

CHARACTERIZATION OF MASONRY MORTARS USED IN SOME
ANATOLIAN SELJUK MONUMENTS IN KONYA, BEYŞEHİR AND AKŞEHİR

A THESIS SUBMITTED TO
THE GRADUATE SCHOOL OF NATURAL AND APPLIED SCIENCES
OF
THE MIDDLE EAST TECHNICAL UNIVERSITY

BY

116577

SELİM SARP TUNCOKU

IN PARTIAL FULFILLMENT OF THE REQUIREMENTS FOR THE DEGREE

OF

DOCTOR OF PHILOSOPHY

IN

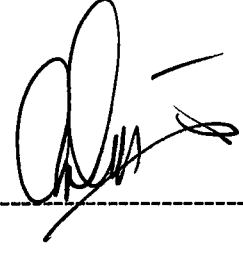
RESTORATION

THE DEPARTMENT OF ARCHITECTURE

JANUARY 2001

116577
T.C. YÜSEKÖĞRETİM KURULU
DOKÜMANTASYON MERKEZİ

Approval of the Graduate School of Natural and Applied Sciences



Prof. Dr. Tayfur ÖZTÜRK
Director

I certify that this thesis satisfies all the requirements as a thesis for the degree of Doctor of Philosophy.



Assoc. Prof. Dr. Selahattin ÖNÜR
Head of Department

This is to certify that we have read this thesis and that in our opinion it is fully adequate, in scope and quality, as a thesis for the degree of Doctor of Philosophy.



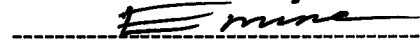
Prof. Dr. Ömür BAKIRER
Co-Supervisor



Prof. Dr. Emine N. Caner SALTİK
Supervisor

Examining Committee Members

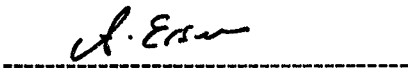
Prof. Dr. Emine N. Caner SALTİK



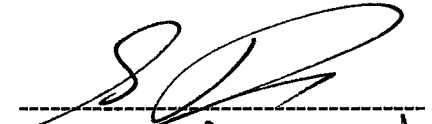
Prof. Dr. Ömür BAKIRER



Prof. Dr. Ahmet ERSEN



Prof. Dr. Şahinde DEMİRCİ



Prof. Dr. Vacit İMAMOĞLU



ABSTRACT

CHARACTERIZATION OF MASONRY MORTARS USED IN SOME ANATOLIAN SELJUK MONUMENTS IN KONYA, BEYŞEHİR AND AKŞEHİR

Tuncoku, S. Sarp

Ph.D., in Restoration, Architecture

Supervisor : Prof. Dr. Emine N. Caner-Saltık

Co-Supervisor : Prof. Dr. Ömür Bakırer

January 2001, 128 pages

The study has involved the examination of mortar technology in twenty two stone and brick masonry structure of Anatolian Seljuk Period in Konya, Beyşehir and Akşehir, in terms of their raw material composition, basic physical and mechanical properties and durability characteristics.

The density and porosities have been determined by using RILEM standard test methods, uniaxial compressive strength (UCS) measurements by ISRM-Point Load Tests, and modulus of elasticity (E_{mod}) by ultrasonic pulse velocity measurements.

Chemical analyses, such as the separation of the insoluble aggregates by hydrochloric acid treatment, complexometric titration with EDTA and Atomic Absorption Spectroscopy (AAS), standard sieve analyses, thin section analyses by optical microscopy, X-Ray Diffraction (XRD), Scanning Electron Microscopy (SEM) coupled with Energy Dispersive X-Ray Analyser (EDX), and thermogravimetric (TGA) analyses were carried out to find the binder/aggregate ratios, element

composition of aggregate parts, aggregate size distribution, mineralogical composition of the binder and aggregate compositions, and the presence of organic additives. Pozzolanic activity estimations of the aggregates were done by electrical conductivity measurements.

The brick masonry mortars are relatively less dense and more porous than the stone masonry ones, but similar to that of adjacent bricks. UCS and E_{mod} values of the mortars were in agreement with those of other historic mortars of pozzolanic nature.

The binder of the mortars was high calcium lime and composed of well-carbonated micritic calcite crystals with a likely organic additive. Lime content in brick masonry mortars was slightly higher than that of stone masonry ones. The use of organic additive was likely to control carbonation process and crystallisation of calcite.

Siliceous aggregates, mostly of opal-A with high pozzolanic activity, formed the major portion of fine aggregates. The use of highly pozzolanic aggregates seemed to promote the formation of silica network for C-S-H formation, prevent damaging attacks of OH⁻ on other aggregates influencing the development of high mechanical strength and durability for wetting and drying cycles.

Those material properties employed in the past have helped the monuments to be durable structures.

Keywords: Medieval masonry, historic lime mortars, pozzolanic mortars, Anatolian Seljuk Period

ÖZ

KONYA, BEYŞEHİR VE AKŞEHİRDEKİ BAZI ANADOLU SELÇUKLU YAPILARINDA KULLANILAN HARÇLARIN ÖZELLİKLERİ

Tuncoku, S. Sarp

Doktora, Restorasyon Programı, Mimarlık Bölümü

Tez Yöneticisi : Prof. Dr. Emine N. Caner-Saltık

Ortak Tez Yöneticisi : Prof. Dr. Ömür Bakırer

Ocak 2001, 128 sayfa

Bu çalışmada Konya, Akşehir ve Beyşehir’de yirmi iki Anadolu Selçuklu Dönemi yığma yapısında uygulanan harç teknolojisi, bu harçlarda kullanılan hammadde kompozisyonları, harçların fiziksel ve mekanik özellikleri ile durabilite özellikleri kapsamında incelenmiştir.

Harçların yoğunluk ve gözeneklilikleri RILEM standart test yöntemleri ile, tek eksenli basınç dayanımları ISRM nokta yükleme testleri ile, elastisite modülleri de ultrasonik hız ölçümleri ile saptanmıştır.

Harçlarda kireç ve agrega yüzdeleri, agrega boyutu dağılımları, kireç ve agregaların mineralojik özellikleri, element kompozisyonları, ve olası organik katkı maddelerinin varlığı araştırılmıştır. Bu çalışmalar kapsamında kireç ve agregaların asit ile

ayrıştırılmasından sonra elek analizleri, asitte çözünen kısımlarında atomik soğurma spektroskopisi (AAS) ve kompleksometrik tirasyon gibi kimyasal analizler yapılmıştır. Ayrıca optik mikroskop ile ince kesit analizleri, X-ışınları toz difraksiyonu (XRD) analizleri, elektron tarama mikroskobu (SEM) ve buna bağlı X-ışınları (EDX) analizleri, ısınma ile ağırlık kaybı tayinleri ve termogravimetrik analizler (TGA) yapılmıştır. Agregaların puzolanik aktiviteleri ise en küçük tanelerin doygun kalsiyum hidroksit çözeltisinde elektrik iletkenliği ölçümleri ile saptanmıştır. Yapıların tuğla örgülerinde kullanılan harçlar taş örgülerdekilere kıyasla daha düşük yoğunlukta ve daha gözeneklidir. Aynı yapılarda kullanılan tuğlaların ve harçların fiziksel özellikleri benzemektedir. Harçların mekanik özellikleri başka Orta Çağ yapılarında kullanılan puzolanik harçlarla benzerlik taşımaktadır.

İncelenen harçlarda saf kireç kullanılmış ve mikritik kalsit şeklinde tam olarak karbonatlaşmıştır. Kireç oranı tuğla örgü harçlarında taş örgülerdekinden daha fazladır. Karbonatlaşma ve kristal oluşumu süreçlerini kontrol altında tutabilmek amacıyla organik katkı maddelerinin kullanılmış olabileceği düşünülmektedir.

İnce agregaların çoğunluğunu puzolanik aktivitesi yüksek olan opal-A minerali oluşturmaktadır. Puzolanik agrega kullanımının harçlarda C-S-H ve silika ağı oluşumunu sağladığı, bazik ortamın diğer agregalara yapacağı tahribatı önlediği, mekanik özellikleri geliştirdiği, ve kuruma-ıslanma tekrarlarına karşı dayanımı sağladığı anlaşılmaktadır.

Bu malzeme özelliklerinin incelenen yapıların dayanımında önemli katkıları olduğu düşünülmektedir.

Anahtar kelimeler: Orta Çağ yığma yapıları, tarihi kireç harçları, puzolanik harçlar, Anadolu Selçuklu Dönemi

ACKNOWLEDGMENTS

I would like to express my gratitude to Prof. Dr. Emine N. Caner Saltık for her supervision and care, and Prof. Dr. Ömür Bakırer for her guidance and encouragement throughout the study.

Special thanks are due to the members of examining committee, Prof. Dr. Şahinde Demirci and Prof. Dr. Vacit İmamoğlu for their contributions in the progress of the thesis.

I should extend my gratitude to Conservation Chemist Dr. Hasan Böke for his helps for the experimental part of the work and invaluable discussions throughout the work.

My deepest thanks are due to Mineralogist Prof. Dr. Asuman Tükmenoğlu, M.E.T.U. - Department of Jeology, Mineralogists Rüksan Teşrekli and Nurgün Güngör, former staffs of The Mineral Research and Exploration Institute of Turkey for their guidance during the XRD analyses, Assoc. Prof. Dr. Tamer Topal, M.E.T.U. - Department of Geology for his helps and guidance during point load tests, Asst. Prof. Dr. Özgen Kangal, Sivas Cumhuriyet University - Department of Geology for his helps during the photographical work on thin sections, Prof. Dr. Haşim Karpuz, Konya Selçuk University - Department of History of Art and Achaelogy for his guidance and invaluable supports during the fieldwork and Res. Asst. Tolga Bozkurt from the same department for his accompany during the photographical survey of the monuments.

The official permission for material sampling given by the General Directorate of Pious Endowments is gratefully acknowledged.

My special thanks are due to Archeologists, Prof. Dr. Rüçhan & Oluş Arık from Ankara University, for providing me Kubadabad Palace samples.

This study was partially supported by the M.E.T.U.- Research Fund Project (AFP).
Therefore, I greatly acknowledge it.

Lastly, I would like to thank to my family for their endurance during my long
absence.



TABLE OF CONTENTS

	Page
ABSTRACT	iii
ÖZ	v
ACKNOWLEDGMENTS	vii
LIST OF TABLES	xv
LIST OF FIGURES	xvi
CHAPTER	
1. INTRODUCTION	1
1.1 The Role and Importance of Mortars in Ancient Masonry	1
1.2 Raw Material Properties of Ancient Masonry Mortars	4
1.2.1 Properties of Binders	5
1.2.1.1 Mixes with Mud	5
1.2.1.2 Mixes with Gypsum	5
1.2.1.3 Mixes with Lime	7
1.2.2 Properties of Aggregates	10
1.2.2.1 Pozzolanic Aggregates	12
1.2.2.2 Lime-Pozzolana Reactions	15
1.2.3 Organic Additives	16

	Page
1.3 The Aim and Scope of the Study	16
1.3.1 Sampling	18
1.3.2 The Monuments Examined	18
2. EXPERIMENTAL METHODS	25
2.1 Determination of Basic Physical Properties	26
2.1.1 Determination of Porosity and Density	26
2.1.2 Determination of Drying Rate	27
2.2 Determination of Basic Mechanical Properties	28
2.2.1 Determination of Modulus of Elasticity (Young's Modulus)	28
2.2.2 Determination of Uniaxial Compressive Strength	29
2.3 Determination of Raw Material Properties	30
2.3.1 Determination of Hygroscopic Water, Organic Matter and Carbonate Content by the Weight Loss on Heating	30
2.3.2 Proportions Binder and Aggregate Parts	31
2.3.3 Determination of Calcium Oxide and Magnesium Oxide Contents by Volumetric Analysis through Complexometric Titration with Standard EDTA Solution	31
2.3.4 Determination of Silicon Dioxide, Aluminium Oxide and Iron Oxide Contents by Atomic Absorption Spectroscopy (AAS)	31
2.3.5 Quantitative Determination of Salt Content by Electrical Conductivity Measurements	32
2.3.6 Pozzolanic Activity Measurements by Electrical Conductivity	32

	Page
2.4 Particle Size Distribution	33
2.4.1 Particle Size Distribution in the Aggregates of Mortars	33
2.5 Petrographic Analyses	33
2.5.1 X-ray Diffraction (XRD) Analyses	33
2.5.2 Thin Section Analyses	33
2.5.3 Scanning Electron Microscopy (SEM) Coupled with Energy Disperse Analysis (EDX)	34
3. EXPERIMENTAL RESULTS	35
3.1 Basic Physical Properties of Mortars	35
3.1.1 Porosity and Density	35
3.1.2 Drying Rates	36
3.1.3 Porosity and Density of Bricks used in some of the Monuments	37
3.2 Basic Mechanical Properties of Mortars	38
3.2.1 Modulus of Elasticity	38
3.2.2 Uniaxial Compressive Strength	40
3.3 Durability Characteristics of Mortars	42
3.4 Raw Material Properties of Mortars	44
3.4.1 Soluble Salt Content	44
3.4.2 Hygroscopic Water, Bound Water and Organic Matter, and Carbonate Contents	45
3.4.3 Binder and Aggregate Proportions	47
3.4.4 Particle Size Distribution in Aggregate Parts	48

	Page
3.4.5 Pozzolanic Activity Estimation in Aggregate Parts ..	52
3.4.6 Chemical Composition of Acid Soluble Parts	52
3.5 Mineralogical Properties of Mortars	54
3.5.1 Thin Section Analyses	54
3.5.2 X-ray Diffraction (XRD) Analyses	58
3.5.2.1 Analysis of the Matrix	58
3.5.2.2 Analysis of the Binder	58
3.5.2.3 Analysis of Aggregates	61
3.5.3 Scanning Electron Microscopy (SEM) and Energy Dispersive X-ray (EDX) Analyses	70
3.5.3.1 Analysis of Matrix	70
3.5.3.2 Analysis of Binder	71
3.5.3.3 Analysis of Fine Aggregates	72
3.5.3.4 Analysis of C-S-H Formations	74
4. DISCUSSION AND CONCLUSION	76
4.1 Raw Material Properties of Mortars	76
4.1.1 Properties of Binder	76
4.1.2 Properties of Aggregates	78
4.1.3 Organic or Inorganic Additives	80
4.2 Physical Properties	81
4.3 Mechanical Properties	82
4.4 Durability Characteristics	83

	Page
4.5 Conclusion	84
REFERENCES	86
APPENDICES	
A. SAHİP ATA COMPLEX AND İNCE MİNARELİ MEDRESE	95
B. TAHİR İLE ZÜHRE MESCİDİ	96
C. SAKAHANE MESCİDİ, HOCA HASAN MESCİDİ AND ZENBURİ MESCİDİ	97
D. HATUNİYE MESCİDİ, THE REMAINS OF LARENDE GATE, EFLAKİ DEDE TOMB AND ŞEKERFURUŞ MESCİDİ	98
E. EVHADEDDİN KIRMANİ TOMB, BEDREDDİN GÜHERTAŞ TOMB AND GÖMEÇ HATUN TOMB	99
F. ZAZADİN HAN	100
G. OBRUK HAN	101
H. KURUÇEŞME HAN	102
I. KIZILÖREN HAN AND THE MESCİD BÜİLDİNG	103
J1. KUBADABAD – THE GREAT PALACE	104
J2. KUBADABAD – THE SMALL PALACE	105
K. TAŞ MEDRESE AND THE MESCİD, ULUCAMİ AND GÜDÜK MİNARELİ MESCİD	106
L. BASIC PHYSICAL PROPERTIES OF STONE AND BRICK MASONRY MORTARS	107
M. PHYSICAL PROPERTIES OF BRICKS USED IN SOME OF THE MONUMENTS	113

	Page
N. ULTRASONIC PULSE VELOCITY MEASUREMENTS AND MODULUS OF ELASTICITY OF STONE AND BRICK MASONRY MORTARS	115
O. UNIAXIAL COMPRESSIVE STRENGTH OF STONE AND BRICK MASONRY MORTARS IN DRY AND WET STATES	118
P. BINDER / AGGREGATE RATIOS AND PARTICLE SIZE DISTRIBUTION IN THE OVERALL COMPOSITION OF MORTAR AND AGGREGATE PARTS OF STONE AND BRICK MASONRY MORTARS	123
R. METAL OXIDE CONTENTS BY AAS AND COMPLEXOMETRIC TITRATION ANALYSES IN ACID SOLUBLE PARTS, AND CEMENTATION INDEX OF STONE AND BRICK MASONRY MORTARS	125
CURRICULUM VITAE	128

LIST OF TABLES

TABLE	Page
1.1 Cementation index for various types of limes	8
3.1 Ultrasonic pulse velocity, density and modulus of elasticity of stone masonry mortars	39
3.2 Ultrasonic pulse velocity, density and modulus of elasticity of brick masonry mortars	39
3.3 Uniaxial compressive strength of stone masonry mortars in dry and wet states	40
3.4 Uniaxial compressive strength of brick masonry mortars in dry and wet states	41
3.5 Durability characteristics of stone and brick masonry mortars ..	43
3.6 Hygroscopic water, bound water and organic matter, and carbonate contents by the weight loss observed on heating	45
3.7 Metal oxide contents in acid soluble parts and cementation Index (CI) of stone and brick masonry mortars	53
3.8 Nomenclature and file numbers of the minerals found in XRD Patterns of the mortar aggregates (<125 μ m)	63
3.9 Metal oxide contents in mortar aggregates	73

LIST OF FIGURES

FIGURE	Page
3.1 Porosity and density of stone masonry mortars	35
3.2 Porosity and density of brick masonry mortars	35
3.3 Drying rates of mortars by weight loss versus time	36
3.4 Drying rates of mortars by weight loss versus time and surface area	37
3.5 Comparison of the porosity of mortars and bricks	37
3.6 Comparison of the density of mortars and bricks	38
3.7 Correlation between modulus of elasticity and uniaxial compressive strength of mortars	42
3.8 Soluble salt content of stone and brick masonry mortars	44
3.9 Thermogravimetric analysis (TGA) of the white lump of Kubadabad Palace	46
3.10 Binder content of stone masonry mortars	47
3.11 Binder content of brick masonry mortars.....	48
3.12 Mortars containing mainly fine aggregates	49
3.13 Mortars containing mainly medium sized aggregates	50
3.14 Mortars containing mainly coarse aggregates	51
3.15 Pozzolanic activity estimations in fine aggregates	52

	Page
3.16 Sparitic limestone aggregate in Obruk Han mortar	55
3.17 Sparitic limestone and sandstone fragments in Kubadabad Palace mortar	55
3.18 White lump and metamorphic rock fragments in the mortar of Kubadabad Palace	55
3.19 Distinction between white lump and limestone aggregate in the mortar of Kubadabad Palace	55
3.20 Sealing of fine cracks by re-crystallisation of micritic calcite and the large pores in the mortar of Zazadin Han	56
3.21 Re-crystallisation at the fine cracks and large pores in the mortar matrix of Kubadabad Palace	56
3.22 Quartz, feldspar and rock fragments in the mortar of Bedreddin Gühertaş Tomb	56
3.23 Quartz and feldspars in the mortar of Hoca Hasan Mescidi ...	56
3.24 Biotite and feldspars in the mortar of Sakahane Mescidi	57
3.25 Abundant inclusions of biotite in the mortar of Zenburi Mescidi	57
3.26 Metamorphic rock fragments in the mortar of Taş Medrese ...	57
3.27 Metamorphic rock fragments, sandstone and feldspars in the mortar of Kubadabad Palace	57
3.28 XRD patterns of mortar matrixes	59
3.29 XRD patterns of the mortar matrix of Kuruçeşme Han and Şekerfuruş Tomb	60
3.30 XRD patterns of mortar binders	60
3.31 XRD patterns of <125µm sized aggregates	62
3.32 XRD patterns of silica polymorphs	64

	Page
3.33 XRD patterns of <math><125\mu\text{m}</math> and <math><45\mu\text{m}</math> sized aggregates in Kubadabad Palace mortar	65
3.34 XRD patterns of <math><125\mu\text{m}</math> and <math><45\mu\text{m}</math> sized aggregates in the mortar of Gömeç Hatun Tomb	65
3.35 XRD patterns of <math><125\mu\text{m}</math> and <math><45\mu\text{m}</math> sized aggregates in the minaret mortar of İnce Minareli Medrese	66
3.36 XRD patterns of <math><125\mu\text{m}</math> and <math><45\mu\text{m}</math> sized aggregates in Zazadin Han mortar	66
3.37 XRD patterns of <math><125\mu\text{m}</math> and <math><45\mu\text{m}</math> sized aggregates in the mortar Sahip Ata Hanikahı	67
3.38 XRD patterns of <math><125\mu\text{m}</math> and <math><45\mu\text{m}</math> sized aggregates in the mortar of Eflaki Dede Tomb	67
3.39 XRD patterns of <math><125\mu\text{m}</math> and <math><45\mu\text{m}</math> sized aggregates in the minaret mortar of Sahip Ata Mosque	68
3.40 XRD patterns of <math><125\mu\text{m}</math> and <math><45\mu\text{m}</math> sized aggregates in the mortar of Evhadeddin Kirmani Tomb	68
3.41 XRD patterns of <math><125\mu\text{m}</math> and <math><45\mu\text{m}</math> sized aggregates in the minaret mortar of Hoca Hasan Mescidi	69
3.42 XRD patterns of <math><125\mu\text{m}</math> and <math><45\mu\text{m}</math> sized aggregates in the minaret mortar Zenburi Mescidi	69
3.43 SEM view of the mortar matrix in Kubadabad Palace	70
3.44 A close SEM view of the mortar matrix of Kubadabad Palace	70
3.45 A close SEM view of the mortar matrix of the minaret of Taşmedrese Mescidi	71
3.46 A close SEM view of the mortar matrix of the minaret of Zenburi Mescidi	71
3.47 SEM view showing the good adhesion between a coarse aggregate and the mortar matrix in Kubadabad Palace	71

	Page
3.48 SEM view showing the good adhesion between a coarse aggregate and the mortar matrix in the minaret of Hatuniye Mescidi	71
3.49 SEM view of micritic calcite crystals in the mortar matrix in Kubadabad Palace	72
3.50 SEM view of micritic crystals in the mortar matrix in the minaret of Sahip Ata Mosque	72
3.51 EDX analysis of a white lump in the mortar in Kubadabad Palace	72
3.52 SEM view of gypsum crystals in the mortar matrix in Şekerfuruş Mescidi	73
3.53 SEM view of the dolomite crystals in the aggregates of Kuruçeşme Han mortar	73
3.54 SEM view of the C-S-H formation in the mortar matrix of Kubadabad Palace	74
3.55 A close SEM view of the C-S-H formation in the mortar of Kubadabad Palace	74

CHAPTER 1

INTRODUCTION

Anatolia is a rich source of masonry structures that form a very important part of our architectural heritage. In spite of many studies on their historical, architectural and stylistic features, the construction techniques, the use of building materials in relation to their preparation techniques attracted little attention (Bakırer, 1967, 1981; Akman *et al.*, 1986; Aktaş, 1988; Güleç, 1992; Satongar, 1994). Besides their architectural characteristics, the use of materials in historic masonry structures depend on many factors such as, the preference or background of master builders, construction trends of the periods, social and economical power of the donors, and especially the availability of the local sources of raw materials.

Thinking of the scarcity of the authentic documentary sources on technological information, it will be realised that these standing edifices are the only sources at hand to be explored. In this context, the mortar, which holds the stone and brick units of those masonry structures as monolithic masses standing for centuries, deserves a special consideration as far as the preservation of this heritage is concerned. Such a consideration demands a scientific approach in order to reveal the properties of original materials, and to develop adequate repair materials for sound interventions.

1.1 The Role and Importance of Mortars in Ancient Masonry

“...The word ‘mortar’ gives no indication of what the material is made of, but the job that it does... It is commonly supposed that the purpose of a mortar is to stick masonry units together, but it is only a minor part of the work to be done. The joints between the units should provide a cushion to spread the loads evenly, particularly with soft bricks and stones. They should act as a wick to draw moisture out of a wall and provide a good surface for evaporation... (Holmes and Wingate, 1997)”.

The meaning and the vital importance of mortar, as it was simply explained by Holmes and Wingate (1997), stem from many duties it undertakes in historic as well as contemporary masonry.

When mortar was used for structural purpose to act as bonding agent in the joints, ancient masons had to consider the structural inputs, such as gravity and thermal load concentrations on the structural members, and the movements due to soil settlements or seismic loads (Salvadori, 1982; Holmes and Wingate, 1997). In addition to those structural inputs, ancient masons were also obliged to consider the certain effects of environmental conditions such as wetting and drying cycles, and frost action *etc.* due to differentiation in ambient temperature and humidity, and wind flow. These are effective parameters on the weathering of building materials and on the long-term durability of the masonry respectively (Schaffer, 1972; Malinowski, 1981).

Within this structural context, the physical and mechanical properties of mortar gain a due importance to hold the masonry units without failure. In the past, this was achieved by the use of purpose-built mortars, the properties of which were compatible with that of masonry units. When the masonry material is brick for instance, ancient masons prepared lightweight mortars with lightweight aggregates and relatively high amount of lime binder compatible with the physical and mechanical properties of the brick units (Malinowski, 1981; Livingston, 1993; Biscontin *et al.*, 1993; Tuncoku *et al.*, 1993). On the other hand, the mortar for stone masonry, on which the lightweight-upper structure rests on, is prepared with the same consideration by using denser mortars with higher strength. Thus, shell-like homogenous structures, which behave uniformly against the possible impacts of environmental conditions, were obtained (Tuncoku *et al.*, 1993; Biscontin *et al.*, 1993).

Different from intermediary tasks between stone and brick units, mortar itself becomes the load-bearing massive core of the structure instead of masonry units as met in numerous structures of Roman Period. The mortar, used in such a way, was customarily termed as 'Roman Concrete' in the building history (Davey, 1961; Cowan, 1977). In those structures, the layers of stone and brick units served as permanent formwork to hold the concrete core while resisting its initial liquid pressure (Davey, 1961; Cowan, 1977). Such formworks of stone or brick, acted also

as evaporation surfaces during hardening phase of the concrete. They remained as mere veneer layers which were designed in various compositions, and they are called in Latin words such as; *opus testaceum*, *opus quadratum*, *opus reticulatum*, *opus incertum*, *opus mixtum etc.* (Davey, 1961; Cowan, 1977).

In many cases, mortars with different physical and mechanical properties were also applied in accordance with different load concentrations in the same component of the same structure (Cowan, 1977; Salvadori, 1982; Mark *et al.*, 1993). The most typical example for this case is the dome of Pantheon in Rome. The lowest part, where thermal expansion forces were higher, was built of mortars with broken brick aggregate being the densest part strengthened against outward thrust and displacements. Going upwards, this layer was gradually replaced with the aggregate layers of brick and tufa, and above the layers of tufa and pumice above forming the lightest zone (Cowan, 1977; Malinowski, 1981; Salvadori, 1982; Hidaka *et al.*, 1993; Holmes and Wingate, 1997). In addition to these considerations in the choice of raw materials and preparation techniques, other devices such as coffers, bottle-bricks, baked clay-hollow tubes *etc.* were also adopted to lighten the upper parts of ancient structures (Davey, 1961; Cowan, 1977).

As it is seen in many other structures of the same period, brick units acted as ribs which were initially placed on timber framework at certain intervals along the transverse and intersection lines of vaults, and along the meridians of cupolas, apses, *etc.* Concrete was then poured in those intervening spaces. When concrete harden enough to support its own weight, the brick ribs did not behave in the same way anymore as those built as true arches (Davey, 1961; Malinowski, 1981). They appear to be mere stiffeners (Çakmak *et al.*, 1994) or inserted reinforcements in the concrete fabric (Livingston, 1993).

By the use of same sort of mortars, with high mechanical properties and impermeable characteristics, ancient masons were also able to construct maritime structures, foundations in waterlogged grounds, cisterns, baths, pavements, pools, wells *etc.* where water insulation was of prime importance in addition to strength. This preference was also due to the fact that such mortars set under water without the need of carbon dioxide (CO₂) in the ambient air (Davey, 1961; Malinowski, 1981; Ashurst and Dimes, 1990; Bugini *et al.*, 1993).

In some other structures however, mortar may not directly contribute to the structural fabric of the masonry. In well-known structures of ancient Egypt for instance, gypsum mortars were used as a soft film layer allowing heavy blocks to be placed gently, thus, preventing their edges from chipping (Davey, 1961).

Other than mortars for jointing, filling or hearting (Davey, 1961) and bedding purpose, there is another term, 'pointing mortar', which is frequently used in the relevant literature. Except for decorative or repair purpose, however, the word 'pointing' or 'pointing mortar', does not refer to a separate work or a mortar with different properties than that used for bedding purpose in the joints. It is a mere struck off flush in the joints as the masonry rises. The job is done by the use of special mason tools, and needs skill (Ashurst and Dimes, 1990; Holmes and Wingate, 1997). The physical and mechanical properties of the mortar, for decorative or repair purpose are very important. Such a mortar is usually more porous and has lower strength than the one in the joints. This is to avoid cracks, which yield in loss of bond between mortar and brick (Duffy *et al.*, 1993). It should also be permeable enough to allow evaporation from the wall through the joints. This is important to avoid salt crystallization problem and its subsequent damage at the surface, or just beneath the surface of masonry units (Schaffer, 1972; Caner-Saltık *et al.*, 1994; Holmes and Wingate, 1997).

As it is seen, mortars in historic masonry undertook numerous different functions, and their physical and mechanical properties were remarkably dependent on each particular case. It is also recognized that those different properties were obtained by the use of different raw materials in varying proportions and different preparation techniques.

1.2 Raw Material Properties of Ancient Mortars

The major components of these mortar mixes are binder and aggregate. The most frequently used binders are mud, lime, gypsum and asphaltic bitumen. If they are used alone they develop cracks on drying. The tendency has therefore been to add them other materials such as natural sand, crushed stone, tile dust, ashes *etc.* which form their filler or aggregate part (Davey, 1961). Besides these major components many other additives, of organic or inorganic origin, which impart different physical

and mechanical properties, can also be found in historic mortars (Davey, 1961; Sickels, 1981).

The raw material properties of mortars can be examined under two groups; the properties of binders and the properties of aggregates (Davey, 1961; Ashurst and Dimes, 1990).

1.2.1 Properties of Binders

1.2.1.1 Mixes with Mud

The oldest use of mixture for building purpose is mud which is composed of sand, silt and clay size aggregates when clay particles act as binder (Davey, 1961; Brown and Clifton, 1978, Brown *et al.*, 1979). It is still in use in many parts of the world (Davey, 1961; Hughes, 1988; Oliver, 1993). Mud is used in varying earth-walling techniques with several names. If it is used with shuttering or formwork it is called rammed-earth-walling or '*pisé*'. If it is used without shuttering it is called 'cob' or 'chalk mud' construction, and, adobe, being hand-molded mud brick sometimes with the addition of fibers such as straw, palm *etc.* Throughout the building history, numerous mud structures that are still in use and good condition can be found especially in arid regions (Davey, 1961; Brown and Clifton, 1978, Brown *et al.*, 1979; Hughes, 1988; Oliver, 1993; Çokça, 1997).

1.2.1.2 Mixes with Gypsum

Gypsum ($\text{CaSO}_4 \cdot 2\text{H}_2\text{O}$) occurs in many different regions, often in between limestone strata and in association with various minerals such as rock salt (NaCl – halite), calcite (calcium carbonate - CaCO_3) and anhydrite (CaSO_4). Most gypsum deposits were formed originally by the evaporation of seawater containing large amount of calcium sulfate in solution (Eckel, 1928; Davey, 1961; Mora *et al.*, 1984).

By the application of different calcination temperatures, different kinds of gypsum can be obtained. When gypsum is calcined at low temperatures between 125°C and 130°C for about three hours more than half of the chemically combined water is driven off; the reaction yields the material known as plaster of Paris ($\text{CaSO}_4 \cdot \frac{1}{2}\text{H}_2\text{O}$) or hemihydrate (or hemihydrate plaster). If burned at higher temperatures of about 200–400°C, the remaining water is totally driven off and anhydrous calcium sulfate

(CaSO_4) is obtained (Eckel, 1928; Davey, 1961; Mora *et al.*, 1984). Moreover, if it is calcined between 900-1300°C a substance ($\text{CaSO}_4 \cdot n\text{CaO}$), which is called hydraulic or flooring plaster is obtained (Davey, 1961). In the course of calcination, partial decomposition of calcium sulfate takes place to form calcium oxide (CaO) and sulfur dioxide (SO_2). It sets slowly and becomes very hard and durable. Due to such properties hydraulic (or flooring) plaster is used to obtain smooth surfaces.

Plaster of Paris sets rapidly when mixed with water forming hard crystalline gypsum ($\text{CaSO}_4 \cdot 2\text{H}_2\text{O}$). Varying sorts of retarders such as keratin (obtained by cooking animal hair, horns, and hoofs in caustic soda solution) or glue-like materials are added to prevent rapid setting, which may cause difficulties in its application. In case of anhydrous calcium sulfate, which hardens rather late however, some accelerators may be needed. This resulted in the production of various patented brands of plasters as Keene's, Parian, and Martin's Cements where the additives of alum (potassium aluminium sulfate), borax and soda have been added respectively as accelerators for hardening (Davey, 1961).

Although gypsum is highly soluble in water, which is a great disadvantage for a building material, mortars, containing gypsum were widely used in the complex components such as domes, vaults and arches of masonry. It was used even in underground parts of many medieval religious buildings with hydraulic lime and/or other hydraulic additives (Kaviak, 1990; Middendorf and Knöfel, 1994) as well as decorative pointing material or fixative material for decorative ceramic tiles (Bakırer, 1981; Tuncoku *et al.*, 1993). It has recently been found that the solubility of gypsum is very low in the historic gypsum mortars in comparison to the solubility of gypsum mineral. This must have been provided by the addition of some organic additives (Middendorf and Knöfel, 1994). In some recent studies, the type of organic additives used in gypsum mortars are being investigated by simulation experiments since it is hardly possible to detect the original organic compounds which have been added for this purpose (Middendorf and Knöfel, 1994). The wide use of gypsum mortars is likely to be due to their advantages over lime in terms of lower energy requirements for their calcination, higher mechanical properties especially of compressive strength and early setting time (Livingston *et al.*, 1991; Middendorf and Knöfel, 1994).

1.2.1.3 Mixes with Lime

Limestone provides the raw material for lime, which is the most frequently used binder. Theoretically, limestone is formed of mineral calcite, calcium carbonate (CaCO_3), which is chemically composed of 56% calcium oxide (CaO) and 44% carbon dioxide (CO_2). Such a pure form of calcite however, is hardly found in the nature. During or after the formation of rock a certain amount of magnesia (MgO) and other impurities such as silica (SiO_2), alumina (Al_2O_3), iron (or ferric) oxide (Fe_2O_3), and alkalis such as sodium and potassium oxides in the form of complex silicates are always introduced. The quantity of these impurities determines the type of limestone and the resultant limes respectively (Eckel, 1928; Davey, 1961; Boynton, 1966).

If the amount of magnesia and other impurities are less than 5% the lime is termed as high calcium lime or rich lime or fat lime. The further classification is usually based on the percentage of magnesia and silicates in the limestone (Davey, 1961; Holmes and Wingate, 1997); if the amount of magnesia exceeds 5%, it is no more pure lime. When the magnesium carbonate amount in limestone reaches 45%, it is called dolomitic lime, and if more, it is magnesian lime. If the amount of silicates exceeds 5% the lime becomes to have hydraulic properties. Different from high calcium limes; hydraulic components set without the need of CO_2 from the air, which makes them different from other limes. Hydraulic limes can be classified under several sub-groups depending on the amount of siliceous or hydraulic components in them which may vary between 10% to 35-40%. Another classification of hydraulic limes can be made by the use of cementation index. It is defined as the ratio of the percentage of silica and alumina content to the percentage of calcium and magnesium oxides in lime (Boynton, 1966; Holmes and Wingate, 1997).

$$\text{Cementation Index (C.I.)} = \frac{2.8 (\% \text{SiO}_2) + 1.1 (\% \text{Al}_2\text{O}_3) + 0.7 (\% \text{Fe}_2\text{O}_3)}{\% \text{CaO} + 1.4 (\% \text{MgO})}$$

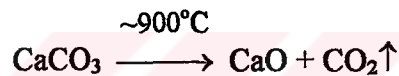
By using cementation index hydraulic limes can be classified as follows (Davey, 1961; Boynton, 1966; Holmes and Wingate, 1997):

Table 1. Cementation index for various types of limes (*)

Lime Description	Cementation Index	Active siliceous compounds
Fat Limes	Close to zero	Very little
Slightly (or feebly) hydraulic limes	0.3 to 0.5	Around 8%
Moderately hydraulic limes	0.5 to 0.7	Around 15%
Eminently hydraulic limes	0.7 to 1.1	Around 25%
Natural cements	1.7	Up to 45%

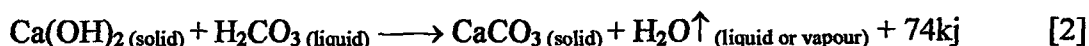
* *Holmes and Wingate, 1997*

Lime is obtained by breaking limestone into lumps of fist size and calcining them in several kinds of kilns at the temperatures around 900°C. The process is called calcination. By the calcination process CaCO₃ gives off CO₂ and any water in it reducing to CaO which is called quicklime or un-slaked lime (Eckel, 1928; Davey, 1961; Boynton, 1966).



Although calcining process of limestone in kilns is almost the same for all types of limestone, the firing temperature at which the material decompose by chemical reactions is a very important parameter on the final product (Eckel, 1928; Boynton, 1966). For hydraulic limes the firing temperature is same with that of calcitic limes. At higher temperatures, lime begins to sinter and cannot slake unless it is finely ground up (Holmes and Wingate, 1997). Different from calcitic limes, hydraulic limes undergoes more complex chemical reactions (Eckel, 1928; Boynton, 1966). The level of firing temperature has another importance on the ability of quicklime slaking into lime putty in water, or, to dry hydrate in the air. And in turn, it will also affect the ability of slaked lime to react with CO₂ to achieve a good set (Holmes and Wingate, 1997).

To obtain lime hydrate or lime putty quicklime is treated with water. The end product is calcium hydroxide, Ca(OH)₂, and the process of hydrating quicklime is called slaking process. The lime putty is then, mixed with sand in certain proportions to produce mortars. When this mixture is exposed to the air, Ca(OH)₂ absorbs CO₂ from the air and converts to CaCO₃. This process is called carbonation process. The reaction occurs in the following steps (Morehead, 1986; Balen and Gemert, 1994; Elvfing *et al.*, 1996);



Initially, atmospheric CO₂ reacts with surface water of Ca(OH)₂ and forms carbonic acid (H₂CO₃) shown in equation [1], and carbonic acid thereafter, reacts with lime hydrate and forms calcite (CaCO₃) shown in equation [2]. During the reaction some heat (74kJ) is also produced. The formation of carbonate leads to an increase in volume, which is accommodated in the larger pores of the mortars thus making the mortar less permeable for CO₂ diffusion for further carbonation (Morehead, 1986). The rate and the range of carbonation in such a case, is also influenced by the construction techniques, involving the thickness of the joints which determines the depth of the initial carbonation, and the physical properties, especially porosity, of the adjacent masonry units, that are serving as galleries for CO₂ diffusion into the reaction site (Balen and Gemert, 1994). Cracks, occurred due to initial shrinkage on drying or structural settlements, large pores in the mortar and porous aggregates are also the source of CO₂ to react with condensation water in them and un-carbonated Ca(OH)₂. The heat generated during the reaction on the other hand, is said to be enough to evaporate the water produced by the reaction, thus leading to premature set of the mortar without a complete carbonation (Morehead, 1986) in the case of the scarcity of water. In case of excess amount of water however, the diffusion rate of CO₂ decreases since its diffusion in water is much slower than in the air and thus retarding the carbonation (Balen and Gemert, 1994). As it is seen, both cases imply the critical importance of mixing (or working) water. The environmental conditions, such as the temperature, relative humidity and wind speed are also effective factors, which work in combination by influencing the rate of CO₂ diffusion, the quantity of water to react with CO₂, and the rate of carbonation (Morehead, 1986; Balen and Gemert, 1994).

In some cases slaking process is carried out together with sand to provoke the covering of all particles with lime paste in a more effective way than conventional mixing methods. The process is called hot lime process and it was used in Ancient Europe and other parts of the world and favored especially in cold and wet regions (Wisser *et al.*, 1988; Ashurst and Dimes, 1990; Holmes and Wingate, 1997). With respect to their slaking, high calcium limes slake rapidly, evolve much heat and

expand more giving a large bulk of slaked lime (Eckel, 1928). On the contrary of high calcium limes, magnesian limes slake slowly, evolves less heat with less expansion and they give less bulk of slaked lime. However, when compared to high calcium limes, these limes yield mortars with high strength, they set early (Eckel, 1928; Holmes and Wingate, 1997).

As previously mentioned, mortars prepared with hydraulic limes are well known for their high mechanical properties when compared to the mortars prepared with non-hydraulic limes. Non-hydraulic limes in the mortars impart an astonishing self-curing ability to the fabric. This happens by the successive cycles of rain penetration and drying which lead to the redistribution and re-crystallization processes of calcium carbonate. Thus, cracks, crevices and fissures caused by freezing, swelling or temperature changes which form micropores (or microcracks) disadvantages for the durability (Schaffer, 1972) are often found to be filled again (Davison, 1977; Wisser *et al.*, 1988; Sickels 1995). Such a property is also available for hydraulic mortars since they always contain considerable amount of calcium carbonate, which may be called free-lime (Wisser *et al.*, 1988).

In addition to those parameters, either hydraulic or non-hydraulic, the grain size of the lime is also important as the smaller the grain size, the higher the specific surface area and the higher the water demand. That will also give a porous mortar with lower strength (Schäfer and Hilsdorf, 1993). In addition to mineralogical properties of the limestone from which lime is obtained, the grain size of the lime hydrate is related to its slaking process; the higher the slaking rate, the smaller is the grain size (Boynton, 1966).

1.2.2 Properties of Aggregates

Aggregates, of natural or artificial origin, perform important duties in mortars. Simply, they act as filler reducing the requirements of lime and prevent mortar from shrinkage on drying and cracking respectively (Davey, 1961; Mora *et al.*, 1984; Ashurst and Dimes, 1990). Their natural sources are sand quarries (or sand pits) and river or coastal beds (Davey, 1961; Mora *et al.*, 1984). Some of those aggregates act as inert dilutants in the mortar, because they do not react with lime (Davey, 1961). Some others however, may readily react with lime and yields hydraulic mortars

(Davey, 1961; Ashurst and Dimes, 1990; Holmes and Wingate, 1997) similar to those prepared with hydraulic limes. As will be explained in detail below, this difference is attributed mostly to their different mineral compositions and different crystal structures (Lea, 1970). Besides natural sources, aggregates may also be obtained artificially by grinding various types of rocks, bricks, tiles, pottery *etc.* into desired size (Mora *et al.*, 1984). In some cases, aggregates may have to be washed to remove clayey and organic matters, and water-soluble salts that are considered to be deficiencies in mortars (Davey, 1961; Mora *et al.*, 1984; Ashurst and Dimes, 1990). The presence of clay minerals, the ones unbaked and not of volcanic origin, may cause shrinkage on drying, but it is also suggested that they may introduce a slight hydraulic effect to the mortar (Holmes and Wingate, 1997), such as lateritic soils in controlled amounts (Falade, 1993; Osunade, 1993). Within those impurities, the most dangerous one is the presence of soluble salts eg. mostly found in sea sands. Soluble salts make the mortar hygroscopic which is leading to slower drying and thus, to slower hardening of mortar (Davey, 1961). In addition, the salts also cause salt crystallization, which is introduced by wetting and drying cycles. This is one of the major decay forms observed in historic masonry structures. The use of sea sand without a thorough-washing is therefore never advisable (Davey, 1961; Schaffer, 1972; Mora *et al.*, 1984; Ashurst and Dimes, 1990).

Besides their mineralogical composition and structure, the particle size distribution of aggregates in the mortar is another important factor, because it determines the volume of the space between particles and the quantity of binder needed (Mora *et al.*, 1984). For the particle size distribution in inert aggregates it is suggested that the voids between large grains must be filled with smaller ones (ASTM C144-76; Davey, 1961; Mora *et al.*, 1984). Thus, the total surface area to be covered with lime will be small. This means less amount of carbon dioxide and less amount of lime, which requires less amount of water. Upon drying, this results in minimum contraction and a less porous mortar with high strength (Davey, 1961; Mora *et al.*, 1984). For such an ideal case, the ratio of binder to aggregate would correspond to 1/2~3 by volume (Mora *et al.*, 1984; Ashurst and Dimes, 1990). If those voids are in great amount, much lime and hence much water will be required. This yields a porous mortar with lower strength. In addition, much carbon dioxide intake due to high amount of voids

between grains will cause lime to set prematurely without covering the whole grain surfaces (Lewin, 1981). This will also be another reason for a mortar with lower strength.

Similar to the grain size distribution, the average grain size of the aggregates in a given mortar is also effective on its physical and mechanical properties. Excessive use of fine sand, for instance, will provide higher surface area to be covered with lime, which means more water and, which result in a porous mortar with lower strength respectively (Ashurst and Dimes, 1990; Schäfer and Hilsdorf, 1993).

In addition to average grain size and its distribution in the mortar, the shape of the aggregate grains is also effective on the physical and mechanical properties and workability of mortar. It is suggested that, aggregates with rough surface provide larger specific area and they increase the friction in between. In spite of difficulties in the workability with such a mortar, the aggregate of this kind will provide higher strength and better adherence with the binder after setting (Mora *et al.*, 1984) when compared with rounded aggregates. The ancient masons improved the workability (or plasticity) of such mortars by the use of organic or inorganic additives (Sickel, 1981).

With respect to physical and mechanical properties of a mortar, the mineralogical composition of the aggregates is extremely important to such an extent that the above-mentioned parameters may become less important. As explained below, this may be due to their ability to combine with lime and produce new compounds, which may cause remarkable differences in the favour of the strength properties in the mortar.

1.2.2.1 Pozzolanic Aggregates

Pozzolanic aggregates are defined as the materials, though not cementitious in themselves, contain the compounds such as silica, alumina and iron oxides, which readily react with lime at ordinary temperatures in the presence of water, and form stable insoluble compounds with cementing properties (Davey, 1961; Lea, 1970; Ashurst and Dimes, 1990; ASTM C 593-76a). Such materials of volcanic origin are called 'pozzolana', which has become a generic name since they are supposed to be found and used first in Puzzuoli near Naples in Campania Region in Italy (Davey,

1961; Mora *et al.*, 1984; Ashurst and Dimes, 1990). Depending on the regions where they are found, pozzolanas can be called with different names, such as German *trass*, Santorin earth, *tosca* in Teneriffe, *tetin* in Asores *etc.* (Lea, 1970). Pozzolanas are well known for their cementing properties, and they impart high mechanical strength to the mortars. As of volcanic origin, they can also be naturally occurred earths by sedimentation process (such as diatomaceous earth) or obtained artificially (burnt clay). Either natural or artificial origin, they must contain siliceous compounds in certain amounts to react with lime and form silicate hydrates.

a. Volcanic Pozzolanas: They are glassy incoherent materials or compacted tuffs originated from the deposition of volcanic dust and ash (Lea, 1970), which have undergone rapid cooling and, in some cases subjected to chemical alterations thus, leading to the formation of zeolitic compounds (Lea, 1970). The volcanic materials owe their pozzolanic properties both to the volcanic glass and to the altered zeolitic compounds (Lea, 1970).

b. High Silica Minerals: These materials, showing pozzolanic properties, include the diatomaceous earths and siliceous rocks of biogenic origin (petrified wood and plant remains) and silica of inorganic origin such as; cherts, flints, shales, sandstones (Lea, 1970; Diamond, 1976; Drees *et al.*, 1995). The reactive constituent of these materials is opal, which is one of the polymorphs of silica group minerals, such as; quartz, cristobalite, tridymite *etc* (Drees *et al.*, 1995). Within this group of minerals opal is the only hydrated 'amorphous' silica which contains water in the range of 4 to 10% by weight (Diamond, 1976; Drees *et al.*, 1995). Contrary to quartz, which is known as the purest mineral with a well-ordered crystal structure, opal minerals, such as opal-CT and cristobalite, and opal-A may contain impurities of Al, Fe, Ti, Mn, Cu, N, C, alkalies and alkaline earths mostly depending on the physical and chemical environments (Drees *et al.*, 1995). It should also be noted that, carbonates or metal hydroxides (Mg, Fe, Al, Mn) may provoke the condensation reaction for the formation of silica polymerization, which in turn act as reactive sites for further silica precipitation (Drees *et al.*, 1995). In addition to its chemical properties, the reactivity of opal with alkalies, in the case of historic mortars, with $\text{Ca}(\text{OH})_2$ for instance, is attributed to its amorphous character and its structure, which provide an interconnected pore system absorbing alkali solutions quickly to all parts

of the affected aggregate grain (Diamond, 1976). This may better explain the role of amorphous silica on the advantageous properties of pozzolanic mortars. However, some inactive minerals may also react with alkalies upon morphological changes (Diamond, 1976). Quartz for instance, as suggested in a recent study, becomes reactive when its particle size is reduced below 5 μm which was defined as 'critical diameter' associated with 'critical surface area' of 10.000g/cm² (Benezet and Benhassaine, 1999).

c. Artificial pozzolanas: Throughout the history of building practice ancient builders also used artificial pozzolanas, such as burnt-clays (tiles, brick, pottery *etc.*) in mortar combinations to obtain hydraulic properties. Such mortars as Roman concrete or *cocciopesto* (Malinowski, 1981; Massazza and Pezzuoli, 1981; Bugini *et al.*, 1993) were well-known to Romans. The value of burnt-clay addition to non-hydraulic lime however, have also long been common practice in India named as *surkhi*, in Egypt known as *homra* (Lea, 1970; Holmes and Wingate, 1997), and in Ottoman Period in Anatolia used as *Horasan (or Khorasan)* (Akman *et al.*, 1986, Güleç, 1992; Satongar, 1994).

Burnt-clay pozzolanas are produced by burning suitable clays (or shales) at the approximate temperatures of 500-900°C (Lea, 1970). Raw clays consist essentially of a group of hydrated aluminium silicates which sometimes replaced by ferric oxide and by bases such as magnesium oxide (MgO), sodium oxide (Na₂O) and calcium oxide (CaO). These clays contain considerable amount of combined water. Some of them, such as kaolinite types, loose the combined water at 500°C while others, such as montmorillonite at relatively lower temperatures (Lea, 1970). It is suggested that for better results the clays fired at low temperatures are usually preferred (Teutonico *et al.*, 1994).

In modern building practice, there are many ongoing researches to find alternative sources to materials with pozzolanic activity to be used in low-cost concrete. Those potential sources involve mainly; fly ash and geothermal wastes from power plants, rice husk, straw ash, sugar cane *etc.* from agricultural wastes (Martirena *et al.*, 1998; Escalante *et al.*, 1999; Qijun *et al.*, 1999; Biricik *et al.*, 1999).

Either natural or artificial, the particle size of pozzolanas has notable effects on the physical and mechanical properties of mortars in which they are used (Lea, 1970; Holmes and Wingate, 1997). The coarser particles act as more or less inert aggregates slowing down the rate of hardening. Thus, the use of finely ground pozzolana not only helps in having a higher reactivity and higher mechanical strength, but also accelerates the rate of hardening (Lea, 1970; Robert and Caijun, 1994). The use of porous aggregates either natural, such as limestone, or artificial such as, coarser grains of burnt clay act as air entrainers and may lead to lightweight mortars (Teutonico *et al.*, 1994; Ashall *et al.*, 1996).

1.2.2.2 Lime-Pozzolana Reactions

Different from the mortar combinations prepared with fat limes and inert aggregates, the mortars prepared with high calcium limes and pozzolanic aggregates involve chemical reactions, which turn the mortar to be of a hydraulic one with entirely different physical and mechanical properties. The chemical reactions are called pozzolanic reactions and the resulting product is of hydraulic or pozzolanic mortar (Eckel, 1928; Davey, 1961; Boynton, 1966; Lea, 1970). As it is already stated, the fundamental property of a natural pozzolana is its ability to combine with lime hydrate, Ca(OH)_2 , at ordinary temperatures in moist curing environment or under water (Eckel, 1928; Davey, 1961; Lea, 1970; Boynton, 1966; Ashurst and Dimes, 1990).

The silicas of such amorphous or vitreous nature can readily dissolve in alkaline media of high pH values such as Ca(OH)_2 (Wang and Gillot, 1991) The reaction starts with the absorption of hydroxide (OH^-) ions by pozzolanic aggregates on Ca(OH)_2 solution and silicic acid is formed on the surface of aggregates. Silicic acid, hereafter, reacts with Ca(OH)_2 and forms calcium-silicate-hydrates quoted as C-S-H in cement chemistry notation ($\text{C}=\text{CaO}$, $\text{S}=\text{SiO}_2$, $\text{H}=\text{H}_2\text{O}$). Those final products of C-S-H connect the aggregate particles to a certain degree after which no more reaction takes place on the surface of the siliceous particle. This is due to the formation of a layer of C-S-H gel on the surface of the particle, which prevents further penetration of OH^- ions into the aggregate. The crystal form of C-S-H gel is known as tobermorite (Lewin, 1981; Wang and Gillot, 1991; Erdoğan, 1995).

The mineralogical and chemical composition of the aggregates used, and the concentration of lime has notable effects on the reaction rate as well as the final properties of C-S-H gels (Barret *et al.*, 1977, Aardt and Visser, 1977).

The use of feldspathic aggregates in mortars, such as orthoclase, microcline, albite, anorthite, labradorite minerals with high content of potassium oxide (K_2O) and sodium oxide (Na_2O), may have deleterious effects on the properties of the final gel and the resulting product (Aardt and Visser, 1977; Wang and Gillott, 1991). Similar to pozzolanic reaction explained above, initially a bond of C-S-H gel is formed on the aggregate grain, which contains silica together with alkali feldspar. $Ca(OH)_2$ also react with feldspathic part of the aggregate and alkalis are liberated in the form of potassium hydroxide (KOH) and sodium hydroxide (NaOH), and potassium and sodium silicate gels that are soluble. This migration proceeds until KOH and NaOH alkalis reach a certain concentration in the solution. After this point, the initially formed C-S-H bond will start to dissolve in sodium and potassium silicates forming weaker gels that are soluble in water. If the initial solution has a high concentration in lime and pozzolanic aggregates, the formation rate of C-S-H gel is higher (Barret *et al.*, 1977). Therefore, the relatively stable layer of C-S-H will not allow further penetration of OH^- ions into the aggregates, such as feldspars, and thus protect them from degradation (Aardt and Visser, 1977; Benharbit, 1994).

1.2.3 Organic Additives

According to some documentary sources the ancient masons also used organic or synthetic additives in addition to binders and fillers. The additives, such as, egg whites, blood, fig juice, rye dough, hogs' lard, curdled milk, casein, fats, oils *etc* were probably used to improve workability, to extend or retard the setting time, to increase cohesion and the strength of mortars (Sickels, 1981; Knöfel and Wisser, 1988). The issue however, is still open to debate and calls for further research.

1.3 The Aim and Scope of the Study

Anatolian Seljuk Period, covered the 12th and 13th centuries was one of the most glorious periods which was able to convey its evidences to the present through its numerous standing edifices that are met in many parts of Anatolia. Konya with its

nearby surroundings in this respect, has a due importance regarding the population as well as the diversities in the function of those edifices. Among these edifices, religious buildings, such as mosques and ‘mesjids’ (small scaled mosques), commemorative buildings, such as the tombs of nobles, buildings of educational purpose, such as ‘medreses’ (theological schools), buildings for short-period stay for traders or the army, such as ‘kervansarays’ or ‘hans’, and palaces for permanent or seasonal use are the most frequently found monuments in Konya and its vicinity. All of these monuments are masonry structures built of stone, brick or both, and mortar, as a binding medium, being the subject of this study, which successfully held them for centuries. The objective of the study is therefore to understand the technological properties of the mortars employed in the masonry structures of this period. This was done by the determination of their basic physical and mechanical properties, raw material properties, possible additives and preparation techniques. The related physical and/or chemical mechanisms through which those physical and mechanical properties obtained were studied and tried to be understood. In addition to those essential parameters, the durability characteristics and the contribution of the mortars in the masonry were tried to be estimated. Hence, the criteria in the selection of the monuments to be investigated for their mortars were; to concentrate on the buildings with different functions and different construction dates, and, to choose those structures, which have been subjected to little or no intervention to obtain original samples, and thus to highlight the mortar technology employed in the period as much as possible. The monuments determined for the study are located in Konya, on its connection roads to Aksaray, Beyşehir and Karaman, and in the nearby towns, Akşehir and Beyşehir. The monuments in Konya are: the Complex of Sahip Ata (Hanikah and the Mosque); the tombs of Evhadeddin Kirmani, Gömeç Hatun, Eflaki Dede and Şekerfuruş; the ‘mescids’ of Zenburi, Hatuniye, Sakahane, Tahir ile Zühre (or Sahip Ata) and Hoca Hasan; and the recently found remains of a stone masonry wall, which was attributed to the Larende Gate of the city defences of Konya. The monuments in Akşehir are: Ulucami (The Great Mosque), Taşmedrese and its ‘mescid’, and the ‘mescid’ of Güdük Minareli. Other monuments are: Kubadabad Palace located on the southwestern shores of Lake Beyşehir; the ‘hans’ of Kızılören and Kuruçeşme on Konya-Beyşehir Highway; the ‘hans’ of Zazadin and Obruk on

Konya-Aksaray Highway, and the tomb of Bedreddin Gühertaş in Selim Sultan District on Konya-Karaman Highway.

The exact construction date and the donors of some of the monuments above are not known. However, their approximate dating were done by the historians of art and architecture through the comparison with well-known monuments of the same period with respect to their architectural and stylistic features, construction techniques and workmanship in addition to various legendary sources, foundation charters *etc.*

(Öney, 1967; Bakırer, 1968,1981; Arık, 1968, 1992; Dülgerler, 1979; Karamağaralı, 1982; İpekoğlu-Acar, 1992).

1.3.1 Sampling

Following the selection of the monuments, mortar samples were collected from the relatively sound and untouched parts of the walls, arches, vaults, the domes and the minarets of these structures. The places, from where the samples were collected have been indicated on photographs and plans of the structures (Appendix A-K). The samples were collected by the use of chisels and hammer with maximum care not to damage the monuments. The samples were then packed in polyethylene bags, and they were labelled by the abbreviated name of the monument, masonry material of brick or stone, and the sample number. For example, in the sample of ‘kub.SM1’: ‘kub’ indicates the name of the monument Kubadabad Palace, ‘SM’ indicates the stone masonry mortar, and ‘1’ is the sample number. Another abbreviation used is ‘BM’ representing the mortar of brick masonry, *eg.* ‘kub.BM2’. Other remarks, such as a brief description of the collection spot, the condition of the sample *etc.* were also noted on the label cards. The labels without sample number, as ‘kub.SM’ or ‘kub.BM’, represented the average values of pieces of the same kind of sample. This coding system has been kept throughout the thesis. The plans of the buildings and the photographic documentation of sampling has been presented in Appendix A-K.

1.3.2 The Monuments Examined

The places of the mortar samples from where they were collected, information about the construction date and donor and the type of the masonry of the monuments are as follows:

1. Sahip Ata Complex (Bakırer, 1981)

Construction date of the mosque: 1258 (inscription panel)

Donor: Sahip Ata Fahrettin Ali

Construction date of Hanikah: 1269-1270 (inscription panel)

Construction materials: Cut and rubble stone in lower parts of the walls and brick in the upper parts.

The mortar samples of brick masonry were collected from the entrance hall of the 'hankah' and, from the lower and upper levels of the minaret staircase of the mosque (Appendix A1.1-4).

2. İnce Minareli Medrese and the Mescid (Bakırer, 1981)

Construction date: 1264-1265 (foundation charter)

Donor: Sahip Ata Fahrettin Ali

Construction materials: Cut stone in minaret base and brick on the shaft.

The mortar samples of brick masonry were collected from the lower and medium levels of the staircase of the mescid minaret (Appendix A2.1-2).

3. Tahir ile Zühre Mescidi (Bakırer, 1981)

Construction date: The second half of the 13th century

Donor: Sahip Ata Fahrettin Ali

Construction materials: Cut and rubble stone in lower parts, brick in upper parts.

Brick masonry mortars were collected from the arch of the entrance hall, the arch of the opening above on the north facade, the exterior of the west wall, and from the arch of the southern niche of the tomb space. Stone masonry mortars were collected from the north, south and west facades and south-east corner of the prayer hall (Appendix B1-6).

4. Sakahane Mescidi (Bakırer, 1981)

Construction date: second half of the 13th century (by comparison of the stylistic and architectural features, especially similarity with the 'mihrap' of Tahir ile Zühre)

Donor: unknown

Construction materials: Cut and rubble stone in lower walls, brick in upper parts.

The stone masonry mortar was collected from the north-east corner of the mesjid interior 50cm above ground level (Appendix C1.1-2).

5. Hoca Hasan Mescidi (Bakırer, 1981)

Construction date: second half of the 13th century (the style of the minaret)

Donor: Köle Hasan [?]

Construction materials Cut stone in minaret base and brick on the shaft.

The brick masonry mortars were collected from the lower and medium levels of the minaret staircase of the mesjid (Appendix C2.1-2).

6. Zenburi Mescidi (Bakırer, 1981)

Construction date: the first half of the 13th century (by comparison of the stylistic and architectural features of other monuments of the same period).

Donor: unknown

Construction materials Cut stone in minaret base and brick on the shaft.

The mortar samples of brick masonry were collected from the lower part of the staircase of the mesjid minaret (Appendix C3.1-2).

7. Hatuniye Mescidi (Bakırer, 1981)

The mosque was demolished and it was reconstructed in later periods.

Construction date: 1229-1230 (inscription panel on the minaret)

Donor: Hacı Mahmutzade Bedrettin Bermuti

Construction materials: Cut stone in minaret base and brick on the shaft.

The brick masonry mortars were collected from the lower and medium levels of the minaret staircase of the mesjid (Appendix D1).

8. The remains of the walls of Larende Gate from the city walls of Konya

The dating of the remains has been done by art historians. The wall can now be seen in the basement of a new apartment building (Information was obtained by personal communication with Prof. Dr. Haşim Karpuz from the Department of History of Art and Archaeology, Konya-Selçuk University).

Material collected from the rubble masonry (Appendix D2)

9. Eflaki Dede Tomb (Karpuz, 1998)

Construction date: 1360 (Inscriptions on the tombstone of Eflaki Dede)

Donor: Unknown

Construction materials: Rubble stone and brick.

The brick masonry mortar was collected from the demolished edge of the west wall (Appendix D3.1-2).

10. Şekerfuruş Tomb (Dülgerler, 1979)

Construction date: 13th century (legendary sources)

Donor: Unknown

Construction materials: Cut and rubble stone in lower parts of the walls and brick in upper parts and some sections of the walls.

The brick masonry mortar was collected from the left sidewall of the entrance to the crypt (Appendix D4.1-2).

11. Evhadeddin Kirmani Tomb (Dülgerler, 1979)

Construction date: Second half of the 13th or first half of the 14th century

Donor: Unknown

Construction materials: Cut and rubble stone in lower walls and brick in upper parts.

Mortars from rubble masonry was collected from the entrance and the east façades. The brick masonry mortars were collected from the south-east zone of the dome and from the arch of the on the east side the dome (Appendix E1.1-3).

12. Bedreddin Gühertaş Tomb (Dülgerler, 1979)

Construction date: Second half of the 13th century (legendary sources)

Donor: Unknown

Construction materials: Cut and rubble stone in lower and brick in the upper parts of the wall.

The mortar from rubble masonry was collected from the demolished edge of the north wall. Brick masonry mortars were from the west and east edges of the same wall (Appendix E2.1-2).

13. Gömeç Hatun Tomb (Bakırer, 1981)

Construction date: 1275-1285 (the stylistic features and techniques of ceramic tiles)

Donor: The wife of Kılıçarslan IV (the mother of Gıyasettin Keyhüsrev XIII)

Construction materials: Cut stone in lower parts of the walls, brick in upper parts

The brick masonry mortar wall was collected from the exterior of the south-east corner (Appendix E3.1-3).

14. Zazadin Han (Ethem, 1969).

Construction date: 1236

Donor: The Seljuk Emirate Saadeddin Köpek bin Muhammed.

Construction materials: Cut and rubble stone.

Stone masonry mortars were collected from the vaults of the north-side 'eyvans' of the courtyard and the entrance 'eyvan' (Appendix F1-5).

15. Obruk Han (Ethem, 1969).

Construction date: The first half of the XIIIth Century (by comparison with other hans of the same period)

Donor: Unknown

Construction materials: Cut and rubble stone.

Stone masonry mortars were collected from the vaults of the 'eyvans' on the north-side of the courtyard and the entrance 'eyvan' (Appendix G1-4).

16. Kuruçeşme Han (Ethem, 1969).

Construction date: 1207-1208 (The period of Gıyaseddin Keyhüsrev)

Donor: Unknown

Construction materials: Cut and rubble stone.

Stone masonry mortars were collected from the vault of the 'mescid' space, the right side corner of the entrance gate wall and the main vault of the 'eyvans' on the north-side of the courtyard (Appendix H1-5).

17. Kızılören Han and the 'mescid' building (Ethem, 1969)

Construction date: 1206

Donor: Gıyaseddin Keyhüsrev Period, Muhammed Oğlu Emir Kutlu

Construction materials: Cut and rubble stone masonry.

Stone masonry mortars were collected from the south wall of the 'eyvan' and from the vault covering the central nave of the closed space of the han. Stone masonry

mortars from the 'mescid' building were collected from the pier in front of the south wall, and from the east corner of the entrance facade (Appendix I.1-7).

18. Kubadabad Palace Complex – The Great Palace (Arık, 1968)

Construction date: 1236

Donor: Sultan Aleaddin Keykubad

Construction materials: Cut and rubble stone masonry, minor quantities of brick in arches.

Stone masonry mortars were collected from the rubble and cut stone masonry walls, and brick masonry mortar samples were from the arches (Appendix J1.1-6).

19. Kubadabad Palace - The Small Palace (Arık, 1995)

Construction date: 1236

Donor: Sultan Aleaddin Keykubad

Construction materials: Cut and rubble stone masonry, minor quantities of brick in arches.

Stone masonry mortars were collected from the rubble and cut stone masonry walls, and brick masonry mortar samples were from the arches (Appendix J2.1-6).

20. Taşmedrese and its Mescid (Bakırer, 1981)

Construction date: 1250 (inscription panel)

Donor: Sahip Ata Fahrettin Ali

Construction materials: Cut and rubble stone in lower parts, brick in upper parts

Stone masonry mortar was collected from the rubble wall of the space located on the left-side of the entrance. Brick masonry mortars were from the lower and medium levels of the minaret staircase of the mescid (Appendix K1.1-3).

21. Akşehir Ulucami (Öney, 1967)

Construction date: 1213 (inscription panel)

Donor: Cihanbeyli Yarı Mahmut Ağa

Construction materials: Cut stone in minaret base and brick on the shaft.

Brick masonry mortars was collected from the medium level of the minaret staircase of the mosque (Appendix K2.1-2).

22. Gdk Minare Mescidi (Bakırer, 1981)

Construction date: 1227 (inscription panel)

Donor: Mktesip Hacı Hasan

Construction materials: Cut stone in minaret base and brick on the shaft.

**Brick masonry mortar was collected from the medium level of the minaret
(Appendix K3.1-3).**



CHAPTER 2

EXPERIMENTAL METHODS

As explained in previous sections, the contribution of a given mortar in a given masonry occurs in several ways related to on its function. A mortar serves in the masonry with its physical and mechanical properties. However, to obtain those properties, the raw materials of mortars are selected, processed, mixed and used in different ways for the purpose. Several analyses are necessary to understand those technologies.

The laboratory analyses of the mortars covered the determination of basic physical and mechanical properties, and raw material compositions.

Analyses of basic physical properties involved the determination of porosity, density and drying rate of the mortar samples.

Analyses of basic mechanical properties covered the determination of their uniaxial compressive strength (UCS) and modulus of elasticity (E_{mod}). Uniaxial compressive strength of the mortars were determined by the use of point load tests, and the modulus of elasticity by the measurements of ultrasonic pulse velocity (UPV).

The raw material composition and mineralogical properties of the mortars were determined by thermogravimetric, chemical, particle size distribution and petrographic analyses.

Determination of hygroscopic water, bound water and organic matter, and carbonate contents have been carried out by the weight loss on heating.

Chemical analyses involved; the determination of binder and aggregate proportions by acid treatment, the quantitative determination of metal ions in acid soluble parts by volumetric analysis (complexometric titration by EDTA) and atomic absorption spectroscopy (AAS), the quantitative determination of soluble salt content in the

mortars, and pozzolanic activity estimations in the fine aggregates by the measurement of electrical conductivity.

Particle size distribution analyses were carried out in the aggregate parts of the mortars by standard sieving.

Petrographic analyses were performed to determine mineralogical composition and crystal structure of the mortars. These analyses involved, X-ray diffraction (XRD) analysis, scanning electron microscopy (SEM), which was coupled with energy dispersive X-ray analysis system (EDX), and thin section examinations by optical microscopy.

Detailed explanations of the analyses, related standards and preparation of the samples have been given in the following sections.

2.1 Determination of Basic Physical Properties

For the determination of basic physical properties, the samples, each of which was separated into three pieces (of 15-20g), were dried in the oven at 35°C to constant weight. These weight measurements were recorded as the dry weights of the samples (m_{dry}).

The saturation of samples in distilled water was carried out in vacuum using a (HERAEUS vacuum chamber) at 0.132atm (100torr) pressure. The weights of the water-saturated samples were recorded as saturated weights (m_{sat}). The weight of saturated samples was also measured in water and recorded as the Archimedes weight (m_{arch}) of the samples. All weights were measured with the sensitivity of 0.0001g and they were used in the calculation of porosity and density of the samples (RILEM, 1980; Teutonico, 1986). The results have been given as average values with their standard deviations in tables and/or expressed in diagrams.

2.1.1 Determination of Porosity and Density

Porosity (P) is the fraction of the total volume of a porous material occupied by pores or, more simply, the empty spaces or voids in the mass. Porosity is expressed by the percentage of volume and calculated by the following formula (RILEM, 1980):

$$P (\% \text{volume}) = [(m_{sat} - m_{dry}) / (m_{sat} - m_{arch})] * 100$$

where,

m_{sat} : saturated weight (g)

m_{dry} : dry weight (g)

m_{arch} : the weight of the sample in water (g)

Density (D) is the ratio of the mass to the bulk volume of the sample. It is expressed in g/cm^3 and calculated by the following formula (RILEM, 1980):

$$D (g/cm^3) = (m_{dry}) / (m_{sat} - m_{arch})$$

2.1.2 Determination of Drying Rate

Mortar samples of approximately 15-40g with prismatic shapes, were first dried in the oven at 35°C to constant weight. They were weighed (m_{dry}) and then saturated in distilled water under vacuum at 0,132atm (100torr) pressure. Following their weight measurements in saturated state (m_{sat}) they were left for drying under controlled conditions at 25°C and 30 ± 5% relative humidity. The weight loss of the samples was followed by weight measurements (m_{wet}) at certain time intervals such as 15-30-60 minutes, 1-2-4-8-24 hours and 2-3-4-5-6 days subsequently. All weight measurements were recorded with the sensitivity of .0001grams.

The drying rate is expressed as the density of vapor flow rate (g) evaporated from the surface of the sample and it is calculated as a function of average moisture content for each time span versus surface area of the sample by using the following formula (RILEM, 1980):

$$(g) = M / A * t$$

where,

(g) : density of flow rate (kg / m².s)

M : moisture content of the sample (kg) at the time t

A : total surface of the area of the prismatic test specimen (m²)

t : time span (second)

M (moisture content of the sample) is found by the use of dry, wet and saturated weights of samples:

$$M = (m_{wet} - m_{dry}) / (m_{sat} - m_{dry})$$

where,

m_{sat} : saturated weight (kg)

m_{dry} : dry weight (kg)

m_{wet} : wet weight (kg) at a certain time

The results have been expressed in diagrams as the percentage of the weight loss versus time, and density of water vapor flow rate versus time.

2.2 Determination of Basic Mechanical Properties

The determination of mechanical properties by the use of conventional test techniques usually requires test specimens with the minimum dimensions of 50x50x150mm (ASTM C270-80a; RILEM, 1980). In the case of mortars in historic masonry however, it may hardly be possible to obtain samples of such sizes due to the narrow joints, which were rarely over 20-25mm between brick and stone masonry units. Therefore, the determination of compressive strengths was carried out by the use of point load test, by which it is possible to work on relatively smaller samples (ISRM, 1985, Brook, 1985).

For this purpose the lumps of collected samples were cut into pieces with prismatic shapes with the minimum thickness of 20mm. Cutting was done by the use of an electrical sawing machine (DIAMANT BOART-220). Before crushing them in dry and wet state, ultrasonic velocity measurements were done. Point load tests were carried out by using ELE-Point Load Test Apparatus / 770110.

2.2.1 Determination of Modulus of Elasticity (Young's Modulus)

The modulus of elasticity (E_{mod}) is defined as the ratio of stress to strain and shows deformation ability of a material under external forces (Timoshenko, 1970). The modulus of elasticity of mortars in this study was determined by ultrasonic pulse velocity measurements (ASTM D 2845-90; RILEM, 1980). A pulse generating test equipment, PUNDIT*plus*, with its probes, transmitter and receiver of 500kHz, for small sized samples was used. In this method the impulse is imparted to the specimen and, the time required for the ultrasonic waves to traverse the minimum cross section of the test specimen is measured. The velocity of the waves is calculated by using the following formula (RILEM, 1980; ASTM D 2845-90);

$$V = l/t$$

where,

V : velocity (m/s)

l : the distance traversed by the wave (mm)

t : travel time (s)

The modulus of elasticity is then obtained through the density of the specimen and velocity by the following expression (RILEM, 1980).

$$E_{\text{mod}} = D \cdot V^2 (1 + \nu_{\text{dyn}}) (1 - 2\nu_{\text{dyn}}) / (1 - \nu_{\text{dyn}})$$

where,

E_{mod} : modulus of elasticity (GN/m²)

D : density of the specimen (kg/m³)

V : wave velocity (m/sec)

ν_{dyn} : Poisson's ratio

In this equation, Poisson's ratio refers to the ratio of lateral expansion to the longitudinal reduction of the material under compression (Timoshenko, 1970). In relation to the elasticity of different building materials, Poisson's ratio differs from 0.1 to 0.5. Considering the similarities between mortar and lightweight concrete, and other case studies in historic mortars (Berger, 1989; Hidaka *et al.*, 1989; Aoki *et al.*, 1989; Topal 1995; Moropoulou *et al.*, 1997), $\nu_{\text{dyn}} = 0.18$ seemed a reasonable value to be used in Konya mortars.

The calculated value of modulus of elasticity in GN/m² has been expressed in MPa in the related tables and/or diagrams.

2.2.2 Determination of Uniaxial Compressive Strength

By the use of point load test, at first, the uncorrected point load strength index (I_s) of the mortar samples in dry and wet states were calculated using the formula;

$$I_s = P/De^2$$

where,

P : applied load (kN)

De : equivalent core diameter (mm)

Equivalent core diameter (De) is given by the following formula for axial tests, which is suggested for blocks and lumps;

$$De = \sqrt{4A/\pi}$$

where, A is the minimum cross sectional area of the test specimen found by multiplying the width of the test specimen with its thickness.

The size-corrected point load strength, $Is_{(50)}$, is calculated from Is , uncorrected point load strength index, using equivalent core diameter method suggested by Brook (1985) by the following equation;

$$Is_{(50)} = F * Is$$

where F , the size-correction factor which is obtained from De , equivalent core diameter, using the expression;

$$F = (De/50)^{0.45}$$

To obtain uniaxial compressive strength (U.C.S.), it is customary to multiply by $Is_{(50)}$, by a correlation factor 'k' which covers an extremely wide range of values from 8 to 55 in the literature in rock mechanics (Topal, 1995). However, it is also stated that weak rocks give lower 'k' values than those of strong ones. In a recent study carried out by Topal (1999/2000) on weak tuffs, a linear relationship with a relatively high correlation coefficient ($R^2 = 0.92$) has been proposed to calculate the uniaxial compressive strength from $Is_{(50)}$. It is expressed by the following equation;

$$U.C.S. = 10.6471 * Is_{(50)} + 2.4736$$

The values of $Is_{(50)}$ of Konya mortars that are found by point load tests have been converted into uniaxial compressive strengths by the above equation. The results have been given in MPa together with modulus of elasticity values.

2.3 Determination of Raw Material Properties

2.3.1 Determination of Hygroscopic Water, Bound Water and Organic Matter, and Carbonate Content by Weight Loss on Heating

Two sets of powdered samples (of ~1g) were successively heated at the temperatures of 105°C, 550°C and 900°C in porcelain crucibles in the oven. The weight losses measured after heating have been used to calculate the amounts of free water (at

105°C), bound water and organic matter (at 550°C), and carbonate content (at 900°C) in the samples expressed as carbon dioxide content (Walter, 1974).

2.3.2 Proportions of Binder and Aggregate Parts

The aim of the analysis was to determine the proportions of the raw materials used in the mortars, namely, the percentages of binder and aggregate, which form the main components.

Three pieces of each mortar, of 10-15g, crushed into coarser grains, dried, have been weighed (m_{samp}) with the sensitivity of 0.01, and dissolved in 5% hydrochloric acid. Insoluble part was filtered, washed with distilled water, dried and weighed (m_{insol}). Acid soluble and insoluble parts were calculated by the following formulae and expressed as percentages (Jedrzejvska, 1981).

$$\% \text{ insoluble part} = [(m_{\text{samp}} - m_{\text{insol}}) / (m_{\text{samp}})] * 100$$

$$\% \text{ soluble part} = 100 - \% \text{ insoluble part}$$

where,

m_{samp} : dry weight of the sample (g)

m_{insol} : dry weight of insoluble part (g)

2.3.3 Determination of Calcium Oxide and Magnesium Oxide Contents by Volumetric Analysis through Complexometric Titration with Standard EDTA Solution

The aim of the analysis was to make a quantitative estimation about the acid soluble calcium and magnesium oxides (CaO, MgO). Two sets of samples of (about 1g) were first crushed in an agate mortar to finer grains, dried, weighed and dissolved in %5 hydrochloric acid and diluted to 200ml with distilled water. Insoluble parts were filtered. From each of these solutions, 5ml of each sample was taken and titrated with standard EDTA solution. The results were expressed as the percentages of CaO and MgO in the sample.

2.3.4 Determination of Silicon Dioxide, Aluminium Oxide and Iron Oxide Contents by Atomic Absorption Spectroscopy (AAS)

The solutions above were also used for atomic absorption spectroscopy analysis to determine the contents of silicon dioxide (SiO_2), aluminium oxide (Al_2O_3) and iron oxide (Fe_2O_3), which were expressed as their weight percentages in the samples.

2.3.5 Quantitative Determination of Soluble Salt Content by Electrical Conductivity Measurements

The soluble salt content was determined by electrical conductivity measurements. For this purpose approximately 1g of dried and powdered mortar sample is mixed with a known volume of distilled water. The total soluble salt content is determined by the electrical conductivity measurements of the salt extract solutions by using a conductometer (Metrohm AG Herisau, Kondoktometer E382). Percent salt in the sample was calculated by the following formulae (Black, 1965).

$$EC = [(0.0014 * R_{std}) / (R_{ext})] \text{ (mhocm}^{-1}\text{)}$$

where,

EC : electrical conductivity (mhocm⁻¹)

R_{std} : the cell resistance with standard solution (0.01 N KCl)

R_{ext} : the cell resistance with extract solution

$$\% \text{ salt in the sample} = [A * V_{ext}(\text{ml}) / 1000] * [100 / \text{weight of sample (mg)}]$$

where,

A : salt concentration (mg/l) = 640 * EC (mmhos cm⁻¹)

V_{ext} : volume of the extract solution (milliliter : ml)

The extract solutions, after conductivity measurements have been used for qualitative analyses of sulphate (SO₄⁻) anions by spot tests. The reason for this test was to check the existence of gypsum in the binder parts of the mortars.

2.3.6 Pozzolanic Activity Measurements by Electrical Conductivity

For this purpose, fine aggregates, of <125µm size, obtained from sieve analyses have been reacted with saturated calcium hydroxide solution [Ca(OH)₂] at room temperature with the sample/solution ratio of 5g/200ml. The reaction was followed by the measurements of electrical conductivity and checked with the measurements of pH in reaction media. Variation in the conductivity (mS/cm) was followed when the sample was added into the solution and stirred. The fastest reaction occurred within the first two minutes. The difference in measured electrical conductivity (ΔEC in mS/cm) was used to express the pozzolanic activity (pozzolanicity or hydraulicity)

of the material tested. It was proposed that if the ΔEC is over 1.2mS/cm the tested material has good pozzolanicity (Luxan *et al.*, 1989).

2.4 Particle Size Distribution

2.4.1 Particle Size Distribution in the Aggregates of the Mortars

Determination of particle size distribution in aggregate parts was carried out by standard sieving analyses by the using 1000, 500, 250 and 125 μ m sieves of DIN-4188. These sieve sizes correspond to American mesh numbers of 18, 35, 60 and 120 (ASTM E11-70 *in* Holmes and Wingate, 1997). The results were expressed in the percentages of each particle size in the insoluble parts and shown in diagrams.

A visual examination of the aggregates by a stereo microscope was also done. Their colors and shapes are noted as their visual properties. The distinction of their shapes was expressed with the terms such as rounded, semi-rounded, angular, and sub-angular (Tucker, 1991).

2.5 Petrographic Analyses

2.5.1 X-ray Diffraction (XRD) Analyses

These analyses aimed to determine mineralogical composition of the mortars. The analyses were performed on powdered samples of lime binder obtained from relatively soft white lumps by scrubbing. The matrix, which contained both binder and fine aggregates, of <125 μ m and <45 μ m size in diameter, have been examined separately.

The analyses were performed using a Philips type PW1352/20 X-ray diffractometer with Co K_{α} radiation with Ni filter adjusted to 35kV and 14mA.

2.5.2 Thin Section Analyses

The analyses aimed to determine petrographical and mineralogical properties of the mortars. For this purpose the samples were placed into plastic molding boxes of 1.5x3x1cm. They were saturated with the polyester (ESKIM-extra POLYESTER) mixed with accelerator and hardener under vacuum of 0.132atm (100torr) pressure. Following their hardening, the molded samples were removed from boxes and cut

into 1mm slices to be fixed and reduced to 30micron thickness on glass plates. Thin sections of the samples were examined by using NIKON AFX-2A optical microscope equipped with a photographic attachment.

Mineralogical and morphological properties of the binder and aggregates, such as their shape, size and distribution in the matrix and adhesion properties were examined qualitatively in thin sections. The macro porosity properties such as the shape, approximate size and distribution of macropores in the matrix were also examined qualitatively in thin sections.

2.5.3 Scanning Electron Microscopy (SEM) coupled with Energy Disperse Analysis (EDX)

SEM analyses aimed to provide complementary information about the morphology and microstructure of binder and aggregate parts and possible reaction products formed in between. For this purpose carefully broken pieces of about 0.5cm in diameter with at least one flat surface were coated with gold. The instrument used was a JEOL JSM-5400 Scanning Electron Microscope operated at 20kV and coupled with EDX system by which semi-quantitative element analysis could be done. EDX analysis was used in the determination of metal oxides, such as CaO, MgO, SiO₂, Al₂O₃, K₂O, Na₂O *etc.* in the binder and aggregate parts of the mortars.

Finest aggregates were separately examined by EDX using their pellets. The aggregates, of <45µm, were pressed into pellets by 10tons/cm² using a hydraulic pellet machine. The pellets were used for the quantitative analysis of the finest aggregates. SEM micrographs were also taken where possible. The results of SEM and EDX analyses have been evaluated together with the results of XRD, volumetric analyses, and AAS analyses and thin section examinations.

CHAPTER 3

EXPERIMENTAL RESULTS

The results of all experiments have been expressed with the figures, tables and summarised in the following sections.

3.1 Basic Physical Properties of Mortars

3.1.1 Porosity and Density

The porosity and density values of stone and brick masonry mortars have shown some differences in comparison to each other (Figure 3.1-2, Appendix B).

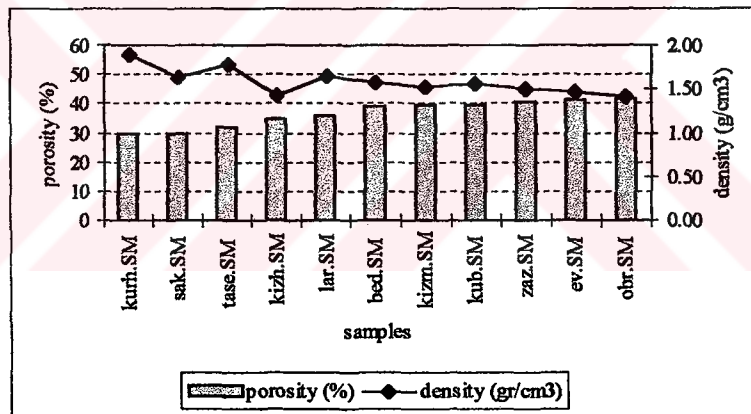


Figure 3.1 Porosity and density of stone masonry mortars

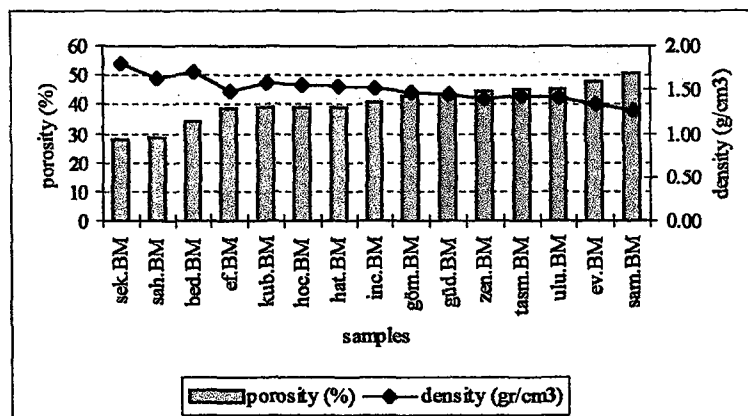


Figure 3.2 Porosity and density of brick masonry mortars

The density of stone masonry mortars varied in the range of $1.39 - 1.85\text{gr/cm}^3$, the average of which was $1.59 \pm 0.15\text{gr/cm}^3$ (Figure 3.1, Appendix L1). In the mortars of brick masonry, this range was in between $1.25 - 1.74\text{gr/cm}^3$ and the average density was $1.50 \pm 0.14\text{gr/cm}^3$ (Figure 3.2, Appendix L2). The porosity values of stone masonry mortars were in the range of $27.36 - 45.88\%$, and the average porosity being $36.91 \pm 5.73\%$. The porosity of the brick masonry mortars varied between $27.81 - 52.26\%$. The average value was $40.71 \pm 6.43\%$.

3.1.2 Drying Rates

The investigation was done by following the loss in the weight of the saturated samples versus time (Figure 3.3). The same data was also used to calculate the density of water vapor flow rate versus time by considering the surface area of the samples (Figure 3.4). A sample of cement repair mortar (tz.CM1) collected from Tahir ile Zühre Mescidi was included in the tests to make a comparison.

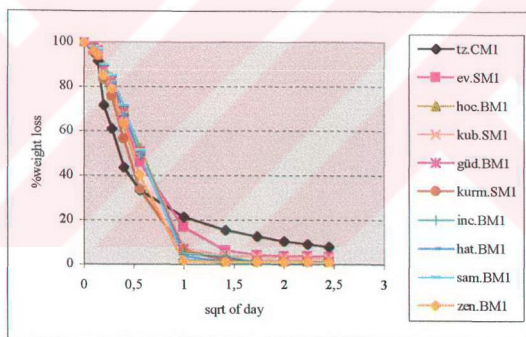


Figure 3.3 Drying rates of mortars by weight loss versus time

Drying rates expressed as percent weight loss showed that the fastest drying occurred at the beginning and almost all samples exhibited a uniform trend in drying. Among the mortars, only the cement repair mortar of Tahir ile Zühre Mescidi appeared to dry relatively slower than the original mortars. All original mortars completely dried within five or six days while cement mortar continued drying (Figure 3.3).

The rate of drying per unit area versus time was lowest again for the cement mortar of Tahir ile Zühre Mescidi in agreement with the results of previous calculations, which were based on the weight loss versus time (Figure 3.4).

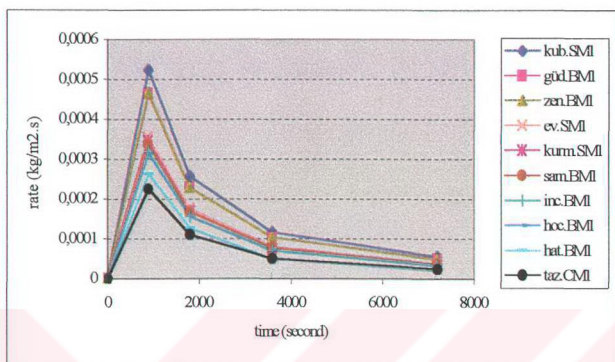


Figure 3.4 Drying rates of the mortars by weight loss versus time and surface area

3.1.3 Porosity and Density of Bricks used in some of the Monuments

The porosity and density of bricks used in the brick masonry were also determined to make comparisons with that of mortars (Figure 3.5-6, Appendix M).

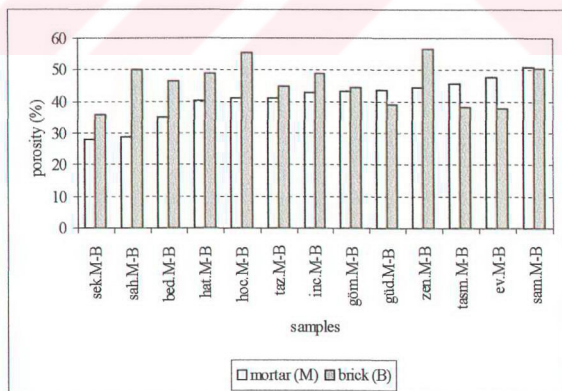


Figure 3.5 Comparison of porosity of the mortars and bricks

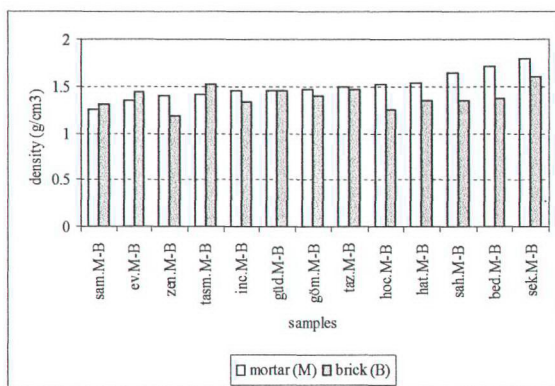


Figure 3.6 Comparison of density of mortars and bricks

The comparisons of physical properties of mortars and bricks indicated that the porosity and density values of the mortars were close to those of bricks used in these monuments (Figure 3.5-6, Appendix M).

3.2 Basic Mechanical Properties of Mortars

Due to the difficulties in obtaining prismatic samples, the mechanical tests had to be carried out on limited number of samples. It was therefore hard to make more precise measurements on the mechanical properties of mortars on the contrary to their physical properties, which could be determined on sufficient number of samples despite their irregular shapes and small sizes.

Modulus of elasticity (E_{mod}) of mortars was determined by ultrasonic pulse velocity (UPV) measurements, and their uniaxial compressive strengths (UCS) by point load tests. Uniaxial compressive strengths were determined on dry and water saturated samples to make estimations about their durability characteristics.

3.2.1 Modulus of Elasticity

Modulus of elasticity (E_{mod}) of stone and brick masonry mortars was in the range of 705.12-8324.72 MPa. The mortars of Kuruçeşme Han (kurh.SM2, kurm.SM1) and Kubadabad Palace (kub.SM) seemed to have relatively higher values of modulus of

elasticity. When the extraordinarily high modulus of elasticity of Kuruçeşme Han mortars were excluded, the rest of the mortars fell in the approximate range of 700-3000MPa (Table 3.1-2, Appendix N1-2).

Table 3.1 Ultrasonic pulse velocity (V), density (D) and modulus of elasticity (E_{mod}) of stone masonry mortars

Sample	V (m/s)	D (kg/m ³)	E.mod. (MPa)
sak.SM1	702,56	1570	714,89
obr.SM1	760,30	1445	780,62
kızım.SM1	790,38	1525	879,98
bed.SM1	797,35	1525	892,92
zaz.SM	868,50	1545	1072,65
ev.SM1	1118,98	1455	1697,44
kub.SM	1288,04	1560	2375,24
kurh.SM2	1792,35	1800	5419,58
kurm.SM1	2166,24	1900	8324,72

Table 3.2 Ultrasonic pulse velocity (V), density (D) and modulus of elasticity (E_{mod}) of brick masonry mortars

Sample	V (m/s)	D (kg/m ³)	E.mod. (MPa)
taşm.BM1	729,51	1433	705,12
ev.BM1	809,12	1360	822,47
ulu.BM1	808,77	1450	878,42
hat.BM2	788,82	1560	894,41
bed.BM1	911,71	1663	1274,65
sam.BM	1056,46	1280	1328,29
inc.BM1	986,33	1473	1338,80
zen.BM1	1042,45	1368	1374,09
güd.BM1	1180,20	1485	1904,80
kub.BM2	1192,43	1720	2286,91
hoc.BM	1275,68	1545	2321,73
sah.BM1	1449,26	1545	2992,97

As the values of modulus of elasticity showed, there was no possibility to make obvious distinctions between the modulus of elasticity of stone and brick masonry mortars as it was done for their physical properties. Modulus of elasticity values of

mortars was variable regardless of their use either in stone or brick masonry (Table 3.1-2, Appendix N1-2).

3.2.2 Uniaxial Compressive Strengths

Uniaxial compressive strength measurements were carried out on dry and water-saturated mortar samples. The strength values in dry state (Table 3.3-4, Appendix O1) have been used for the evaluation of mechanical properties of the mortars. The strength values of water-saturated samples (Table 3.3-4, Appendix O2), together with strength values in dry state were used for the estimation of durability characteristics (Table 3.5). Uniaxial compressive strengths cover a wide range, such that 3.34-18.32MPa. Within this range, the mortars of Kuruçeşme Han, Kubadabad Palace and Evhadeddin Kirmani Tomb seemed to have relatively higher values than the rest. When those high values are excluded, the optimum range was reduced to 3.5-8.0MPa (Table 3.3).

Table 3.3 Uniaxial compressive strength (UCS) of stone masonry mortars in dry and wet states

Sample	U.C.S. (dry) (MPa)	U.C.S. (wet) (MPa)
sak.SM1	3,34	<i>n.d.</i>
zaz.SM2	3,81	<i>n.d.</i>
obr.SM1	3,89	<i>n.d.</i>
kızım.SM1	4,39	<i>n.d.</i>
bed.SM1	4,78	<i>n.d.</i>
zaz.SM1	5,15	<i>n.d.</i>
kub.SM2	8,00	6,94
kub.SM1	11,97	8,07
ev.SM1	14,80	<i>n.d.</i>
kub.SM3	17,18	12,46
kurm.SM1	18,32	17,93
<i>n.d. : not determined</i>		

Table 3.4 Uniaxial compressive strength (UCS) of brick masonry mortars in dry and wet states

Sample	U.C.S. (dry) (MPa)	U.C.S. (wet) (MPa)
hat.BM2	3,52	3,07
ev.BM1	3,72	<i>n.d</i>
taşm.BM1	3,75	<i>n.d</i>
zen.BM1	4,22	3,64
ulu.BM1	4,24	3,65
sam.BM1	4,78	4,19
bed.BM1	4,84	3,74
hat.BM1	5,44	5,30
inc.BM1	5,62	4,94
sam.BM2	6,05	4,42
hoc.BM2	6,52	3,49
güd.BM1	6,61	4,59
sah.BM1	6,80	<i>n.d</i>
hoc.BM1	7,90	6,09
kub.BM2	8,76	8,59

n.d.: not determined

Uniaxial compressive strengths in wet state were in the range of 3.07-17.93MPa. Among those, the mortars of Kuruçeşme Han and Kubadabad Palace had relatively higher values. When they were excluded, the range was reduced to 3.07-6.09MPa (Table 3.4).

As happened in the modulus of elasticity of the same mortars, it was not possible to make a clear distinction between stone and brick masonry mortars with respect to their uniaxial compressive strengths. That is, the strength values of the mortars were variable regardless of the masonry they were used (Table 3.3-4).

There was a direct relationship between the measured ultrasonic velocity and modulus of elasticity. A similar correlation could also be found between uniaxial compressive strength and modulus of elasticity. The increase in the uniaxial compressive strength was proportional to the increase in the modulus of elasticity of mortars (Figure 3.7).

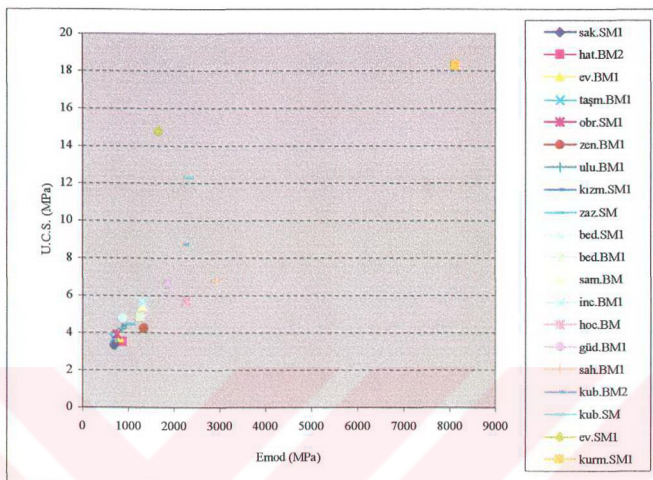


Figure 3.7 Correlation between modulus of elasticity (E_{mod}) and uniaxial compressive strength (UCS) of mortars

3.3 Durability Characteristics of Mortars

Durability estimations have been done by the use of two different durability factors proposed by Winkler (1986) and Rodrigues & Jeramias (1990) respectively, which were developed for the durability of rocks.

The first durability factor, D1, is given by the following equation;

$$D1 = [(UCS_{wet}) / (UCS_{dry})] * 100$$

where;

UCS_{wet} : uniaxial compressive strength in wet state

UCS_{dry} : uniaxial compressive strength in dry state

By the use of this equation, Winkler classifies the durability of rocks from excellent to poor one in the following ranges;

D1: 100-80 excellent durability.

D1: 80-70 very good to good.

D1: 70-60 fair.

D1: 60-50 poor durability.

According to Winkler's equation, almost all mortars of Konya monuments fell in the range of 'very good to excellent durability' (Table 3.5).

Table 3.5 Durability characteristics of stone and brick masonry mortars

Sample	P % volume	UCS (dry) (MPa)	UCS (wet) (MPa)	Is(50)dry (MPa)	D1*	D2**
kub.SM1	42,76	11,97	8,07	0,89	67,38	0,02
kub.SM2	43,82	8,00	6,94	0,52	86,69	0,01
kub.SM3	33,18	17,18	12,46	1,38	72,51	0,04
kurm.SM1	22,71	18,32	17,93	0,17	97,85	0,01
kub.BM2	34,05	8,76	8,59	0,59	98,08	0,02
sam.BM1	49,84	4,78	4,19	0,22	87,68	0,01
sam.BM2	49,98	6,05	4,42	0,34	73,01	0,01
zen.BM1	45,33	4,22	3,65	0,16	86,37	0,01
hoc.BM1	40,89	7,90	6,09	0,51	77,17	0,01
hoc.BM2	37,47	6,52	3,49	0,10	53,52	0,01
bed.BM1	35,12	4,84	3,74	0,22	77,20	0,01
hat.BM2	39,65	3,52	3,07	0,27	87,32	0,01
inc.BM1	42,46	5,62	4,94	0,30	87,98	0,01
ulu.BM1	45,82	4,24	3,65	0,30	86,28	0,01
güd.BM1	42,60	6,61	4,59	0,12	69,45	0,01

* Equation by Winkler : $UCS_{wet} / UCS_{dry} * 100$ (1986)

** Equation by Rodrigues & Jeremias: $Is_{(50)dry} / \%P$ (1990)

In the second classification, proposed by Rodrigues and Jeremias (1990), durability of rocks subjected to soluble salt crystallization cycles was determined by the use of their size-corrected point load strength index [$Is_{(50)dry}$], porosity (by %volume) and their swelling strain (sw_{str}). Durability factor, D2, is thus expressed by the following formula;

$$D2 = Is_{(50)dry} / (P + sw_{str})$$

where;

$Is_{(50)dry}$: size-corrected point load strength.

%P : % porosity.

sw_{str} : swelling strain of the material.

In the durability estimation of Konya mortars however, the swelling strain (sw_{str}) was omitted, since it was too small and difficult to measure.

In this equation of Rodrigues and Jeremias (1990) suggested that the rocks having durability factor over two can be regarded durable especially in terms of salt crystallization cycles. The results have shown that all the mortars have the D2 values much lower than two (0.01-0.04) indicating very poor or no durability to salt crystallisation cycles (Table 3.5).

3.4 Raw Material Properties of Mortars

3.4.1 Soluble Salt Content

The quantitative determination of soluble salt content of the mortars discerned two groups (Figure 3.8). The first group of mortars belonging to Kızılören Han, Sahip Ata Hanikahı, Sakahane Mescidi, Şekerfuruş Mescidi, Eflaki Dede Türbesi, Zazadin Han, Hoca Hasan Mescidi and Obruk Han contained relatively high amount of soluble salt content in the range of 4.62-5.80%. The rest of the mortars, which formed the second group, were easily distinguished from the first group with their smaller salt contents. The range of salt content in this group varied between 0.30-3%.

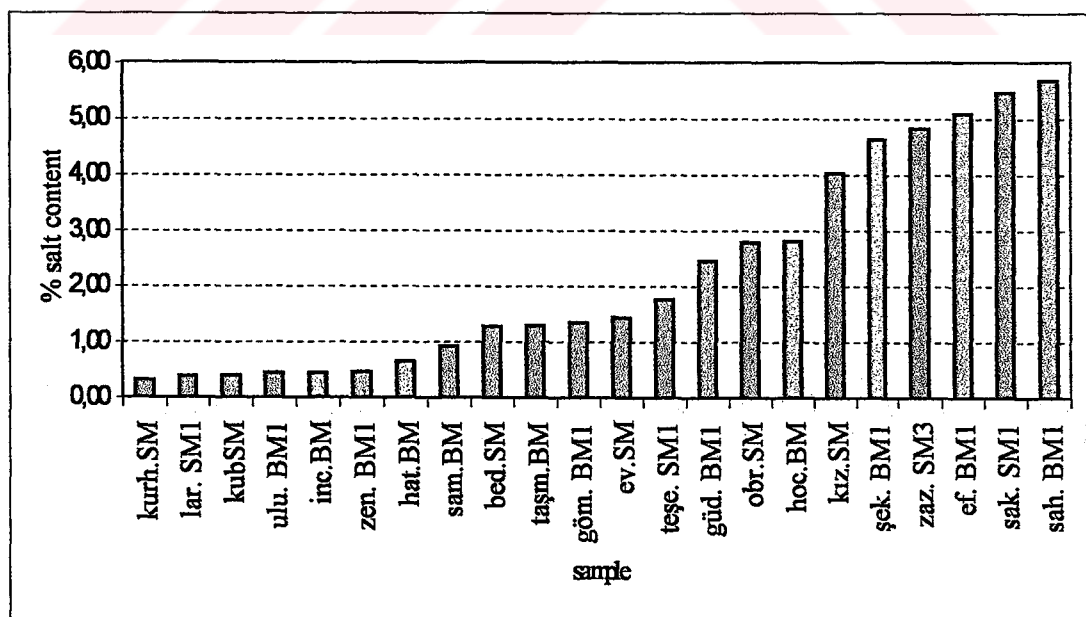


Figure 3.8 Soluble salt content of stone and brick masonry mortars

The results of salt content determination will be evaluated with the results of other analyses. Only the mortar of Şekerfuruş Mescidi, the binder of which contained gypsum was excluded from these evaluations.

3.4.2 Hygroscopic Water, Bound Water and Organic Matter, and Carbonate Contents

Quantitative determination of hygroscopic water (adsorbed water), water in hydraulic compounds (structurally bound water) together with possible organic matter and carbonate content were estimated roughly by following the weight loss at the temperatures of 105°C, 550°C, and 900°C (Walter, 1974) (Table 3.6). The evaluation of the results of these analyses has been done by the following considerations;

Table 3.6 Hygroscopic water (105°C), bound water and/or organic matter (550°C), and carbonate content (900°C) in stone and brick masonry mortars by weight loss (%) observed on heating

Sample	105°C	550°C	900°C
kub.SM	0.88	3.82	22.67
ev.SM	0.84	5.56	20.45
bed.SM1	0.56	3.91	22.14
taşe.SM1	0.37	2.83	21.56
taz.SM	1.44	6.04	20.66
sak.SM1	0.96	5.49	23.11
kurm.SM	0.18	6.53	41.18
kızım.SM	2.51	7.81	20.80
zaz.SM	0.69	3.33	26.21
obr.SM	1.46	7.08	34.73
kub.BM	0.94	2.81	27.24
ev.BM	0.30	4.28	26.61
bed.BM	0.25	2.15	24.94
taşm.BM	0.31	3.49	22.90
taz.BM	0.96	3.81	25.54
sam.BM	0.21	3.24	28.88
sah.BM1	0.97	5.55	22.61
zen.BM1	0.41	3.88	23.29
hoc.BM	0.41	3.22	21.34
göm.BM1	0.29	2.38	22.51
hat.BM	0.43	3.49	19.39
ef.BM1	0.94	7.05	25.81
inc.BM	0.68	5.27	22.60
ulu.BM1	0.29	3.77	24.79
güd.BM1	0.83	4.78	29.62

The losses at 105°C varied in the approximate range of 0.18-1.0% and rarely exceeded 1% as the water content of the mortars of Kızılören Han, Obruk Han and Tahir ile Zühre Mescidi (1.44 - 2.51%).

The losses at 550°C were generally variable between 2-6%. However, the losses at this temperature exceeded 6% in the mortars of Eflaki Dede Tomb, and Kuruçeşme, Kızılören and Obruk Hans (Table 3.6).

The weight losses at 900°C were much more variable than the losses at 105°C and 550°C. The variation range is 19.30-30% (Table 3.6). The highest loss in Kuruçeşme mortars (41.18%) was due do dolomite aggregates in addition to lime.

Thermogravimetric analysis (TGA) carried out in the white lump belonging to the binder of Kubadabad Palace mortar revealed that it was re-carbonated slaked lime since it calcined at 728°C (Bakolas *et al.*, 1995) other than being limestone aggregate which calcines at 900°C (Figure 3.9).

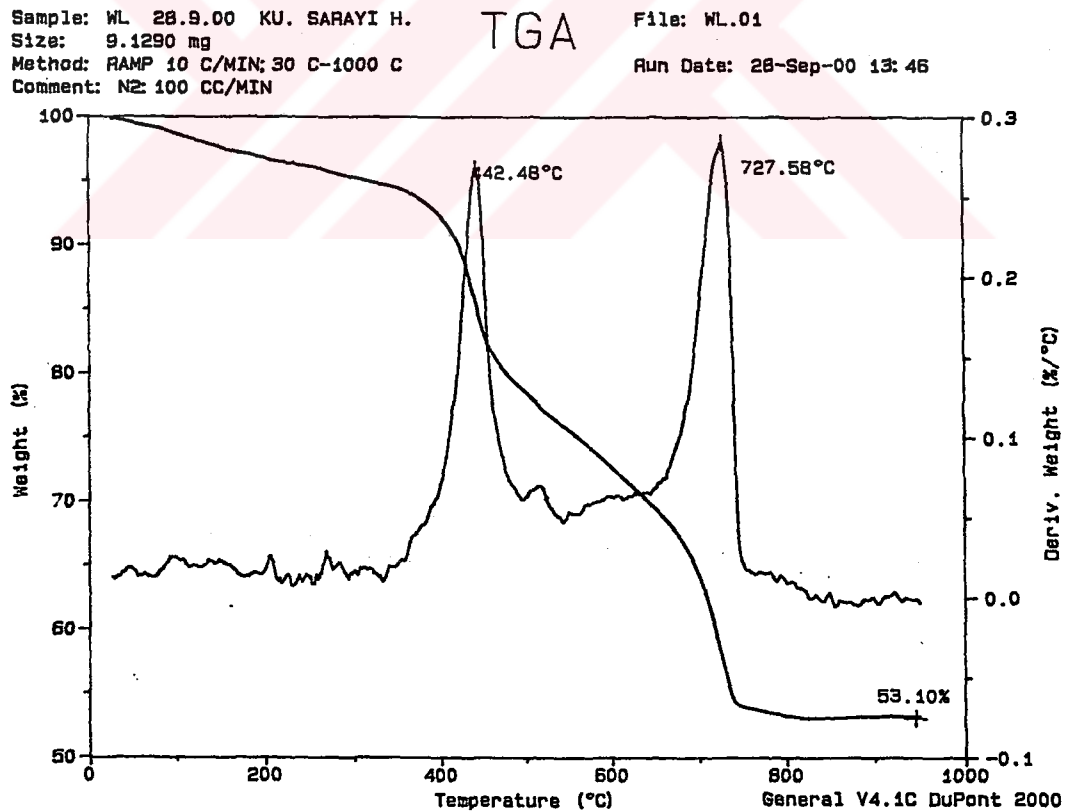


Figure 3.9 Thermogravimetric analysis (TGA) of the white lump of Kubadabad Palace mortar

Excluding the mortars of Obruk Han, which contained limestone aggregates, the weight losses at 900°C therefore can be counted for carbonate content for the rest of mortars belonging to lime binder. In the same analysis another peak at 442°C indicated the likely presence of an organic additive, if it did not belong to the bound water in some possible silicates which could be mixed deliberately.

3.4.3 Binder and Aggregate Proportions

The amounts of carbonated lime (CaCO_3) dissolved in acid (45%-70) indicated that high amount of lime was used in both stone and brick masonry mortars. The average content of carbonated lime in stone masonry mortars was 57.67% and it was 62.08% in brick masonry mortars (Figure 3.10-11, Appendix P1-2)

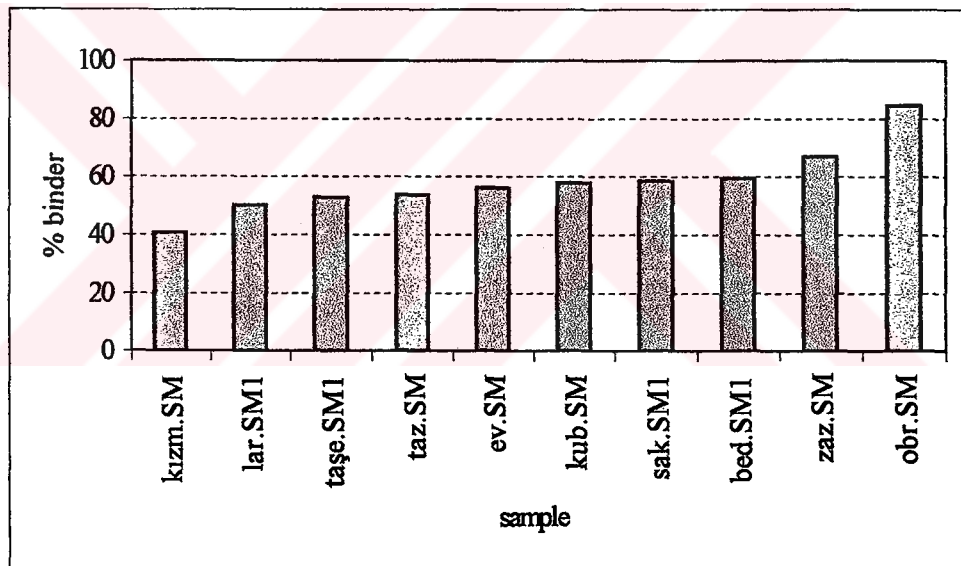


Figure 3.10 Binder content of stone masonry mortars

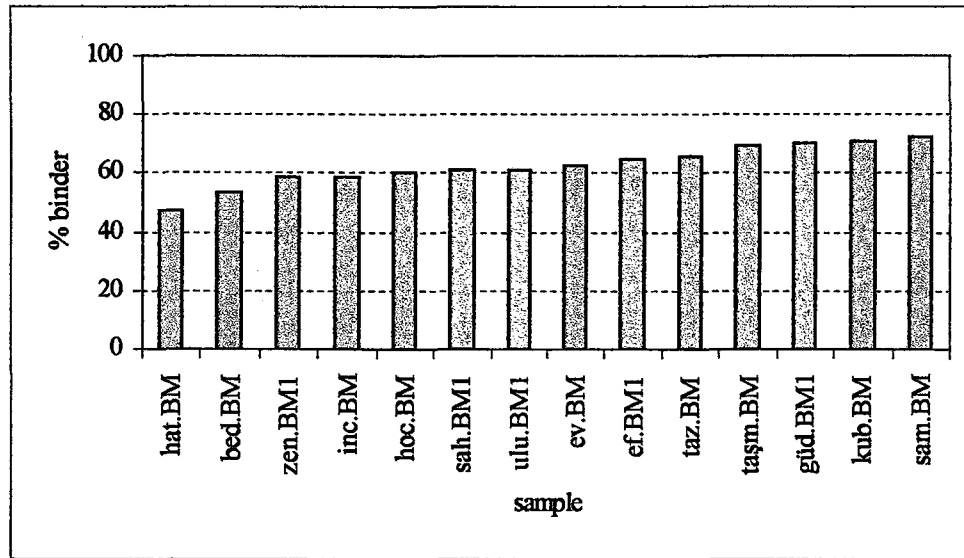


Figure 3.11 Binder content of brick masonry mortars

Due to its high content of dolomitic aggregates, which was proved by XRD and SEM-EDX analyses, the percentage of binder and aggregate parts of Kuruçeşme Han mortars could not be determined by the same analyses. 95% of the mortar of this han was dissolved in hydrochloric acid leaving a small amount of insoluble substance.

The mortar of Şekerfuruş Mescidi on the other hand, contained gypsum, which was also proved by XRD and SEM-EDX analyses. Therefore, the mortars of Kuruçeşme Han and Şekerfuruş Mescidi were not included in the evaluation of lime mortars.

3.4.4 Particle Size Distribution in Aggregate Parts

Classification of aggregates according to the grain size (Norton, 1997) can be made as follows;

BS	ASTM
Gravel : 60 - 2mm	Gravel : 100 - 5mm
Sand : 2 - 0.06mm (2000 - 60 μ m)	Sand : 5 - 0.08mm (5000 - 80 μ m)
Silt : 0.06 - 0.002mm (60 - 2 μ m)	Silt : 0.08 - 0.002mm (80 - 2 μ m)
Clay : <0.002mm (<2 μ m)	Clay : <0.002mm (<2 μ m)

According to those standards the aggregates of Konya mortars can be defined as medium and fine size aggregates.

The coarse aggregates ($>1000\mu\text{m}$) of Akşehir mortars (Güdük Minareli Mescid, Ulucami and Taşmedrese) exceed the limits for sand size reaching 4-5mm diameter which put them in the gravel size.

The mortars examined can be divided into three groups with respect to the majority of fine ($<250\mu\text{m}$), medium ($250-500\mu\text{m}$) and coarse ($>500\mu\text{m}$) aggregates found in them (Figure 3.12-14; Appendix P1-2);

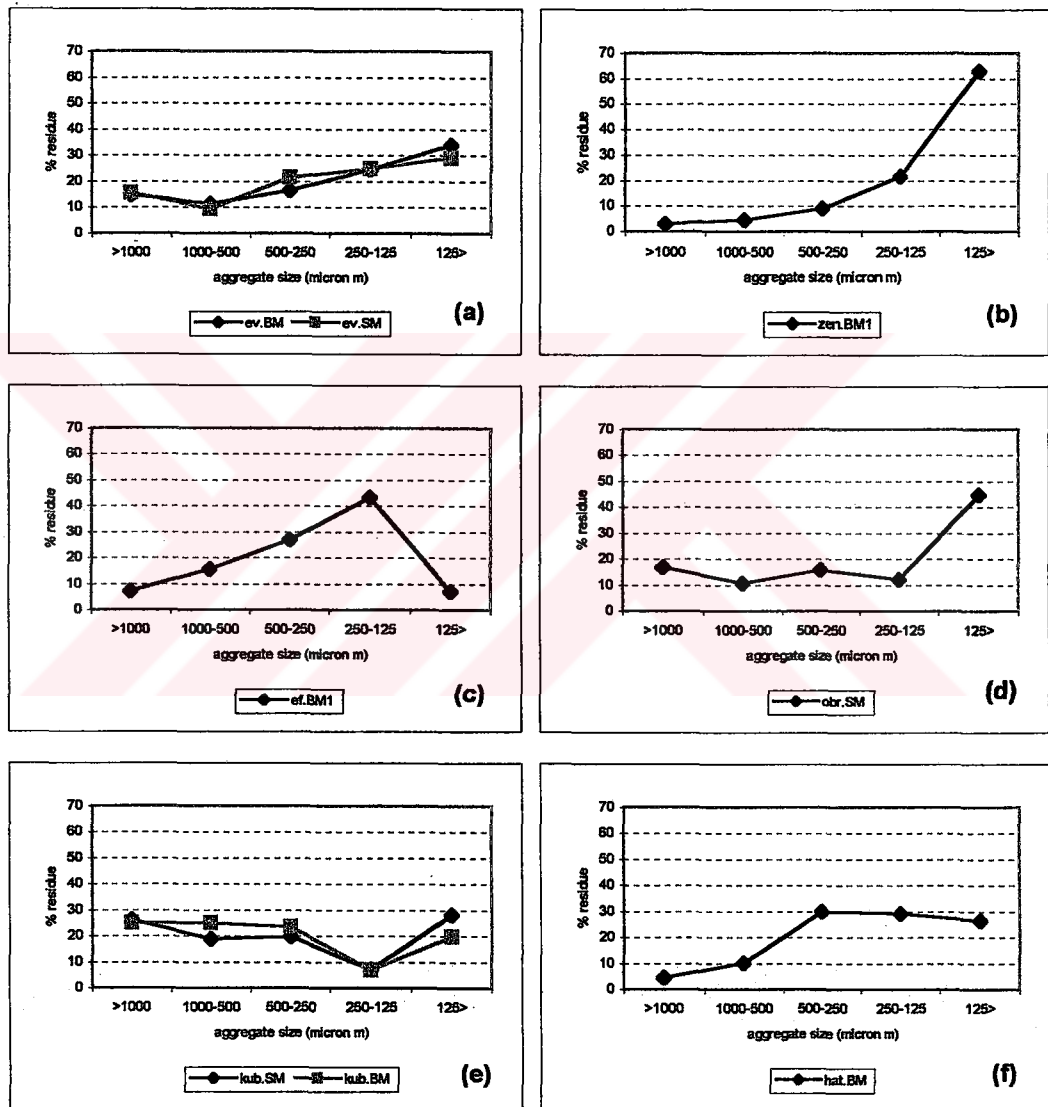


Figure 3.12 Mortars containing mainly fine aggregates

In the second group, the aggregates of medium size (retained on $250\mu\text{m}$ sieve) have formed the major portion of the sand particle in the mortars of Şekerfuruş Mescidi (şek.BM1), Hoca Hasan Mescidi (hoc.BM1), the minaret of Sahip Ata Mosque

sam.BM) and Hanikah (sah.BM1), the tombs of Gömeç Hatun (göm.BM1) and Bedreddin Gühertaş (bed.BM-bed.SM), Tahir ile Zühre Mescidi (taz.BM-taz.SM), the minarets of İnce Minareli Medrese (inc.BM) and Larende Gate (lar.SM1). Fine (<250 μ m) and coarse aggregates (>500 μ m) were in minor amounts (Figure 3.13a-h).

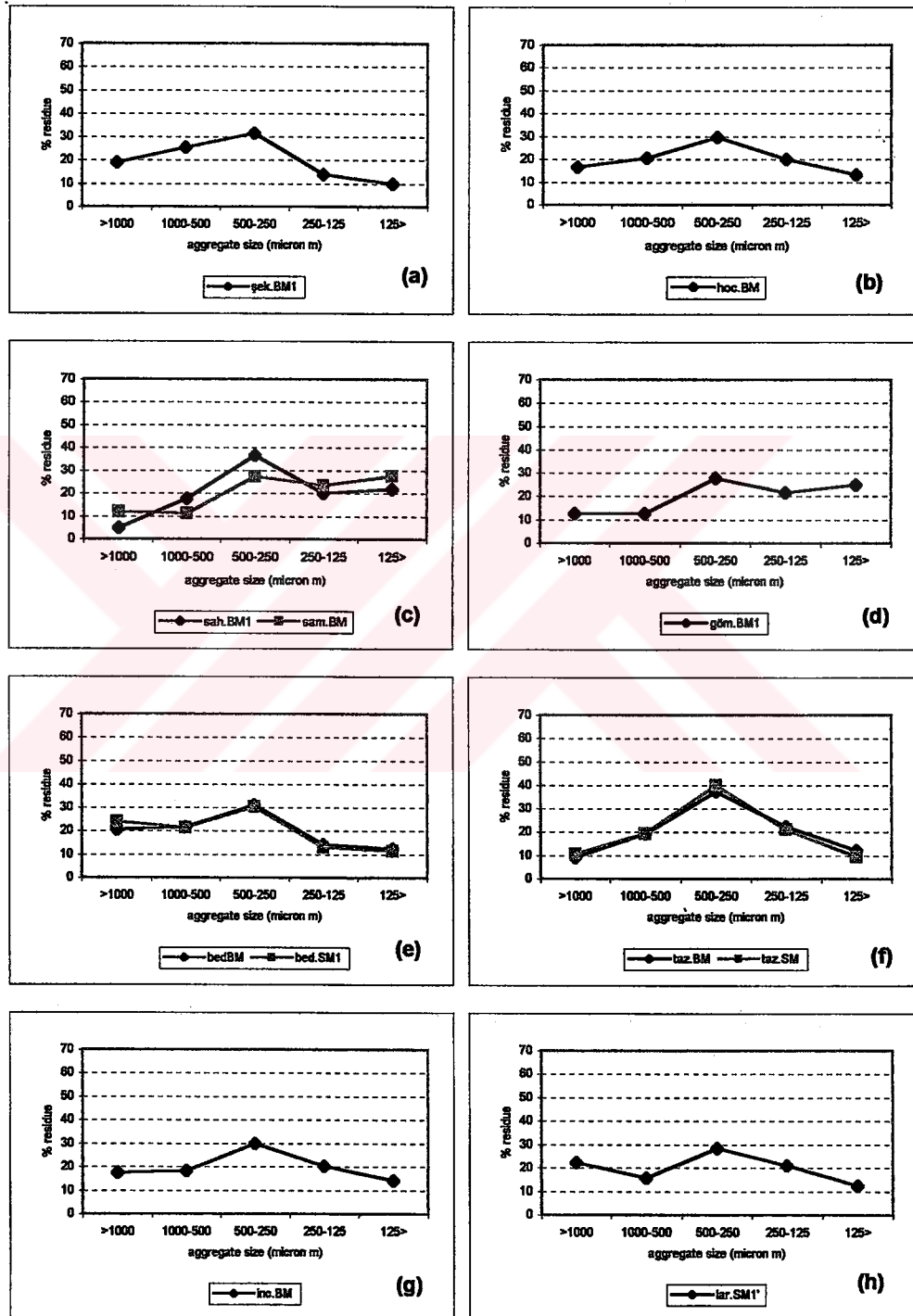


Figure 3.13 Mortars containing mainly medium sized aggregates

In the last group, coarse aggregates ($>500\mu\text{m}$ size) have formed the major part of the sand particle in the mortars of Sakahane Mescidi (sak.SM2), Zazadin Han (zaz.SM), Kızılören Han (kızh.SM) and the mescid (kızm.SM2), Taşmedrese (taşe.SM1) and the minarets of Taşmedrese Mosque (taşm.BM2), Güdük Minareli Mescid (güd.BM2) and Ulucami (ulu.BM2). Medium and fine aggregates were in minor amounts (Figure 3.14a-h).

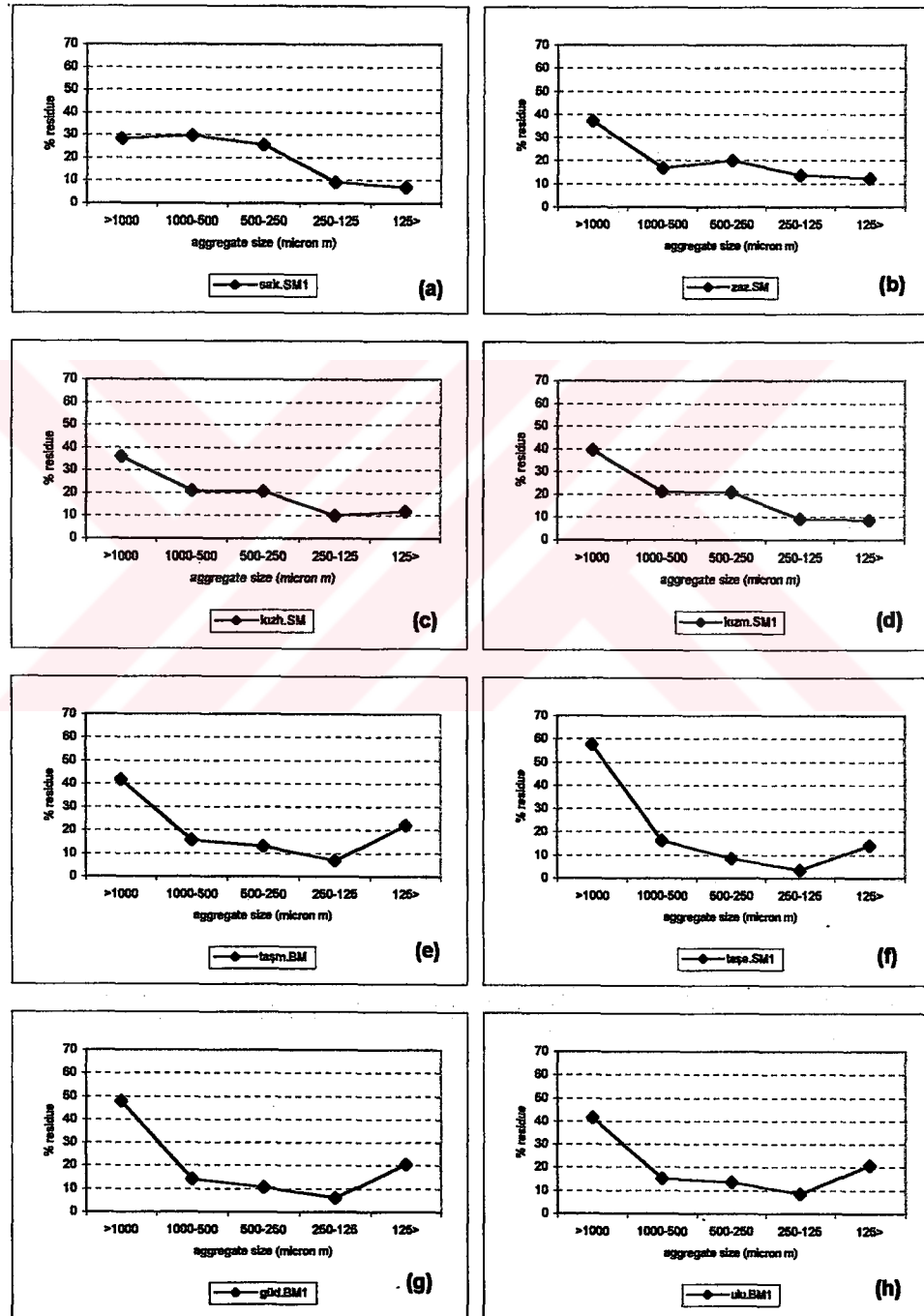


Figure 3.14 Mortars containing mainly coarse aggregates

3.4.5 Pozzolanic Activity Estimation in the Aggregate Parts

Pozzolanic activity estimations were performed for the fine aggregates (of <math><250\mu\text{m}</math> size in diameter) of mortars from the monuments. According to the classification of pozzolanicity (or hydraulicity) suggested by Luxan *et al.*, (1989) the pozzolanas having the values of ΔEC over 1.2mS/cm were considered as good pozzolanas. In the same classification the values between 0.4 - 1.2mS/cm indicate variable pozzolanicity and the materials having ΔEC values less than 0.4mS/cm were considered non-pozzolanic materials. Based on this classification the majority of the mortar aggregates showed good pozzolanicity (Figure 3.15).

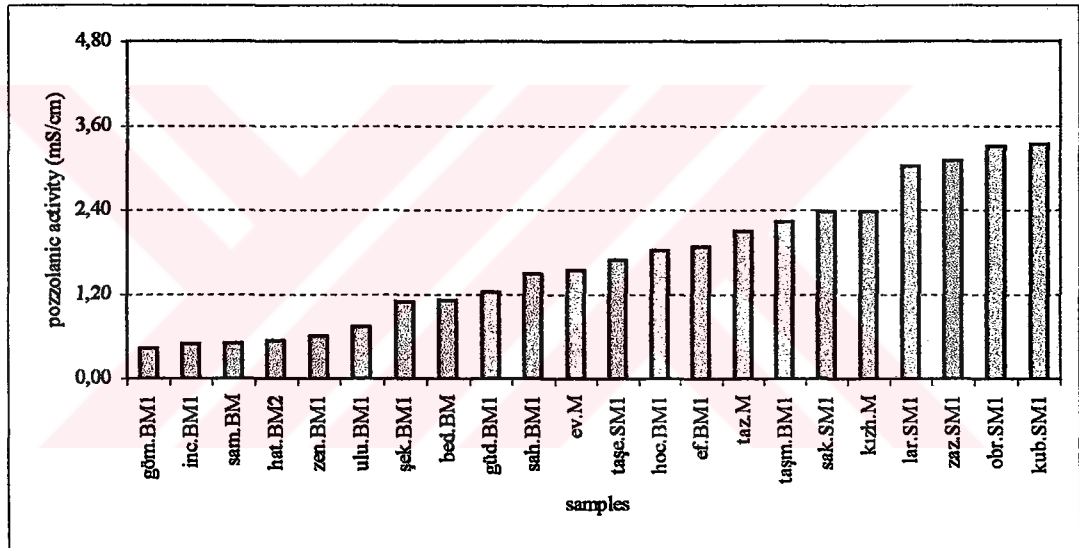


Figure 3.15 Pozzolanic activity estimations in the fine aggregates of mortars

The mortar aggregates of Şekerfuruş Mescidi, Gömeç Hatun and Bedreddin Gühertaş Tombs, the minarets of Sahipata Mosque, Zenburi Mescidi, İnce Minareli Medrese, Hatuniye Mescidi and Ulucami, showed variable pozzolanicity (Figure 3.15).

3.4.6 Chemical Composition of Acid Soluble Parts

Determination of acid soluble CaO and MgO contents were done through volumetric analysis by complexometric titration with standard EDTA solution. Other metal oxides, such as SiO₂, Al₂O₃ and Fe₂O₃ were determined by atomic absorption spectroscopy (AAS). The results of the analyses have been presented in Table 3.7 and Appendix R1-2)

Except the mortars of Kuruçeşme Han, magnesium oxide content found in the mortars was in the range of 0.1-2% (Table 3.7). This indicated that, high-calcium lime was used in the mortars of Konya Monuments. High magnesium content of Kuruçeşme Han was due to its dolomitic aggregates dissolved completely during acid treatment. The thin section and the XRD results will support this later (Figure 3.29). The binder of this mortar was also high-calcium lime as indicated by the CaO and MgO amounts in Table 3.7 showing also the composition of the sum of the dolomite aggregates and the high calcium lime binder.

Table 3.7 Metal oxide contents in acid soluble part, and cementation index (CI) of stone and brick masonry mortars

Sample	EDTA Analysis		AAS Analysis			CI
	%CaO	%MgO	%SiO ₂	%Al ₂ O ₃	%Fe ₂ O ₃	
kub.SM	29,87	0,93	1,27	1,13	1,62	0,20
ev.SM	29,20	1,12	0,30	0,95	0,86	0,10
bed.SM1	30,21	2,34	0,62	0,05	0,66	0,07
sak.SM1	28,56	0,74	0,11	0,48	0,19	0,03
taş.SM1	27,47	0,07	0,37	0,91	1,45	0,11
lar.SM1	32,12	2,43	0,63	1,01	0,84	0,10
kurh.SM	38,42	14,87	0,11	0,32	0,00	0,01
kızım.SM	20,84	0,27	0,77	1,55	0,74	0,20
zaz.SM	36,09	0,20	0,35	0,27	0,28	0,04
obr.SM	39,72	0,38	0,30	0,96	0,38	0,05
taz.SM	27,60	0,25	0,42	0,45	0,20	0,07
kub.BM	39,77	1,19	0,69	0,76	1,13	0,09
sah.BM1	30,41	0,81	0,13	0,57	0,35	0,04
sam.BM	39,76	0,87	0,67	0,94	0,54	0,08
zen.BM1	31,39	0,53	0,11	0,38	0,74	0,04
ev.BM	29,68	1,12	0,24	0,74	0,79	0,06
şek.BM1	25,06	0,07	0,11	0,37	0,19	0,03
hoc.BM	29,33	0,26	0,35	0,56	0,26	0,06
göm.BM1	29,89	0,20	0,31	0,47	0,24	0,05
bed.BM	28,53	1,58	0,21	0,47	0,62	0,05
hat.BM	26,12	0,87	0,21	0,00	0,25	0,03
ef.BM1	33,08	1,28	0,11	0,74	0,57	0,04
inc.BM	30,31	0,14	0,31	0,27	0,31	0,04
taşm.BM	31,66	0,00	0,55	0,90	1,49	0,11
ulu.BM1	35,43	0,27	0,43	0,91	1,51	0,09
güd.BM1	41,74	0,00	1,05	0,69	1,27	0,11
taz.BM	33,80	0,27	0,53	0,52	0,14	0,06

3.5 Mineralogical Properties of Mortars

3.5.1 Thin Section Analyses

The analyses performed on polished thin sections showed that the slaked lime used in the mortars has carbonated into micritic calcite crystals. This was recognized best in the white lumps that were the previous slaked lime lumps not mixed with the aggregates. In addition to white lumps, calcitic aggregates were also found in some samples. The distinction between white lumps and limestone aggregates in thin sections was done by their boundaries with the matrix. While limestone aggregates, which were composed of sparitic calcite crystals appeared with clearly visible boundaries, white lumps did not well-defined edges (Figures 3.16-19). In thin sections, it was observed that large pores were present and the cracks were sealed by the re-crystallisation of calcite minerals (Figures 3.20-21). Very fine opaque minerals, which were proved to be of opal later, perfectly mixed with lime binder that carbonated into micritic calcite were also noticed in almost all thin sections of mortar samples.

In spite of the variations in the types of aggregates, quartz, feldspars (Figures 3.22-23) and biotite (Figures 3.24-25) were the most common minerals in the aggregates. In addition to these, metamorphic rock fragments and sandstone aggregates were also frequently observed in the thin sections of the mortar samples (Figures 3.26-27).

Thin section analyses also revealed that almost all aggregates were with angular shapes. The exception to these was the mortar aggregates of Akşehir monuments, Taşmedrese and the Minaret of its Mescid, the minaret of Güdük Minareli Mescid and Ulucami. The coarse aggregates of these mortars were round shaped and relatively larger sized (up to 5-6mm in diameter). They consisted of metamorphic rock fragments (Figure 3.26).

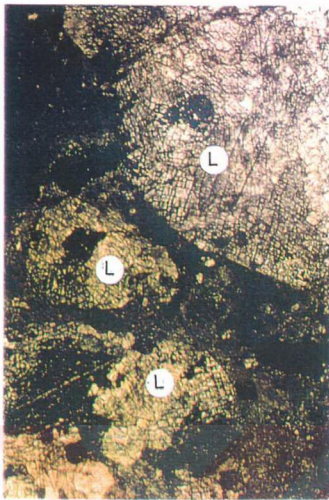


Figure 3.16 Sparitic limestone aggregate in Obruk Han mortar (obr.SM1) L: limestone

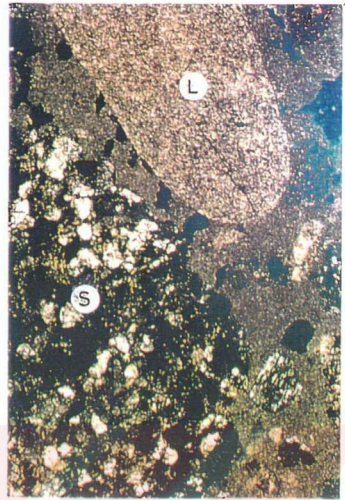


Figure 3.17 Sparitic limestone and sandstone fragments in Kubadabad Palace mortar (kub.BM2) L: limestone S: sandstone

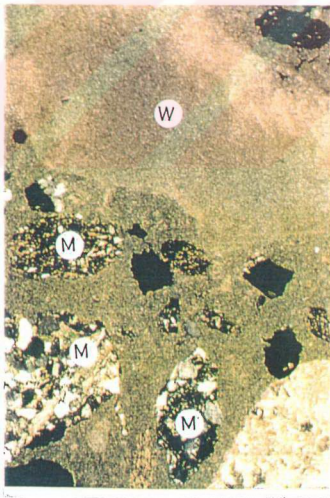


Figure 3.18 White lump and metamorphic rock fragments in Kubadabad Palace mortar (kub.BM1) W: white lump M: metamorphic rock fragment

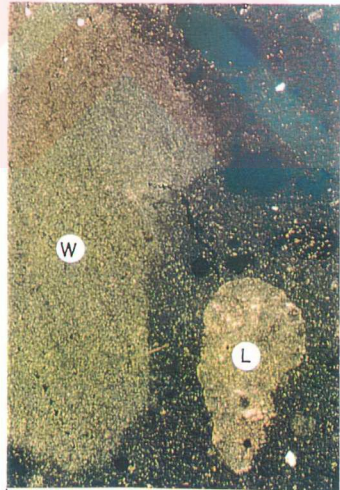


Figure 3.19 Distinction between a white lump and a limestone aggregate in Kubadabad Palace mortar (kub.SM6) W: white lump L: limestone aggregate

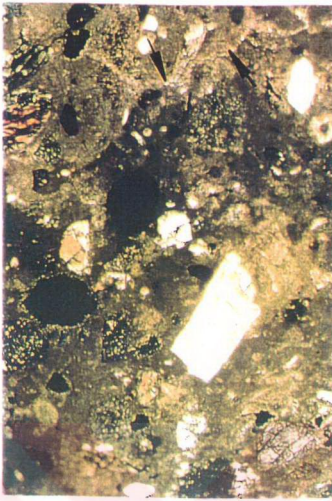


Figure 3.20 Sealing of fine cracks by re-crystallization of micritic calcite and large pores in Zazadin Han Mortar (zaz.SM1)

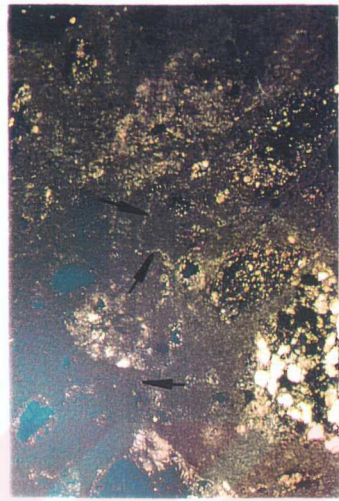


Figure 3.21 Re-crystallization at the fine cracks and large pores in the matrix of Kubadabad Palace mortar (kub.SM4)

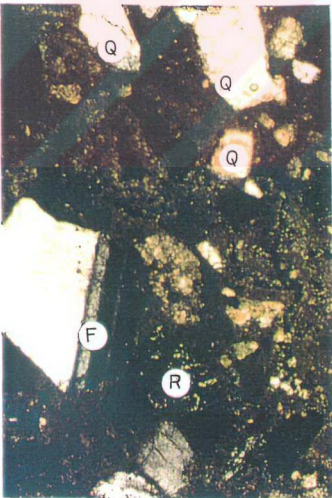


Figure 3.22 Quartz, feldspar and rock fragments in the mortar of Bedreddin Gühertaş Tomb (bed.BM2) Q: quartz F: feldspar R: rock fragment

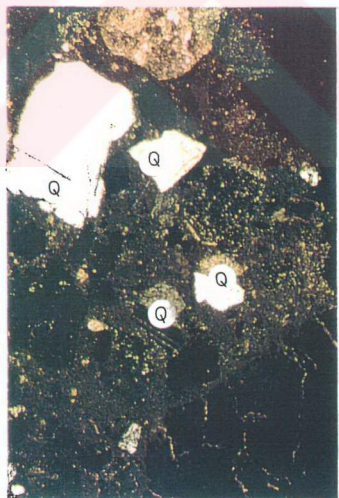


Figure 3.23 Quartz and feldspars in the mortar of Hoca Hasan Mescidi (hoc.BM2) Q: quartz F: feldspar

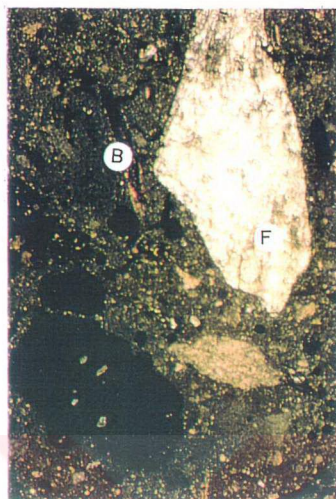


Figure 3.24 Biotite and feldspars in the mortar of Sakahane Mescidi (sak.SM1)
B: biotite F: feldspar



Figure 3.25 Abundant presence of biotite in the mortar of Zenburi Mescidi (zen.BM1)



Figure 3.26 Metamorphic rock fragments in Taşmedrese mortar (teşe.SM1) M: metamorphic rock fragment

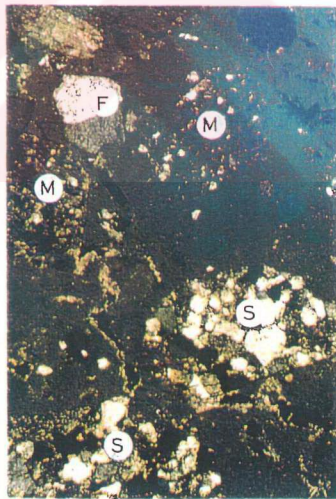


Figure 3.27 Metamorphic rock fragments, sandstone and feldspars in Kubadabad Palace mortar (kub.SM6)
M: metamorphic rock fragment
S: sandstone F: feldspar

3.5.2 X-ray Diffraction (XRD) Analyses

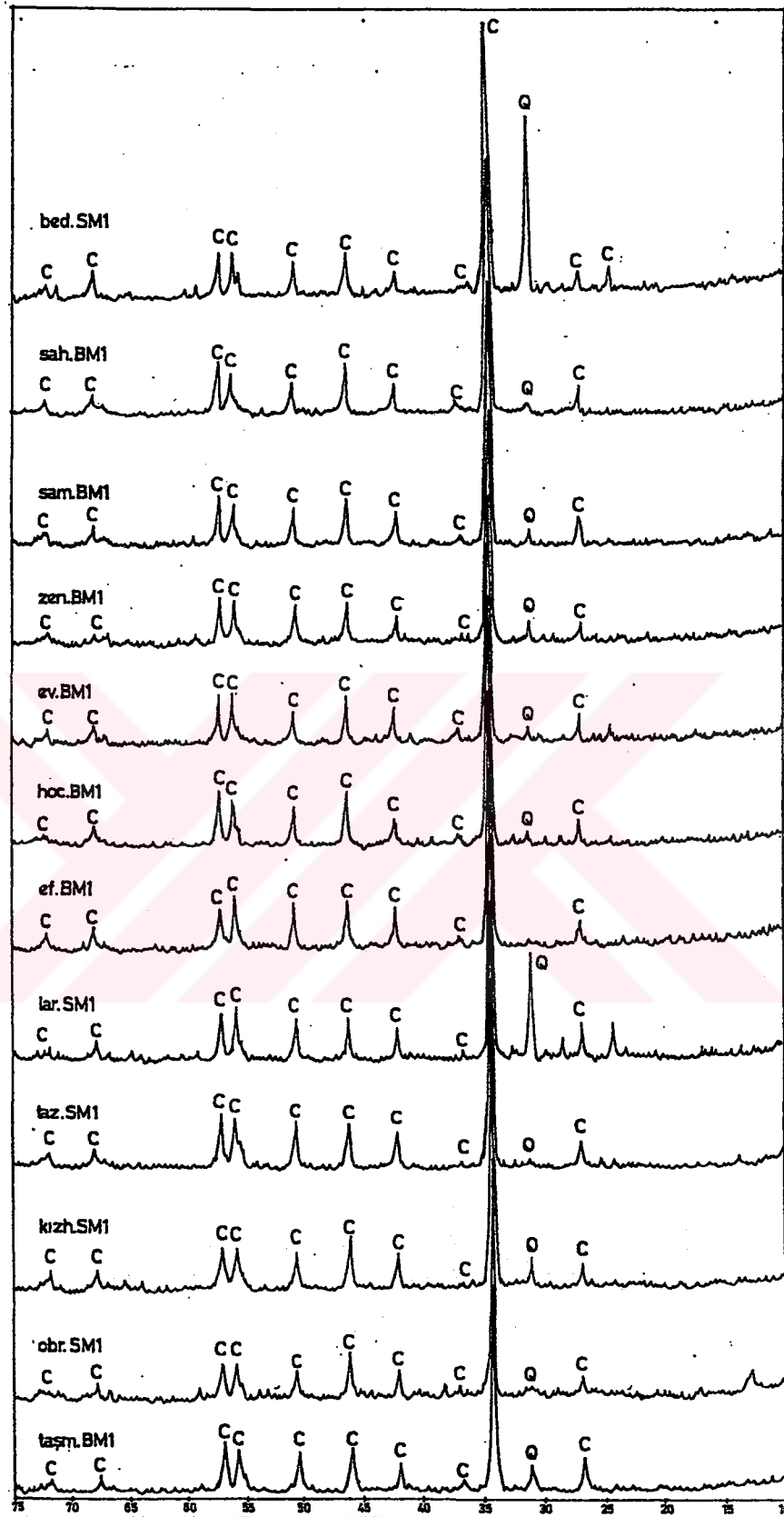
The analyses were carried out in the matrix, which contained both the binder and the fine aggregates, in the white lumps and aggregate parts of the mortars separately to determine their mineral composition.

3.5.2.1 Analyses of the Matrix

The main purpose of the analyses of the matrix was to see the existence of possible C-S-H (calcium-silicate-hydrate) and other new formations in the binder and aggregate mixture. However, in the XRD patterns of calcite mineral (CaCO_3) was dominant in all matrix patterns (Figure 3.28). It is also known from other studies that the strongest and the broadest peak of C-S-H peak coincides with the main calcite peak (Lewin, 1981). For such reasons, it was not possible to detect C-S-H peaks in XRD patterns of matrix. Among these matrix patterns, the mortar matrix of Kuruçeşme Han (kurm.SM) and Şekerfuruş Mescidi (şek.BM) seemed different. In addition to lime, mortar matrix of Kuruçeşme Han contained dolomite aggregates, and the matrix of Şekerfuruş mortar contained gypsum added to the lime binder (Figure 3.29).

3.5.2.2 Analysis of the Binder

XRD analysis of the binder parts were performed on the white lumps, which were the previous slaked lime lumps not mixed with fine aggregates. In their spectra, calcite mineral with all its prominent peaks indicated that pure lime was used in the mortars of almost all monuments studied (Figure 3.30). Among these mortars, the mortar of Şekerfuruş Mescidi (şek.BM1) was very stiff and contained no white lump that was large enough to obtain powder sample for the analysis. Therefore, the evaluation of the binder of Şekerfuruş mortar had to be done through its matrix analysis. This analysis has shown that, in addition to lime, gypsum was also used in the mortar binder of Şekerfuruş Mescidi (Figure 3.29). However, the mortar of Kuruçeşme Han (kurm.SM) contained sufficiently large white lumps. The binder of this mortar was also composed of calcite mineral similar to the mortars binders of other monuments (Figure 3.30).



Co K_α 2θ

Figure 3.28 XRD patterns of mortar matrixes C: calcite Q: quartz

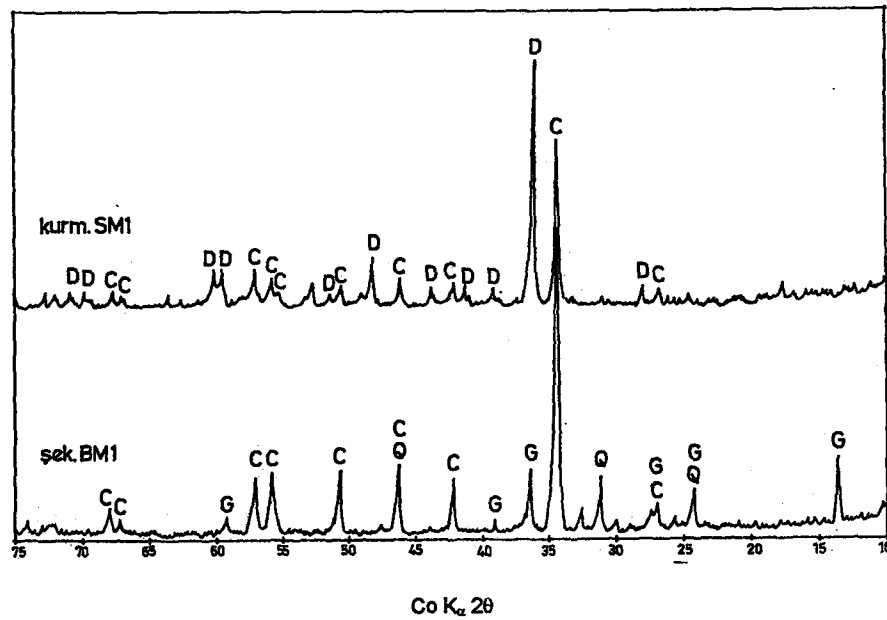


Figure 3.29 XRD patterns of the mortar matrixes of Kuruçeşme Han (kurm.SM1) and Şekerfuruş Tomb (šek.BM1) D: dolomite C: calcite G: gypsum Q: quartz

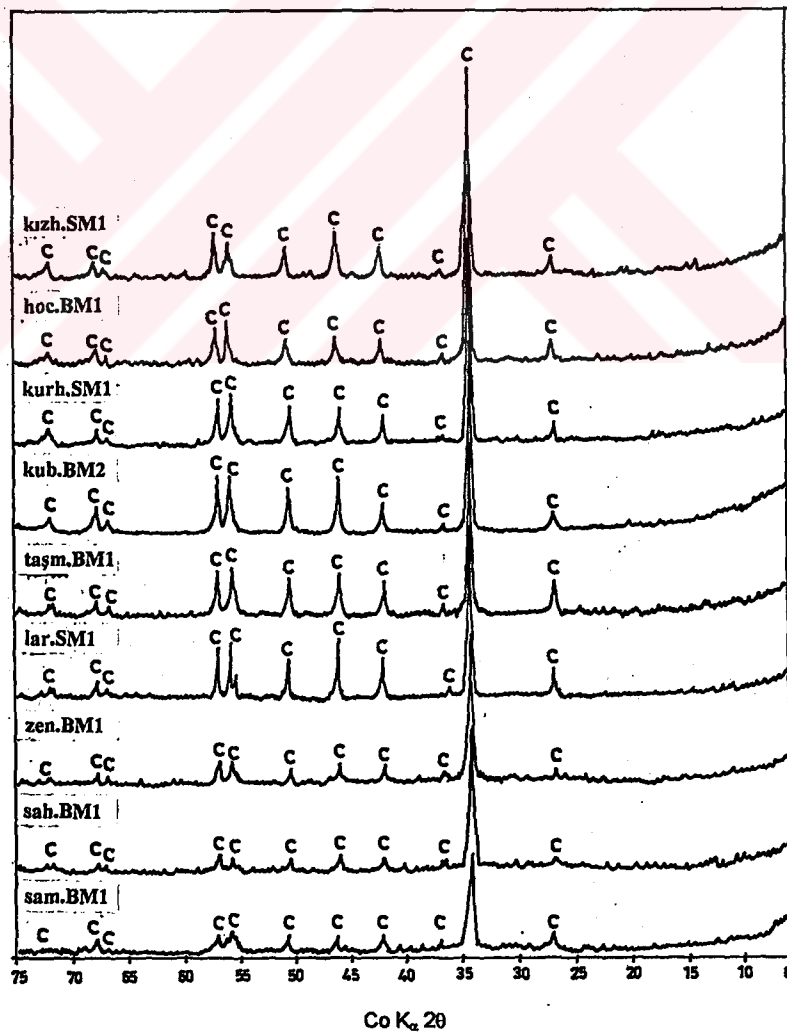


Figure 3.30 XRD patterns of the white lumps C: calcite

3.5.2.3 Analyses of Aggregates

The analyses of aggregate parts were performed on the aggregates of <125 μm and <45 μm size. The analysis of <125 μm sized aggregates was done to determine the mineral composition of sands used in the mortars.

The XRD analyses of <125 μm sized aggregates showed that the majority of sand in the mortars were composed of quartz, plagioclase and alkali feldspars, biotite and muscovite, and, kaolinite and montmorillonite of clay group minerals (Figure 3.31, Table 3.8). The only unique exception to the aggregate composition of these mortars was the mortar aggregates of Kuruçeşme Han (kurm.SM1), which was composed of dolomite mineral [$\text{Ca.Mg}(\text{CO}_3)_2$] (Figure 3.31).

In the general view of XRD patterns of the mortar aggregates, the most significant one was the pattern of the mortar aggregate of Kubadabad Palace (Figure 3.31-kub.SM1). In that pattern, a remarkable rise resembling the band of opal-A, one of the polymorphs of silica (Figure 3.32) indicated the existence of opal-A in the aggregates.

XRD patterns of >125µm sized aggregates

Co K α , 2 θ

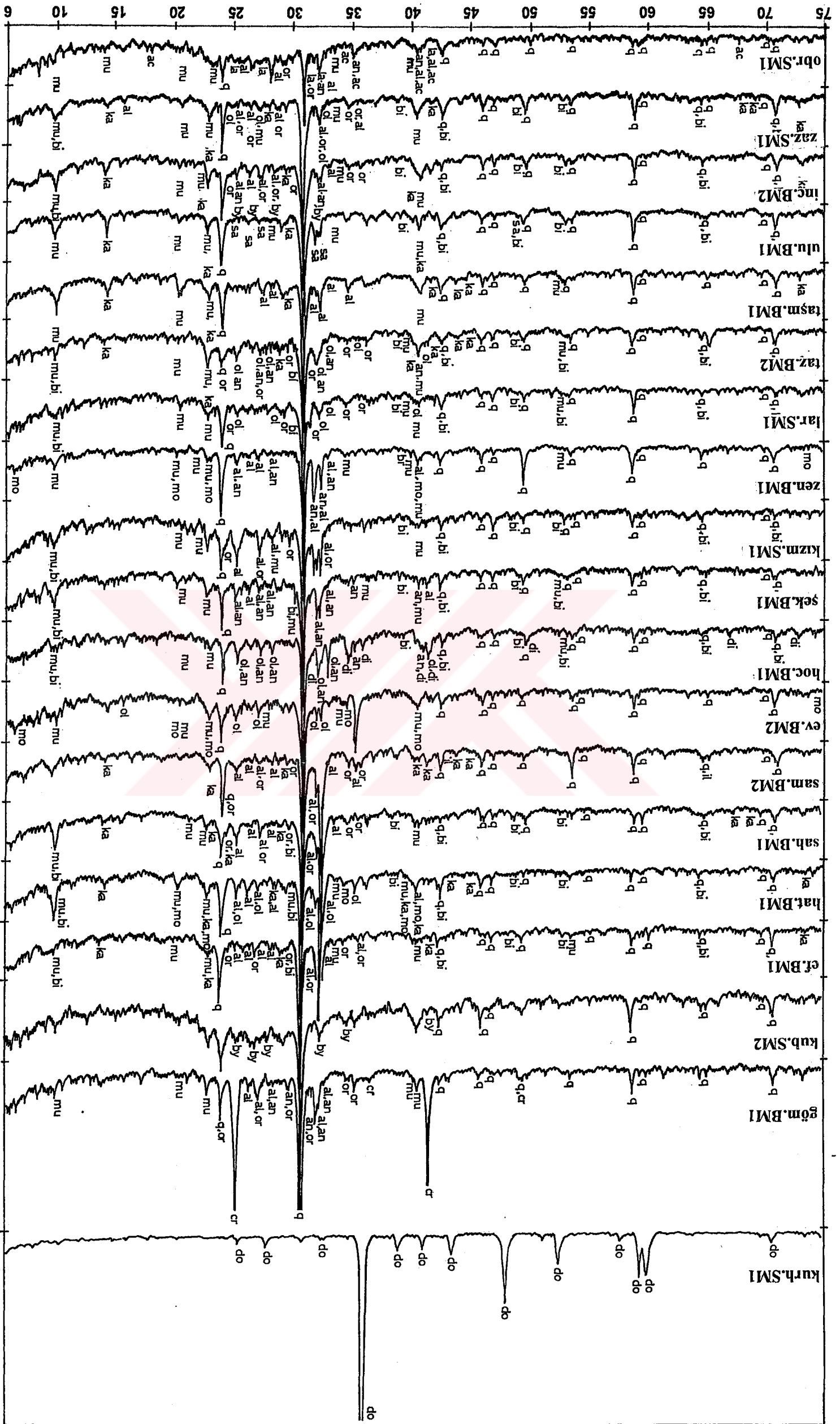


Table 3.8 Nomenclature and file numbers (*) of the minerals identified in XRD patterns of the mortar aggregates (<125µm)

<u>kurh. SM1</u>	<u>ev. BM2</u>	<u>taz. BM2</u>
do : dolomite (11-78)	q : quartz, low (5-490)	q : quartz, low (5-490)
	ol : oligoclase, low (9-457)	an : andesine, low (10-359)
<u>göm. BM1</u>	mu : muscovite 3T (7-42)	ol : oligoclase, low (9-457)
q : quartz, low (5-490)	mo : montmorillonite (13-135)	or : orthoclase (22-1212)
cr : cristobalite,high (27-605)	<u>hoc. BM1</u>	mu : muscovite 3T (7-42)
al : albite, high (20-572)	q : quartz, low (5-490)	bi : biotite (2-45)
an : anorthite, low (12-301)	ol : oligoclase, low (9-457)	ka : kaolinite 1Md (6-221)
or : orthoclase (19-931)	bi : biotite (2-45)	
mu : muscovite 3T (7-42)	mu : muscovite 3T (7-42)	<u>tasm. BM1</u>
<u>kub. SM2</u>	<u>sek. BM1</u>	q : quartz, low (5-490)
q : quartz, low (5-490)	q : quartz, low (5-490)	al : albite, low (20-554)
by : bytownite (20-528)	al : albite, high (20-572)	mu : muscovite 3T (7-42)
<u>ef. BM1</u>	an : andesine, low (10-359)	ka : kaolinite 1Md (6-221)
q : quartz, low (5-490)	mu : muscovite 3T (7-42)	
al : albite, high (10-393)	bi : biotite (2-45)	<u>ulu. BM1</u>
or : orthoclase (19-931)	<u>kız. SM1</u>	q : quartz, low (5-490)
bi : biotite (2-45)	q : quartz, low (5-490)	sa : sanidine (19-1227)
mu : muscovite 3T (7-42)	al : albite, high (20-572)	mu : muscovite 3T (7-42)
ka : kaolinite 1T (14-164)	or : orthoclase (19-931)	ka : kaolinite 1Md (6-221)
<u>hat. BM1</u>	mu : muscovite 3T (7-42)	
q : quartz, low (5-490)	bi : biotite (2-45)	<u>inc. BM2</u>
al : albite, low (20-554)	<u>zen. BM1</u>	q : quartz, low (5-490)
ol : oligoclase, low (9-457)	q : quartz, low (5-490)	al : albite, high (20-572)
bi : biotite (2-45)	al : albite, high (20-572)	an : anorthite, low (12-301)
mu : muscovite 3T (7-42)	an : anorthite, low (12-301)	or : orthoclase (19-931)
mo : montmorillonite (13-135)	bi : biotite (2-45)	by : bytownite (20-528)
ka : kaolinite 1Md (6-221)	mu : muscovite 3T (7-42)	mu : muscovite 3T (7-42)
<u>sah. BM1</u>	mo : montmorillonite (13-135)	ka : kaolinite 1Md (6-221)
q : quartz, low (5-490)	<u>lar. SM1</u>	
al : albite, high (10-393)	q : quartz, low (5-490)	<u>zaz. SM1</u>
or : orthoclase (22-1212)	or : orthoclase (22-1212)	q : quartz, low (5-490)
bi : biotite (2-45)	ol : oligoclase, low (9-457)	al : albite, low (9-466)
mu : muscovite 3T (7-42)	bi : biotite (2-45)	or : orthoclase (19-931)
ka : kaolinite 1T (14-164)	mu : muscovite 3T (7-42)	ol : oligoclase, high (20-548)
<u>sam. BM2</u>		mu : muscovite 3T (7-42)
q : quartz, low (5-490)		ka : kaolinite 1T (14-164)
al : albite, high (10-393)		<u>obr. SM1</u>
or : orthoclase (22-1212)		q : quartz, low (5-490)
		al : albite, high (20-572)
		an : andesine, low (10-359)
		or : orthoclase (22-1212)
		la : labradorite, inter (22-1212)
		mu : muscovite 3T (7-42)

(*) Hanawalt Method (1978)

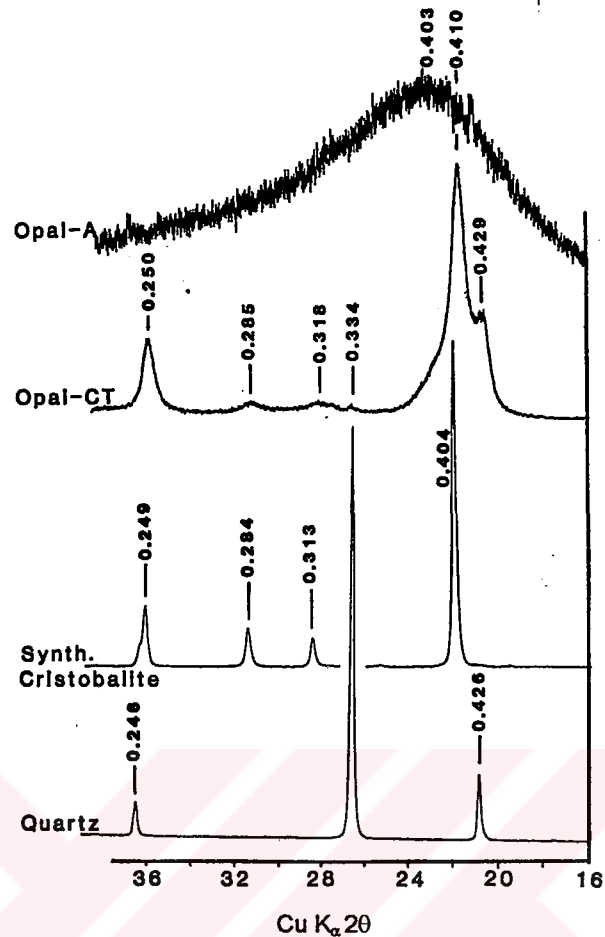


Figure 3.32 XRD patterns of silica polymorphs (Drees *et al.*, 1995)

It has been known that opal in soil environments is extremely small in size, in most cases less than $0.5\mu\text{m}$ and due to its amorphous nature it can easily be masked in the XRD patterns in the presence of other minerals even its percentage is high (Drees *et al.*, 1995; Güngör, 2000). Therefore, the enrichment of $<125\mu\text{m}$ sized aggregates were done to prove their presence. This was done by sieving the $<125\mu\text{m}$ sized aggregates using $<45\mu\text{m}$ size sieve to remove coarser part, which may not be of opal. XRD spectra of $<45\mu\text{m}$ sized aggregates revealed that in most of the mortar aggregates opal and its derivatives are present showing the broad band of opal-A. The differences in XRD patterns of $<125\mu\text{m}$ and $<45\mu\text{m}$ sized aggregates and the appearance of opal-A band with its peak at 0.403nm have been shown in diagrams in pairs (Figures 3.33-42).

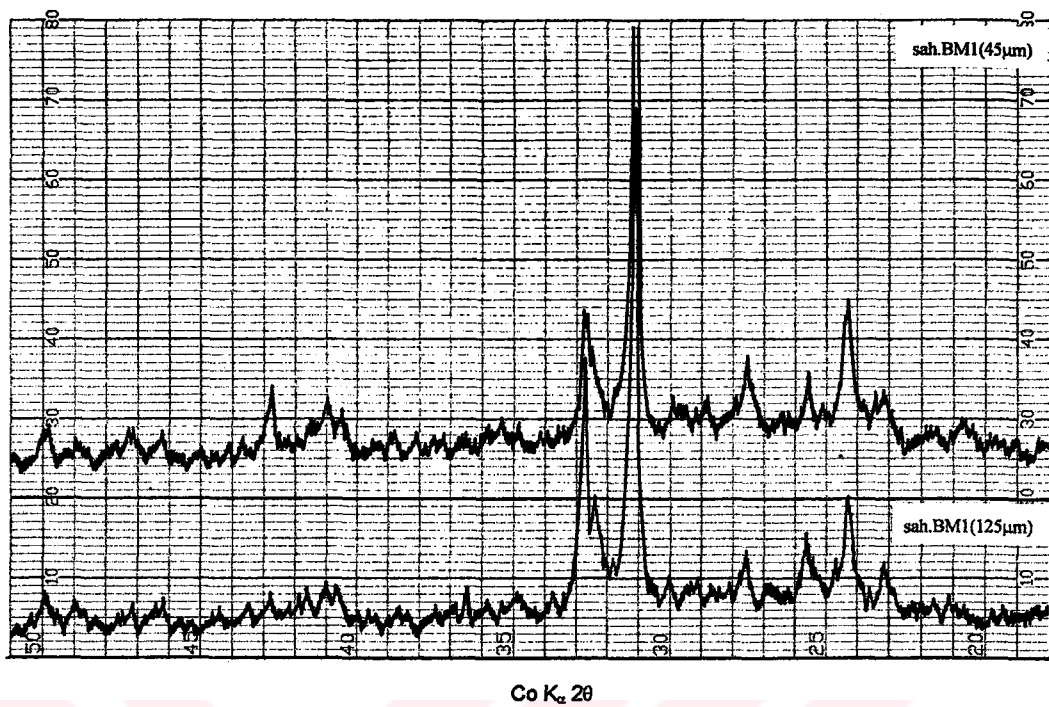


Figure 3.37 XRD patterns of <125μm and <45μm sized aggregates of the mortar of Sahip Ata Hanikahı (sah.BM1)

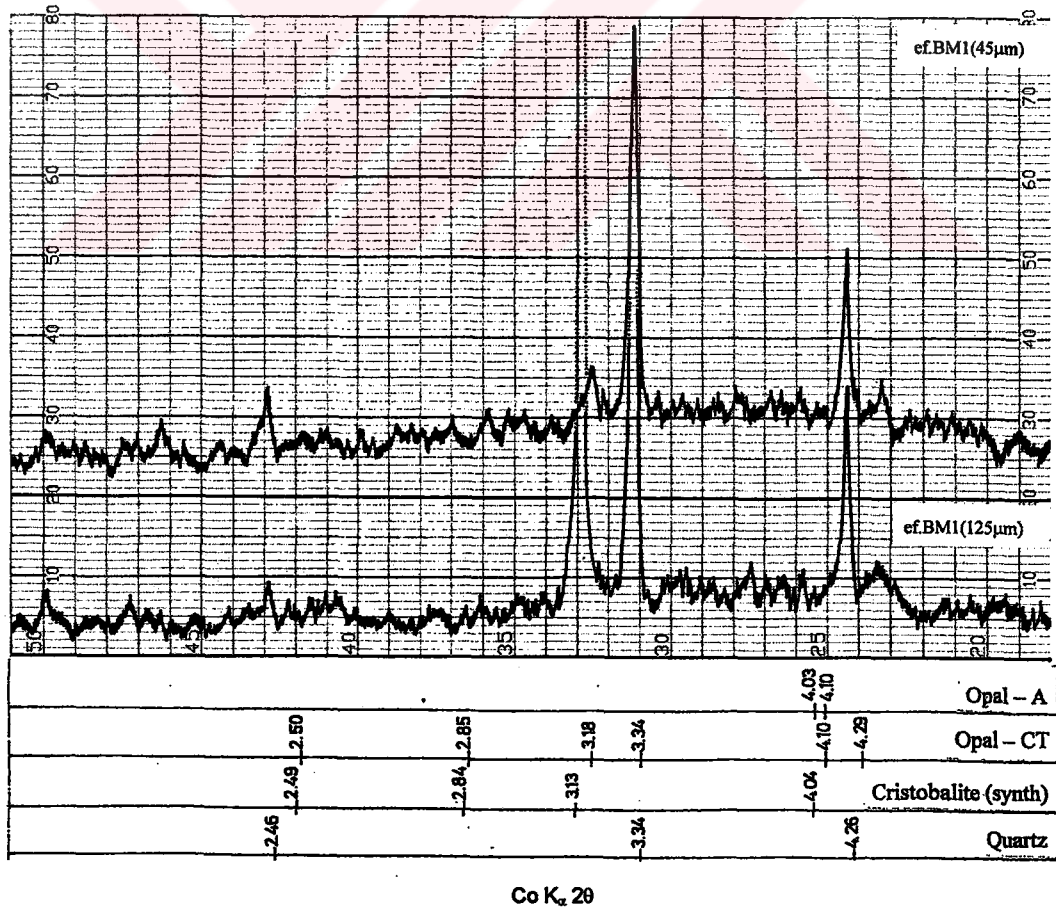


Figure 3.38 XRD patterns of <125μm and <45μm sized aggregates of the mortar of Eflaki Dede Tomb (ef.BM1)

3.5.3 Scanning Electron Microscopy (SEM) and Energy Dispersive X-Ray (EDX) Analyses

SEM images and EDX analyses were performed on the matrix, binder and aggregate parts of the mortars to determine their morphology, microstructure and chemical compositions. The aggregate-binder interfaces were also examined to identify possible reaction products, such as C-S-H (calcium-silicate-hydrate) formations. The results of SEM examinations, which show morphology and microstructure of the samples have been presented in micrographs. The percentages of metal oxide contents of the mortar aggregates have been given in a table (Table 3.9).

3.5.3.1 Analysis of Matrix

The SEM images of mortar matrixes indicated that they were composed of micritic calcite crystals of $\sim 1\mu\text{m}$ (Figure 3.49-50) together with very fine siliceous grains ($<5\mu\text{m}$), which were later proved to be mainly of opal (Figure 3.43-46). It was also seen that this mixture enveloped coarser aggregates with a very good adhesion (Figures 3.47-48). SEM-EDX analyses of the mortar matrix of Şekerfuruş Tomb showed that gypsum was also used in the lime binder (Figure 3.51).

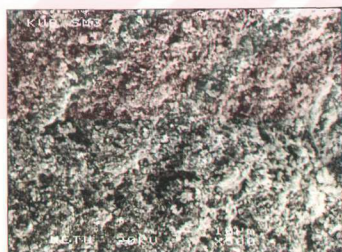


Figure 3.43 SEM view of the mortar matrix of Kubadabad Palace (kub.SM3) x 500



Figure 3.44 A close SEM view of the mortar matrix of Kubadabad Palace (kub.SM1) x 2000

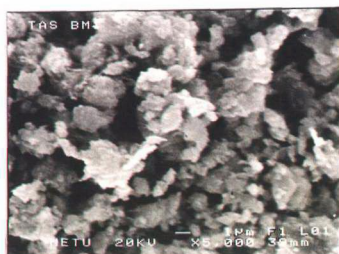


Figure 3.45 A close SEM view of the mortar matrix of the minaret of Taşmedrese Mescidi (taşm.BM1) x 5000

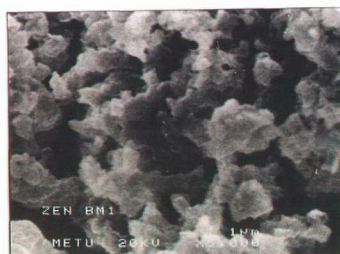


Figure 3.46 A close SEM view of the mortar matrix of the minaret of Zenburi Mescidi (zen.BM1) x 5000

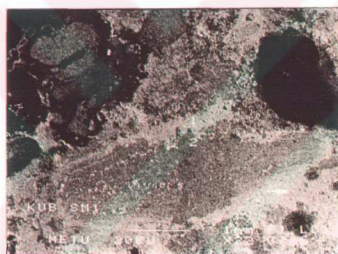


Figure 3.47 SEM view showing the good adhesion between a coarse aggregate and the mortar matrix of Kubadabad Palace (kub.SM1) x 22



Figure 3.48 SEM view showing the good adhesion between a coarse aggregate and the mortar matrix of the minaret of Hatuniye Mescidi (hat.BM1) x 500

3.5.3.2 Analysis of Binder

The SEM micrographs of binder parts showed that the lime, used in the mortars, was composed of micrite type calcite crystals of $<1\mu\text{m}$ size in diameter (Figures 3.49-50). The relatively small amount of other metal oxides, such as SiO_2 , Al_2O_3 , MgO , Fe_2O_3 , which was found by EDX analyses also revealed that high-calcium lime was used as binder in these mortars. The composition of the white lump of Kubadabad Palace mortar, have shown that the total amount of impurities, such as MgO and SiO_2 not

more than 5%. This reveals that the lime used in this mortar was high calcium lime (Figure 3.51). That was common to the white lumps of all other mortars except the binder of Şekerfuruş Tomb (şek.BM1) being a mixture of calcite and gypsum (Figure 3.52).

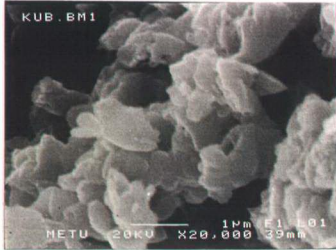


Figure 3.49 SEM view of micrite type calcite crystals in the mortar matrix of Kubadabad Palace (kub.SM1) x 20000

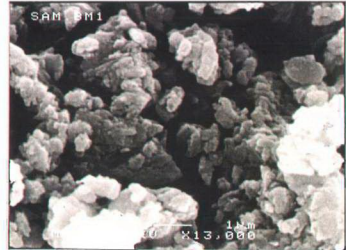


Figure 3.50 SEM view of micrite type calcite crystals in the mortar matrix of the minaret Sahip Ata Mosque (sam.BM1) x 13000

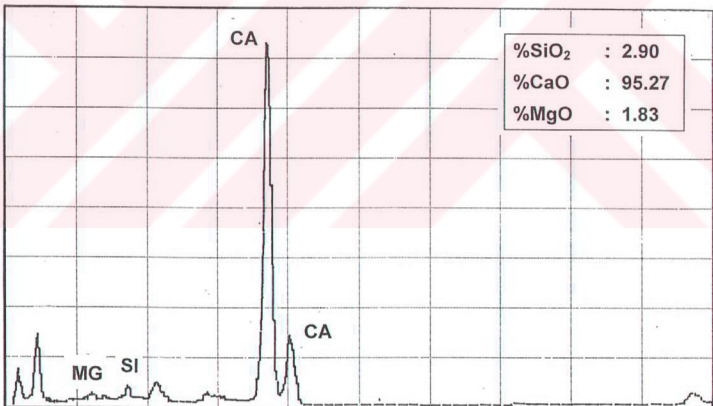


Figure 3.51 EDX analysis of a white lump in Kubadabad Palace mortar (kub.SM1)

3.5.3.3 Analysis of Fine Aggregates:

EDX analyses for the chemical composition of fine aggregate parts were performed on pellets of fine aggregates that were <math><45\mu\text{m}</math> size, except Kuruçeşme Han mortars

where aggregates were mainly dolomite (Figure 3.53). Metal oxide content of the aggregates exhibit a homogeneous character in spite of small differences (Table 3.9).

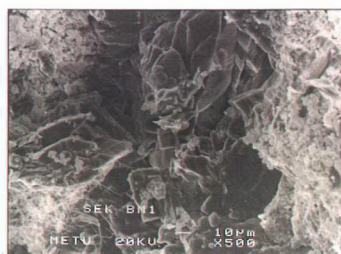


Figure 3.52 SEM view of gypsum crystals in the mortar matrix of Şekerfuruş Tomb (şek.BM1) x 5000

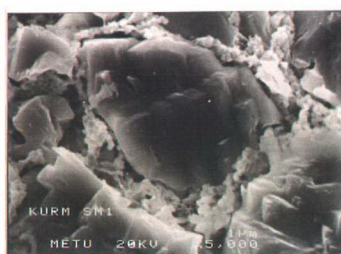


Figure 3.53 SEM view of dolomite crystals in the aggregates of Kuruçeşme Han (kurm.SM.BM1) x 5000

Table3.9 Metal oxide contents in mortar aggregates

sample	%CaO	%MgO	%SiO ₂	%Al ₂ O ₃	%Fe ₂ O ₃	%Na ₂ O	%K ₂ O	%TiO ₂
kub.SM1	-	-	92.66	5.62	0.98	-	0.75	-
zen.BM1	0.45	1.45	72.12	17.41	4.85	-	2.94	0.78
obr.SM1	0.75	2.56	81.64	9.41	3.45	-	1.36	0.88
lar.SM1	0.23	0.71	78.6	13.74	3.89	-	1.94	0.89
bed.BM2	0.59	1.56	75.74	13.58	5.05	-	2.23	1.24
zaz.SM1	0.81	1.16	74.05	15.99	4.56	-	2.50	0.98
hat.BM1	0.80	2.26	69.78	18.79	4.88	-	2.84	0.71
ulu.BM1	0.91	1.20	71.31	18.58	4.38	-	3.01	0.62
tz.BM1	0.81	1.31	70.81	17.95	6.24	-	2.38	0.49
kız.SM1	0.77	1.54	75.59	15.43	3.64	-	2.10	0.93
güd.BM1	0.97	1.09	74.06	15.40	5.12	-	2.76	0.59
sam.BM1	7.52	1.68	69.81	13.01	5.20	-	1.54	1.24
kurm.SM1	59.42	38.00	2.58	-	-	-	-	-
inc.BM1	0.88	2.45	68.68	19.53	5.18	-	2.80	0.49
ev.SM3	1.10	1.71	70.92	17.17	5.12	-	3.15	0.82
şek.BM1	1.45	1.26	74.04	16.27	3.91	-	2.32	0.75
sak.SM1	0.65	1.44	76.1	15.40	3.92	-	2.00	0.49
hoc.BM1	1.77	2.47	69.86	17.58	4.52	-	2.59	1.20
taşm.BM1	0.52	1.57	67.15	19.93	5.37	2.08	2.59	0.84
sah.BM1	1.22	1.47	67.22	18.14	4.60	3.19	3.23	0.92

As the metal oxide contents revealed, silicon dioxide (SiO_2) seemed the main component, which varied in the range of 67-80%. Only, the SiO_2 content of Kubadabad aggregates fell out of this range with a relatively higher value of 92.66%. Next to the silica content, aluminium oxide (Al_2O_3) varied in the range of 13-20%, being the second, and iron oxide, varied in the range of 3-5% was the third important component in the aggregates. Except the mortar aggregates of Taşmedrese Mescidi and Sahip Ata Hanikahı, the absence of sodium oxide (Na_2O) in these analyses may indicate the majority of feldspar minerals were of K-feldspars. The small amount of calcium oxide fractions in the aggregates were likely from the acid insoluble silicates, or the remains undissolved calcite.

3.5.3.4 Analysis of C-S-H Formations

The interface zone between aggregates and binder was examined to detect the possible reaction products, such as C-S-H (calcium silicate hydrate) around pozzolanic aggregates. Such a formation, around a macro-scale aggregate (~2.5mm in diameter), was first noticed on one of the mortar samples of Kubadabad Palace (kub.SM1) during the microscopic examination for the visual properties of mortars (Figure 3.54). SEM image of this gel-like formation resembles a tobermoritic gel, which was formed probably by the reaction between lime and the pozzolanic aggregate (Figure 3.55, lower right).



Figure 3.54 SEM view of the C-S-H formation in the mortar matrix of Kubadabad Palace (kub.SM1) x 20

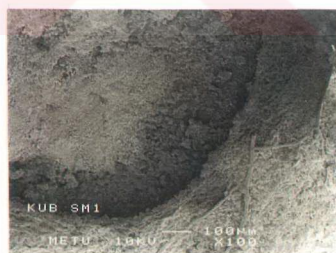


Figure 3.55 A close SEM view of the C-S-H formation in the mortar of Kubadabad Palace (kub.SM1) x 100

By EDX analyses it was found that this zone was composed of 23.93% SiO_2 (silicon dioxide), 74.17% CaO (calcium oxide) and 1.9% MgO (magnesium oxide). Due to the

interference of calcite minerals stuck on the grain, the composition of the aggregate could not be determined (Figure 27, upper left).



CHAPTER 4

DISCUSSION AND CONCLUSION

In this chapter, the experimental results, that have been obtained by the examination of the mortars from twenty two monuments in Konya, Beyşehir and Akşehir, have been interpreted in terms of raw materials properties, physical and mechanical properties and durability characteristics of mortars. Most of the brick and stone masonry mortars have been found to have pozzolanic character although there were two exceptions to it. Discussions have been made during the interpretation of the results. Future studies have been suggested at the end.

4.1 Raw Material Properties of Mortars

It is known that the raw material properties of mortars largely define their final properties, their function within masonry units and structure. Each component of the mortars, namely binder, aggregates, organic and/or inorganic additives all take their own part within this context affecting the long term durability. In the following sections, experimental results will be interpreted in terms of the properties of the components only.

4.1.1 Properties of Binder

The main binder of all mortars has been found to be calcium hydroxide, $\text{Ca}(\text{OH})_2$, or slaked lime. The average lime content (CaCO_3 – carbonated lime) in stone and brick masonry mortars are 57.67% and 62.08% respectively (Figures 3.10-11; Appendix P1-2) much higher than the percentage of lime used in present day building practice (Ashurst and Dimes, 1990; Mora *et al.*, 1984). The exceptionally high content of lime (88.61%) found in the mortars of Obruk Han (Figure 3.10, Appendix P1) was due to the lime aggregates which were observed in thin section analyses (Figure 3.16). The difference (~5%) in the lime content of stone and brick masonry mortars caused brick masonry mortars to be lighter and more porous than

those of stone masonry ones. This will be discussed below in relation to the materials compatibility.

It was possible to examine the properties of binder by the examination of white lumps. White lumps were the previous slaked lime lumps, which were not mixed with the fine aggregates (Bakolas *et al.*, 1995; Bruni *et al.*, 1997). Therefore, the examination of white lumps through several analyses has revealed the properties of the binder.

The preliminary distinction between the white lumps and the limestone aggregates was done in thin sections. White lumps did not have well-defined edges. They were composed of micritic calcite crystals which were tightly packed and indicated a complete carbonation (Figures 3.16-19). Limestone aggregates on the other hand were rarely met in the mortars. Kubadabad Palace mortars had some, but they were abundant in the mortar of Obruk Han. They had rather sharp edges, which made them distinguishable in the matrix from the white lumps (Figure 3.18-19). The crystal structure of limestone aggregates was composed of sparitic calcite crystals (Figures 3.16-19) whereas white lumps were composed of micritic calcite.

TGA analysis was also carried out although on a single sample of white lump from Kubadabad Palace mortars (kub.SM1, Figure 3.9). The calcination of the lump at 728°C also indicated that it was re-carbonated lime (Bakolas *et al.*, 1995), but not the calcite of limestone aggregate which usually decomposes around 900°C (Walter, 1974). Another peak at 442°C observed on the same diagram indicates the likely presence of an organic additive (Walter, 1974) which will be discussed later.

The complete carbonation of white lumps, therefore the binder was proved through XRD traces of several lumps, observing the dominance of calcite, and the absence of portlandite [$\text{Ca}(\text{OH})_2$] minerals in their composition (Figure 3.30).

EDX analyses of white lumps under the SEM (Figures 3.49-50) have shown that calcium oxide was dominant in the composition containing very low percentages of other oxides (*eg.* kubSM1, Figure 3.51).

Therefore the binder may be considered to be high calcium lime or fat lime which has totally carbonated. Most probably the slaked lime had fine particle size and high plasticity inherited from the properties of quicklime (Boynton, 1966).

4.1.2 Properties of Aggregates

The aggregate properties such as their size distribution, shape, mineralogical composition and pozzolanic properties affect the physical and mechanical properties of the mortars.

The average aggregate content in stone and brick masonry mortars have been found to be 42% and 38% respectively (Figures 3.10-11; Appendix P1-2). In the overall size distribution of the aggregates, medium (500-250 μ m) and fine (<125 μ m) aggregates form the major group (Figures 3.12-14). In the total of medium and fine aggregates, the fine aggregates occupy the larger portion.

Thin section analyses have given information about the mineralogical properties of the aggregates in the mortars. Coarse and medium sized aggregates were composed of siliceous sedimentary or metamorphic rock fragments in addition to some quartz and feldspars. They were in good contact with the matrix proving good adhesion (Figures 3.22, 23, 26, 27). Fine aggregates on the other hand, including opal, quartz, feldspar and mica minerals have also been identified in thin sections (Figures 3.24-25) while most of them have formed the matrix as very fine opaque minerals homogenously distributed in the micritic calcite binder.

As far as the monuments in Konya, Akşehir and Beyşehir are concerned, the pozzolanic properties of the aggregates and their interactions with the lime seem to be one of the most prominent features affecting the physical and mechanical properties of the mortars. Fine aggregates have played the major role in that.

As it was mentioned in the previous sections of the study (Section 1.2.2), pozzolanic aggregates are defined as the materials, not cementitious in themselves, but their constituents, such as silica and alumina readily react with lime to form stable and water-insoluble compounds with cementing properties in the presence of water (ASTM C593-76a; Lea, 1970). The most important feature of these materials is the relatively high strength they impart to the mortar when compared with the ones prepared with inert aggregates and non-hydraulic limes. These reactive aggregates can be of volcanic origin or naturally occurred in earth by the sedimentation processes (Lea, 1970; Diamond, 1976; Drees *et al.*, 1995). They can also be artificially prepared by burning suitable clays at certain temperatures. Kaolin for

instance, has the potential to be converted to opal-A when heated to above 500°C (Benharbit, 1994). Either natural or artificial origin, the most important features of pozzolanic materials are their very small particle size and thus high specific surface area, largely amorphous and reactive structure containing SiO₂, Al₂O₃ and Fe₂O₃ constituents (Lea, 1970; Diamond, 1976; Benharbit, 1994; Drees *et al.*, 1995).

The mineralogical and chemical composition of fine aggregates and their pozzolanic characteristics have been determined by the combined results of several analyses due to the difficulties inherent in the examination of fine opaque minerals. The XRD traces of aggregates smaller than 125µm in Kubadabad mortars have shown a diffused broad peak at about 0.41nm (Figure 3.31) while in the others it was not possible to observe it. The opal-A peaks are easily masked in the presence of other silicate minerals even if their percentages may be as high as twenty percent (Güngör, 2000). Therefore, it was necessary to enrich the opal-A proportion in the sample in order to prove its presence. Since opal-A particles are usually of very fine particle size (Drees *et al.*, 1995), the enrichment of opal-A has been done by sieving the finest portion of aggregates (<45µm). The XRD traces of those finest aggregates have shown the typical broad band of opal-A, which has proved its presence in considerable amounts (Figures 3.32-42). In addition to opal-A, most frequently met minerals in the composition of fine aggregates are quartz, plagioclase and alkali feldspars, biotite, muscovite and some clay minerals (Figure 3.31, Table 3.8).

The fine aggregates have also been observed and analysed by SEM-EDX. The pellets were prepared with aggregates of very fine particle size (<45µm). Silica content of the fine aggregates was high, the Kubadabad Palace ones being the highest (~93%)(Figure 3.43-46; Table 3.9). That has supported the XRD results about the abundant presence of opal-A in these mortars. In addition to silica content, aluminium oxide and iron oxide contents of the mortars are also accepted as effective compounds in pozzolanicity (Price, 1995). EDX results have shown that the sum of SiO₂, Al₂O₃ and Fe₂O₃ contents in these mortars was higher than 70% which is the value of pozzolanicity required from pozzolanic aggregates by the present day standards (ASTM C618-73). The contents of potassium oxide (K₂O: 0.75-3.23%) and sodium oxide which was found only in Taşmedrese and Sahip Ata Hanikah

mortars (Na_2O : 2.08, 3.19%) (Table 3.9) were small enough not to be considered as potential sources to produce new damaging formations (Aardt and Visser, 1977).

Fine aggregates have also been characterised by their direct pozzolanic activity measurements. Pozzolanic activity measurements were carried out on $<125\mu\text{m}$ sized aggregates indicated that most of the fine aggregates had the pozzolanic activity values well over 1.20mS/cm above which was accepted as good pozzolanicity (Luxan *et al.*, 1989)(Figure 3.15). Based on this classification, the fine aggregates of the mortars of 22 monuments can be defined as good pozzolanas.

It is seen that the use of very fine aggregates of good pozzolanicity in large amounts, increased the specific surface area and increased the importance of pozzolanic reactions. Considerable amount of very fine amorphous opal-A in their composition has played the major role in that (Diamond, 1976; Benezet and Benhassaine, 1999). It is a fact that in a solution with high lime concentration and reactive pozzolanic material, the formation rate of C-S-H gel is higher, the formation of silica polymerisation is important (Barret *et al.*, 1977). These mechanisms played an important role in the development of high strength in the mortars. On the other hand, pozzolanic material largely prevents the alkaline attack on aggregates and protect them from further physical and chemical damage during the carbonation of slaked lime. (Aardt and Visser, 1977).

The aggregate composition of Kuruçeşme Han mortars was the only exception to the characteristics above. Kuruçeşme Han mortars were composed of dolomitic aggregates and high calcium lime (Figure 3.31). The highest compressive strength and the highest modulus of elasticity when compared with the other mortars must have been due to the use of dolomitic aggregates and the carbonation characteristics of the high calcium lime used (Figure 3.1, 3). Further study is needed to understand better the factors affecting their physical and mechanical properties.

4.1.3 Organic or Inorganic Additives

The significance of additives, of organic or inorganic origin, on the properties of historic mortars is well mentioned. However, there is not much scientific information about their roles, composition and original raw material sources. The possible roles of additives could be to improve workability, to extend or retard the setting time, to

control the carbonation process, the alkaline reactions, pozzolanic reactions *etc.* (Livingston *et al.*, 1991; Knöfel and Wissler, 1988; Sickel, 1981; Young and Miller, 2000; Martinez-Ramirez *et al.*, 1995; Kaviak, 1991; Middendorf and Knöfel, 1994).

Although further analyses are needed to prove the existence of organic additives in Konya mortars, their likely presence is found by TGA analysis of a white lump from Kubadabad Palace mortars. A peak observed at 442°C (Figure 3.9) was taken as a possible evidence of an organic additive. However, further analyses are needed to verify it. Studies on the reaction of CaCO₃ with oleic acid have shown the importance of the formation of insoluble calcium oleate affecting the surface properties of calcite and its recrystallisation (Young and Miller, 2000). Carbonation process is likely to be influenced by such organic additives.

Some studies are done on the role of organic additives in gypsum mortars, which may control the setting time and decrease the water-susceptibility of gypsum (Livingston *et al.*, 1991; Kaviak, 1991; Middendorf and Knöfel, 1994). Despite the abundance of the recipes in various historical sources, the subject calls for more scientific research (Sickels, 1981; Middendorf and Knöfel, 1994).

On the other hand, carbonation of lime is also found to be affected by the addition of clay minerals to the mortar. It was shown that the addition of a few percent of sepiolite (Martinez-Ramirez *et al.*, 1995) slowed down the carbonation rate which can be an advantage for the development of C-S-H formation while improving the workability of mortar and hence affecting the physical and mechanical properties.

4.2 Physical Properties

The comparison of basic physical properties of stone and brick masonry mortars revealed that brick masonry mortars were lighter and porous than the stone masonry ones.

The average densities of stone and brick masonry mortars were ~1.60g/cm³ and ~1.50g/cm³ respectively. Their porosities were also varied similarly, being ~37 and ~41% respectively. (Figures 3.1-2, Appendix M1-2). These mortars have proved to be of high porosity and relatively low density.

Some information about the pore size characteristics of the mortars was obtained by

following their drying rates and thin section analyses. Drying rate characteristics (Figures 3.5-6) have shown that both stone and brick masonry mortars dried quickly when compared with cement mortar. It is known that small capillary pores prevent faster drying, whereas larger pores promote quick drying (Schaffer, 1972). The ease of drying of historic mortars indicated the presence of larger pores and the absence of fine capillaries.

In fact, in the examination of thin sections, it was observed that the fine cracks were sealed by the recrystallisation of calcite minerals. The elimination of capillaries and small cracks by this phenomenon lead faster drying (Figure 3.20-21). Such properties of mortars increased their durability against wetting and drying cycles, and other possible weathering factors (Schaffer, 1972).

The comparison of the physical properties of bricks with that of the adjacent mortars in the same monument indicated that they were in the similar ranges (Figures 3.5-6). This proves that, in these masonry structures, relatively light and porous mortars compatible with the bricks were used. Such a material compatibility have lead to homogeneous shell-like structural properties to the upper parts that are arches, vaults and domes and the transition elements of the monuments enabling them to behave coherently against weathering factors and disruptive forces.

4.3 Mechanical Properties

The mechanical properties of mortars were expressed by their uniaxial compressive strength and modulus of elasticity values. These values were obtained indirectly from the point load strength measurements and ultrasonic pulse velocity measurements together with the density values by using mathematical equations (Section 2.2).

Uniaxial compressive strengths of stone and brick masonry mortars in dry state were mostly in the range of 3.5-8.00MPa (Table 3.3-4, Appendix O1-2). However, some mortars had considerably higher strengths, such as the mortars of Kubadabad Palace (12.93MPa and 17.18MPa), Evhadeddin Kirmani Tomb (14.80MPa) and Kuruçeşme Han being the highest (18.32MPa) (Table 3.3, Appendix O1-2). Unlike all the other mortars, Kuruçeşme ones were composed of high calcium lime binder and dolomitic aggregates. The pozzolanic aggregates were absent in them. The development of high strength in these mortars must be due to carbonation properties of its high

calcium lime and the use of dolomitic aggregates, which need further investigations. Modulus of elasticity of stone and brick masonry mortars are in agreement with their uniaxial compressive strengths values although they have been calculated by using different experimental parameters. (Table 3.1-2). The modulus of elasticity values varied in the range of 700-3000MPa. The modulus of elasticity value of Kuruçeşme Han mortar (Table 3.1) was the highest of all (~8325MPa) as it was in its compressive strength. It can be said that the strength of the mortars was sufficient enough as a structural agent and they are resistant against possible deformations as their modulus of elasticities revealed. The modulus of elasticity and uniaxial compressive strength of Konya mortars are in the similar ranges with the pozzolanic (or hydraulic) mortars of other historic buildings (Schäfer and Hilsdorf, 1993; Penelis *et al.*, 1989; Papayianni and Stefanidou, 1997; Papayianni, 1997).

4.4 Durability Characteristics

Durability factors of the mortars, which have been expressed either by the ratio of their uniaxial compressive strengths in wet and dry states, or by the ratio of dry strength to porosity, revealed two important facts about their durability.

In the first durability factor based on wet to dry strength ratio (Winkler, 1989), the calculated values for the durability of mortars are in the range of 65-98 (Table 3.5, D1). These values indicated that Konya mortars are perfectly resistant against wetting and drying cycles. Such a property must have developed largely due to their aggregates good pozzolanic nature. However, it was also seen that despite their aggregates with poor pozzolanicity (Figure 3.15) and high lime content, the mortars of İnce Minareli Medrese (inc.BM1), the minaret of Sahip Ata Mosque (sam.BM1, BM2), the minaret of Hatuniye Mosque (hat.BM2), the minaret of Zenburi Mescidi (zen.BM1) and the minaret of Ulucami (ulu.BM1) showed similar durability characteristics with that of the mortars of good pozzolanicity. This must be due to the properties of lime and a good carbonation process. Organic or inorganic additives may have played an important role in that process (Young and Miller, 2000; Martinez-Ramirez *et al.*, 1995).

According to the second expression of durability factor, which was based on the dry strength over porosity ratio (Rodrigues and Jeremias, 1990), the calculated values of

durability for Konya mortars were in the range of 0.01-04 (Table 3.5, D2). These values have indicated very poor durability since D=2 was the lower limit for the durability. That durability factor was established by considering the resistance of stone to salt crystallisation cycles. Therefore, it may be concluded that although the Konya mortars are quite durable to wetting and drying cycles, they are not durable at all to salt crystallisation cycles. It shows that soluble salts are dangerous for these structures.

4.5 Conclusion

The examination of the mortars from twenty-two monuments in Konya, Akşehir and Beyşehir has revealed information on the technological characteristics of these materials, which has helped to better understanding of those structures. A lot of information has also been produced that would lead to the preparation of repair mortars for those structures.

The binder used in the mortars of these monuments was high calcium lime, which has well carbonated to micritic calcite crystals.

The amount of binder used was in remarkably high amounts being 58-62 % by weight. The TGA analysis indicated the likely evidence of an organic additive mixed with lime, which would influence the carbonation process affecting physical properties and the development of mechanical strength. It may also be effective on the workability of mortar and on the establishment of good adhesion of the matrix with coarser aggregates. Further research is needed on this subject.

The lime content of brick masonry mortars has been found to be more than that of stone masonry ones. It was also found that the physical properties of brick masonry mortars were close to the properties of the bricks used with these mortars. By the achievement of such a material compatibility, light, porous and homogeneous upper structures were obtained.

The most prominent feature of the aggregates has been found to be the use of opal-A, which formed the major part of the aggregates. It seems that the use siliceous aggregates, such as opal-A with high pozzolanic activity had effects in promoting the formation of silica network and C-S-H formation, preventing damaging attacks of

OH⁻ ions on other aggregates and helped in the development of high mechanical strength found in these mortars.

Such pozzolanic properties with the likely addition of organic additives have lead these mortars to be durable against wetting and drying cycles. However, the presence of soluble salts has been found to be damaging for these mortars and the masonry structures respectively.

In the light of these results the future studies to be suggested are as follows;

Explorations to find the pozzolanic raw material sources, having the similar characteristics with those of original ones have to be done. Investigations must be done to develop standard raw materials in the market. Several interdisciplinary research is needed on this subject involving chemists, civil engineers, geologists *etc.* together with the architects. Similar investigations should also be extended to the market to find alternative materials to them for the monuments and other buildings.

Studies on the organic additives and their possible sources have to be profoundly done by interdisciplinary research involving chemists, biologists *etc.*

This study has also shown that the materials analyses as well as the structural examination by contemporary non-destructive techniques should be an essential part of the studies on the monuments to be performed before any interventions.

REFERENCES

- Aardt Van J.H.P. and Visser S. (1977) Formation of hydrogarnets: Calcium hydroxide attack on feldspars and clays, *Cement and Concrete Research*, Vol.7, pp. 39-44
- Akman S. M., Güner A. and Aksoy İ.H. (1986) Horasan harcı ve betonunun tarihi ve teknik özellikleri (*The historical and technical aspects of Khorosan Mortar*), 2. *Uluslararası Türk-Islam Bilim ve Teknoloji Tarih Kongresi*, I.T.Ü. (28Nisan-2Mayıs), Ayırbaşım, 18p.
- Aktaş A. (1988) Konyadaki Anadolu Selçuklu Dönemi yapılarında malzeme ve teknik (Materials and techniques in the buildings of Anatolian Seljuk Monuments in Konya), Unpublished Ms Thesis, Hacettepe University, Ankara.
- Aoki T., Hidaka K. and Kato S. (1989) Structural Stability and Profile in the Dome of Santa Maria del Fiore, Proceedings of *Structural Repair and Maintenance of Historical Buildings*, ed. Brebbia C.A., *Computational Mechanics Publications*, Southampton, Boston, pp. 211-220
- Arık O. (1968) Kubadabad Sarayı, *Önasya*, No.38, pp. 6-7
- Arık R. (1992) Kubad-Abad Excavations (1980-1991), *Anatolica*, Annuaire International Pour Les Civilizations de L'Asie Anterieure, No. 18, pp. 101-118
- Ashall, G., Butlin R.N., Teutonico J. M. and Martin W. (1996) Development of lime mortar formulations for use in historic buildings, Proceedings of the Symposium on *Durability of Building Materials and Components*, ed by J. Sjöström, E & FN Spon, Vol. 1, pp. 353-359
- Ashurst J. and Dimes F.G. (1990) Mortars of Stone Buildings in Conservation of Building and Decorative Stone, V.2, Butterworth-Heinemann, pp. 78-93
- ASTM, C144-93 (1980) American Society for Testing and Materials, Specification for Aggregate for Masonry Mortar, pp. 103-104
- ASTM, C270-80a (1980) American Society for Testing and Materials, Specification for Mortar for Unit Masonry, pp. 232-235
- ASTM C 593-89 (1989) American Society for Testing and Materials, Specification for Fly Ash and other Pozzolans for Use with Lime, pp. 294-298

- ASTM, C618-73 (1974) American Society for Testing and Materials, Specification for Fly ash and Raw or Calcined Natural Pozzolan for use in Portland Cement Concrete, pp. 353-356
- ASTM D 2845-90 (1990) American Society for Testing and Materials, Standard Test Method for Laboratory Determination of Pulse Velocities and Ultrasonic Elastic Constants for Rock, pp. 361-365
- Bakırer Ö. (1967) A description of existing XIIIth Century mescids in Konya, Unpublished research report in M.E.T.U., Ankara
- Bakırer Ö. (1981) Selçuklu Öncesi ve Selçuklu Dönemi Anadolu Mimarisinde Tuğla Kullanımı -I- (The use of brick in Anatolian Architecture before and during Sejuk Period), Middle East Technical University, Ankara, pp. 52-53
- Bakolas A., Biscontin G., Moropoulou A. and Zendri E. (1995) Characterization of the lumps in the mortars of historic masonry, *Thermochimica Acta*. 269/270, pp. 809-816
- Balen Van K. and Gemert Van D. (1994) Modelling lime mortar carbonation, *Materials and Structures*, 27, pp. 393-398
- Barret P., Menetrier D. and Cottin B. (1977) Study of silica-lime solution reactions, *Cement and Concrete Research*, Vol.7, pp. 61-67
- Benezet J.C. and Benhassaine A. (1999) Grinding and pozzolanic reactivity of quartz powders, *Powder Technology*, no.105, pp. 167-171
- Benharbit, M. (1994) Interface Pierre-Mortier, Mechanismes de Transfert et d'Alteration, Procède Passivation, Thèse de Doctorat, Université Montpellier II., 196p
- Berger F. (1989) Assessment of Old Masonry by means of Partially Destructive Methods, in the proceedings of *Structural Repair and Maintenance of Historical Buildings*, ed. Brebbia C.A., Computational Mechanics Publications, Southampton Boston, pp. 103-117
- Biricik H., Aköz F., Berktaş I. and Tulgar A.N. (1999) Study of pozzolanic properties of wheat straw ash, *Cement and Concrete Research*, Vol.29, pp. 637-643
- Biscontin G., Bakolas A., Zendri E. and Maravelaki P. (1993) Microstructural and composition characteristics of historic mortars in Venice, *Conservation of Stone and Other Materials*, Proceedings of the International UNESCO-RILEM Congress, Ed by Thiel M.J., E & FN Spon, Paris (June), Vol.1, pp. 178-185
- Black, C.A. (1985) Methods of Soil Analysis, Part 2, American Society of Agronomy, inc. Publisher, Madison, Wisconsin, U.S.A. pp. 999-1010

- Boynton R.S. (1966) *Chemistry and Technology of Lime and Limestone*, John Wiley & Sons, 569p
- Brook N. (1985) The Equivalent Core Diameter Method of Size and Shape Correction in Point Load Testing, *Int. J. Rock. Mech. Min. Sci. And Geomech. Abstr.*, Vol.22, No.2, pp. 61-70
- Brown P.W., Robbins C.R. and Clifton J.R. (1978) Adobe I. The properties of adobe, *IIC – Studies in Conservation*, Vol. 23, No: 4, pp. 139-146
- Brown P.W. and Clifton J.R. (1979) Adobe II. Factors affecting the durability of adobe structures, *IIC – Studies in Conservation*, Vol. 24, No: 1, pp. 23-29
- Bruni S., Cariati F., Fermo P., Cairati P., Alessandrini G., Toniolo L. (1997) White Lumps in Fifth-to Seventeenth-Century AD mortars from Northern Italy, *Archaeometry*, 39.1, pp. 1-7
- Bugini R., Salvatori A., Capanessi G., Sedda A.F., D'Agostini C. and Giuliani C.F. (1993) Investigation of the characteristics and properties of 'cociopesto' from the Ancient Roman Period, *Conservation of Stone and Other Materials*, Proceedings of the International UNESCO-RILEM Congress, ed. by Thiel M.J., E & FN Spon, Paris (June), Vol.1, pp. 386-393
- Caner-Saltık E.N., Schuman I. and Franke L. (1994) A review of stages of damage to brickwork due to salt crystallization, *Proceedings of the British Masonry Society*, No.6, pp. 183-187
- Cowan H.J. (1977) Structure in the Ancient World (pp. 25-75), in *The Master Builders*, John Willey & Sons, Inc. 299p
- Çakmak A.Ş., Davidson R., Mullen C.L. and Erdik M. (1994) Dynamic analysis and earthquake response of Hagia Sophia, *Structural Repair and Maintenance of Historic Buildings III*, eds. Brebbia C.A., Frewer R.J.B., Computational Mechanics Publications, Southampton Boston, pp. 67-84
- Çokça E. (1997) Investigation of some mineralogical, physical and mechanical properties of soils used as structural materials in Van Castle, Proceedings of International Conference on *Studies in Ancient Structures*, ed. by Görün Özşen, Yıldız Technical University, Faculty of Architecture, pp. 275-282
- Davey N. (1961) Gypsum Plaster-Limes and Cements-Stucco-Mortar and Concrete, in; *A History of Building Materials*, Phoenix House, London, pp. 86-128
- Davison J. I. (1976) Mortar technology, Division of Building Research (DBR) Paper No. 692, Rep. from Proceedings of *First Canadian Masonry Symposium*, Calgary, Canada, pp. 12-21
- Diamond S. (1976) A Review of alkali-silica reaction and expansion mechanisms

- (2. Reactive aggregates), *Cement and Concrete Research*, Vol.6, pp. 549-560
- Drees R.L., Wilding L.P., Smeck N.E. and Senkayi A.L. (1995) Silica in Soils: Quartz and disordered silica polymorphs, in; *Minerals in Soil Environments*, SSSA Book Series: 1, Co-Eds; Dixon J.B. and Weed S.B., Soil Society of America, Madison, Wisconsin, U.S.A., pp. 913-975
- Duffy A.P., Copper T.P. and Perry S.H. (1993) Repointing Mortars for Conservation of a Historic Stone Building in Trinity College, Dublin, *Matériaux et Constructions*, Vol.26, No.159, pp.302-306
- Dülgerler O.N. (1979) Konya'da Türk-İslam Dönemi mezar anıtlarının özellikleri, Unpublished dissertation for the qualification for Ph. D., V.1. (Metin-text), Konya
- Eckel-Edwin C. (1928) Cements, Limes and Plasters (Their Materials, Manufacture and Properties), New York, pp. 91-583
- Elfvig P., Panas I. and Lindqvist O. (1996) *In situ* IR study on the initial sulphation and carbonation of Ca(OH)₂ and CaO by SO₂ polluted air, *Atmospheric Environment*, Elsevier Science Ltd., Vol.30, No.23, pp. 4085-4089
- Erdoğan, T.Y. (1995) Betonun Oluşturan Malzemeler - Çimentolar (Materials Constitute Concrete - Cements), Türkiye Hazır Beton Birliği (Turkish Pre-cast Concrete Association), İstanbul, 121p
- Escalante J.I., Mendoza G., Mancha H., Lopez J. and Vargas G. (1999) Pozzolanic properties of a geothermal silica waste material, *Cement and Concrete Research*, Vol. 29, pp. 623-625
- Ethem İ. (1969) Tarihi Türk Hanları (Historical Turkish Hans), Karayolları Genel Müdürlüğü (General Directorate of Highways), 121p.
- Falade F. (1993) The Compressive Strength of Lateritic Mortars: The Effect of Mix Proportion, Source and Water/Cement Ratio, *Masonry International*, Vol.7, No.1, pp.2-5
- Güleç A. (1992) Bazı tarihi anıt harç ve sıvalarının incelenmesi (Characterization of mortars and plasters of some historic monuments), Unpublished Ph.D. Thesis, Istanbul Technical University, Institute of Natural and Applied Science
- Güngör N. (2000) (Personal communication), Former staff in 'Maden Analizleri Teknoloji Dairesi, M.T.A. (The Mineral Research and Exploration Institute of Turkey), Ankara
- Hanawalt Method (1978) Powder Diffraction File Search Manual, Inorganic Compounds, JCPDS-International Center for Diffraction Data, Pennsylvania, U.S.A.

- Hidaka K., Aoki T. and Kato S. (1989) Structural Stability and Profile in the Dome of HagiaSophia, Istanbul, *Structural Repair and Maintenance of Historical Buildings*, ed. Brebbia C.A., Computational Mechanics Publications, Southampton Boston, pp. 267-273
- Holmes S. and Wingate M. (1997) Building with Lime (A Practical Introduction), Intermediate Technology Publications, London, 306p.
- Hughes R.E. (1988) The geotechnical study of soils used as structural materials in historic monuments, *The Engineering Geology of Ancient Works and Historical Sites*, V.2, eds. Marinos & Koukis, Balkema, Rotterdam, pp. 1041-1048
- İpekoğlu-Acar B. (1993) Buildings with combined Functions in Anatolian Seljuk Architecture (An evaluation of design principles, past and present functions), Unpublished Ph.D. Thesis, Middle East Technical University, Graduate School of Natural and Applied Science
- ISRM, POINT LOAD TEST (1985) Suggested Method for Determining Point Load Strength, in: *Int. J. Rock Mech. Min. Sci. & Geomech. Abstr.*, Vol.22, No.2, pp. 51-70
- Jedrzejewska H. (1981) Ancient Mortars as Criterion in Analysis of Old Architecture, in the Proceedings of Symposium on, *Mortars, Cements and Grouts Used in the Conservation of Historic Buildings*, Rome pp. 311-329
- Karamağaralı, H. (1982) Sahip Ata Camii'nin restitüsyonu hakkında bir deneme, *Rölöve ve Restorasyon Dergisi*, Vakıflar Genel Müdürlüğü Yayınları, No.3, Ankara
- Karpuz E. (1998) 1997 Yılı Konya Eflaki Dede Türbesi sondaj ve kurtarma kazısı çalışmaları, *IX. Müze Kurtarma Kazıları Semineri, 27-29 Nisan (Antalya)* T.C. Kültür Bakanlığı, Anıtlar ve Müzeler Genel Müdürlüğü Yayınları, Yayın No. 64, Ankara, pp. 111-124
- Kaviak T. (1990) Gypsum mortars from a Twelfth Century Church in Wislica, Poland, *Studies in Conservation*, Iss.36, pp. 142-150
- Knöfel D.F.E. and Wisser S.G. (1988) Microscopical investigations of some historic mortars, Conservation of Brick Structures, *Proceedings of the 2nd Expert Meeting of the NATO-CCMS-Pilot Study*, Berlin (April) pp. 212-222
- Lea, F.M. (1970) The Chemistry of Cement, Ed. Edward Arnold (3rd ed.), London, pp. 414-453
- Lewin S.Z. (1981) X-Ray diffraction and scanning electron microscope analysis of conventional mortars, in the Proceedings of Symposium on, *Mortars, Cements and Grouts Used in the Conservation of Historic Buildings*, Rome, pp. 101-131

- Livingston R.A., Wolde-Tinsae A. and Chaturbahai A. (1991) The use of gypsum mortar in historic buildings, *Structure and Maintenance of Historic Buildings II*, eds. Brebbia C.A., Domingues J, Escrig F., Computational Mechanics Publications, Southampton Boston, pp. 157-165
- Livingston R.A. (1993) Materials analysis of the masonry of the Hagia Sophia Basilica, Istanbul, *Structural Repair and Maintenance of Historic Buildings III*, eds. Brebbia C.A., Frewer R.J.B., Computational Mechanics Publications, Southampton Boston, pp. 15-32
- Luxan M.P. , Madruga F. and Saavedra J. (1989) Rapid Evaluation of Pozzolanic Activity of Natural Products by Conductivity Measurement, *Cement and Concrete Research*, Vol. 19, pp. 63-68
- Malinowski R. (1981) Ancient mortars and concretes: Durability aspects, *Mortars, Cements and Grouts Used in the Conservation of Historic Buildings*, Proceedings of Symposium in Rome, pp. 341-350
- Mark R., Çakmak A.S., Hill K. and Davidson R. (1993) Structural analysis of Hagia Sophia: A Historical perspective, *Structural Repair and Maintenance of Historic Buildings III*, ed. by Brebbia C.A. and Frewer R.J.B., Computational Mechanics Publications, Southampton, Boston, pp. 33-46
- Martirena-Hernandez J.F., Middendorf B., Gehrke M. and Budelmann H. (1998) Use of waste of the sugar industry as pozzolana in lime-pozzolana binders: study of the reaction, *Cement and Concrete Research*, Vol. 28, no.11, pp. 1525-1536
- Martinez-Ramirez (1995) Carbonation process and properties of new lime mortar with added sepiolite, *Cement and Concrete Research*, Vol.25, No.1, pp.39-50
- Massazza F. and Pezzuoli M. (1981) Some teachings of a Roman Concrete, *Mortars, Cements and Grouts Used in the Conservation of Historic Buildings*, Proceedings of Symposium in Rome, pp. 219-245
- Middendorf B. and Knöfel D. (1994) Characterization of mortars from historic German brick buildings and requirements for restoration materials, Proceedings of the *Third International Masonry Conference*, London (Oct. 1992), ed. by West H.W.H., British Masonry Society, No.6, pp. 24-29
- Morehead D.R. (1986) Cementation of hydrated lime, *Cement and Concrete Research*, Vol. 16, pp. 700-708
- Mora L., Mora P. and Philippot P. (1984) Technology of the principal constituents of renderings, in Conservation of Wall Paintings, ICCROM, Butterworths, p. 35-56
- Moropoulou A., Biscontin G, Bakolas A., Michailidis P. and Basiotis J. (1997) Historic Mortars in Mediterranean Monuments, in the Proceedings of the 4th

International Symposium on the Conservation of Monuments in Mediterranean, ed. Moropoulou A., Zezza F. and Papachristodoulou, (6-11 May), Vol.3, Rhodous, pp. 213-237

Norton John (1997) *Building with Earth; A Handbook, Intermediate Technology Publications*, by SRP, Exeter, London. p. 9

Oliver M. and Mesbah A. (1993) Behavior of ancient and new structures made out of raw earth, *Structural Repair and Maintenance of Historic Buildings III*, ed. by Brebbia C.A., and Frewer R.J.B., Computational Mechanics Publications, Southampton, Boston, pp. 440-447

Osunade, J.A. (1993) The compressive strength of lateritic Concrete: The Effect of Types and Sizes of Coarse Aggregate, *Masonry International*, Vol.7, No.1, pp. 1-2

Öney G. (1967) Akşehir Ulu Camisi, Anadolu (Anatolia) IX, 1965'den ayrışım, Türk Tarih Kurumu Basımevi, Ankara

Papayianni I. (1997) Technology of mortars and bricks used in Ottoman Monuments of Thessaloniki, *Proceedings of Conference on Studies in Ancient Structures* ed. by Görün Özşen, Yıldız Technical University, Faculty of Architecture, pp. 245-253

Papayianni I. and Stefanidou M. (1997) Repair mortars suitable for interventions of Ottoman buildings, *Proceedings of Conference on Studies in Ancient Structures*, ed. by Görün Özşen, Yıldız Technical University, Faculty of Architecture, pp. 255-263

Penelis G., Papayianni J. and Karaveziroglou M (1989) Pozzolanic mortars for repair of masonry structures, *Proceedings of Structural Repair and Maintenance of Historical Buildings*, ed. Brebbia C.A., Computational Mechanics Publications, Southampton, Boston, pp. 161-169

Price W.H. (1975) Pozzolans – A Review, *ACI Journal*, (May), pp. 225-232

Qijun Y., Sawayama K., Sugita S., Shoya M. and Isojima Y. (1999) The reaction between rice husk ash and $\text{Ca}(\text{OH})_2$ solution and the nature of its product, *Cement and Concrete Research*, Vol.29, pp. 37-43

RILEM (1980) Tentative Recommendations, Comission-25-PEM, Recommended Tests to Measure the Deterioration of Stone and to Assess the Effectiveness of Treatment Methods, *Materiaux and Construction*, Vol.13, No.73, pp.173-253

Robert L. D. and Caijun S. (1994) Influence of the fineness of pozzolan on the strength of lime-natural pozzolan cement pastes, *Cement and Concrete Research*, Vol. 24, No. 8, pp. 1485-1491

- Rodriguez J.D. and Jeremias F.T. (1990) Assessment of Rock Durability through Index Properties, *6th International IAEG Congress*, V.4, pp. 493-499
- Salvadori M. (1982) *Why Buildings Stand Up (The Strength of Architecture)*, McGraw-Hill, 311p.
- Satongar (Laçinyurt) Ş. (1994) İstanbul şehir surları Horasan harçları üzerine bir araştırma (An Investigation on Horasan Mortars of Istanbul City Walls), Unpublished MS Thesis, Institute of Natural and Applied Science, Istanbul Technical University
- Schaffer R.J. (1972) *The Weathering of Natural Building Stones*, Department of Scientific and Industrial Research, Special Report No.18, London, 149p.
- Schäfer J. and Hilsdorf H.K. (1993) Ancient and new lime mortars: The correlation between their composition, structure and properties, *Conservation of Stone and Other Materials*, Proceedings of the International UNESCO-RILEM Congress, ed. by Thiel M.J., E & FN Spon, Paris (June), Vol.2, pp. 605-612
- Sickels L.B. (1981) Organics vs synthetics: Their use as additives in mortars, *Mortars, Cements and Grouts Used in the Conservation of Historic Buildings*, Proceedings of Symposium in Rome, pp. 25-52
- Taves L.B.S. (1995) An Analysis of Creep and Shrinkage in Mortars, *Journal of Testing and Evaluation*, *JTEVA*, Vol.22, No.6, pp.548-555
- Teutonico J.M. (1986) *A Laboratory Manual for Architectural Conservators*, ICCROM, Rome, pp. 32-122
- Teutonico J. M., McCaig, I., Burns C. and Ashurst J. (1994) The Smeaton Project: Factors affecting the properties of lime-based mortars, *Lime News*, 2:2, pp. 7-13
- Timoshenko S. (1970) *Strength of Materials*, in Chapter II, Analysis of Stress and Strain, Van Nostrand Reinhold Company, Holland, p.53
- Topal (1995) *Formation and Deterioration of Fairy Chimneys of the Kavak Tuff in Ürgüp-Göreme Area (Nevşehir-Turkey)*, Unpublished Ph.D. Thesis, submitted in the Department of Geological Engineering, Middle East Technical University, Ankara, pp. 61-67
- Topal (1999/2000) *Nokta Yükleme Deneyi ile İlgili Uygulamalarda Karşılaşılan Problemler (Problems in the Applications of the Point Load Index Test)*, *Jeoloji Mühendisliği Dergisi (Geological Engineering Journal)*, Vol.23/24, No. 1, pp. 73-86
- Tucker M.E. (1991) *Sedimentary Petrology (an introduction to the origin of sedimentary rocks)*, in Chapter 2: Siliciclastic Sediments, p. 16, Blackwell Scientific Publications, 260 p.

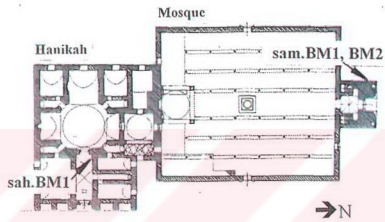
- Tuncoku S.S., Caner-Saltık E.N. and Böke H. (1993) Definition of the materials and related problems of a XIIIth Century Anatolian Seljuk 'Mesjid': A case study in Konya City, *Conservation of Stone and Other Materials*, Proceedings of the International UNESCO-RILEM Congress, ed. by Thiel M.J., E & FN Spon, Paris (June), Vol.1, pp. 368-375
- Vitruvius (1990) Mimarlık Üzerine On Kitap (Ten Books on Architecture), Çev. Suna Güven, Şevki Vanlı Vakfı Mimarlık Yayınları, pp. 29-32
- Walter E. Dean Jr. (1974) Determination of Carbonate and Organic Matter in Calcereous Sediments and Sedimentary Rocks by Loss on Ignition: Comparison with Other Methods, *Journal of Sedimentary Petrology*, Vol. 44,
- Wang H. and Gillott J.E. (1991) Mechanism of alkali-silica reaction and the significance of calcium hydroxide, *Cement and Concrete Research*, Vol.21, pp. 647-654
- Winkler E.M. (1986) Durability Index of Stone. *Bulletin of Association of Engineering Geologist*. Vol.23. p. 344
- Wisser S., Kraus K. and Knöfel D. (1988) Composition and properties of historic lime mortars, 6th International Congress on *Deterioration and Conservation of Stone*, ed. by J. Ciabach, Nicolas Copernicus University Press, Torun, pp. 426-431
- Young C.A. and Miller J.D. (2000) Effect of temperature on oleate adsorption at a calcite surface: an FT-NIR/IRS study and review, *Int. J. Miner. Process*, pp.331-350

APPENDIX A

A1: Sahip Ata Complex **A2:** İnce Minareli Medrese and the Mescid



A1.1 Hanikah, Entrance Façade



A1.2 Sahip Ata Hanikahı and Mosque, Plan
(Redrawn from Karamağaralı, 1982)



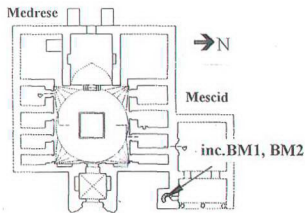
A1.3 Hanikah Hall, Corner of North Wall
(● sah.BM1)



A1.4 The Minaret of the Mosque
(● sam.BM1, ● sam. BM2)



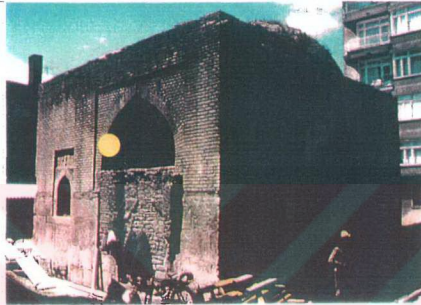
A2.2 The Minaret of the Mescid
(● inc.BM1, ● inc.BM2)



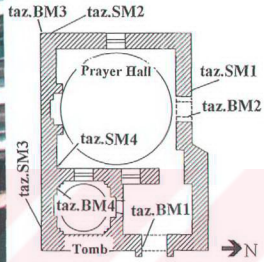
A2.1 İnce Minareli Medrese and Mescid
Plan (İpekoğlu, 1993)

APPENDIX B

Tahir ile Zühre Mescidi



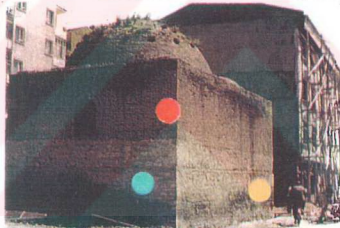
B1. Tahir ile Zühre Mescidi, Entrance Façade
(● taz.BM1)



B2. Tahir ile Zühre Mescidi,
Plan (Redrawn from Tuncoku, 1993)



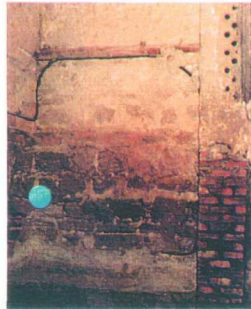
B3. Entrance of the Prayer Hall
(● taz.BM2, ● taz.SM1)



B4. South and West Walls, Exterior
(● taz.BM3, ● taz.SM2, ● taz.SM3)



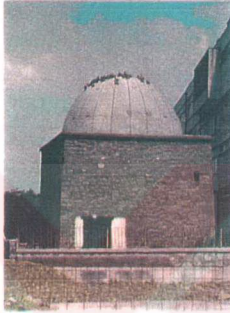
B5. Tomb Space, South-West Corner
(● taz.BM4)



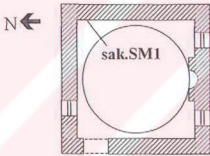
B6. Prayer Hall, South-East Corner
(● taz.SM4)

APPENDIX C

C1: Sakahane Mescidi C2: Hoca Hasan Mescidi C3: Zenburi Mescidi



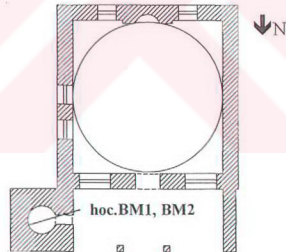
C1.1 Sakahane Mescidi, Entrance Facade



C1.2 Sakahane Mescidi, Plan
(Redrawn from Bakrer, 1967)



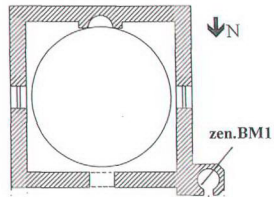
C2.2 The Minaret of Hoca Hasan Mescidi
(● hoc.BM1, ● hoc.BM2)



C2.1 Hoca Hasan Mescidi, Plan
(Redrawn from Bakrer, 1967)



C3.2 The Minaret of Zenburi Mescidi
(● zen.BM1)



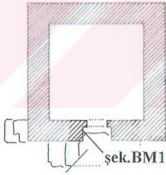
C3.1 Zenburi Mescidi, Plan
(Redrawn from Bakrer, 1967)

APPENDIX D

D1: Hatuniye Mescidi D2: The Remains of Larende Gate D3: Eflaki Dede Tomb
D4: Şekerfuruş Tomb



D1 The Minaret of Hatuniye Mescidi
(● hat. BM1, ● hat. BM2)



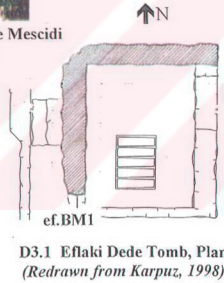
D4.1 Şekerfuruş Tomb, Plan



D4.2 Şekerfuruş Tomb, Entrance Façade



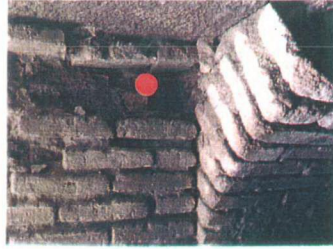
D2 The Remains of Larende Gate (● lar.SM1)



D3.1 Eflaki Dede Tomb, Plan
(Redrawn from Karpuz, 1998)



D3.2 Eflaki Dede Tomb, West Wall
(● ef.BM1)



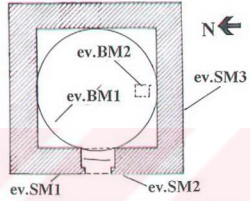
D4.3 Entrance Space, North Wall, Interior
(● şek.BM1)

APPENDIX E

E1: Evhadeddin Kirmani Tomb E2: Bedreddin Gühertaş Tomb
E3: Gömeç Hatun Tomb



E1.1 Evhadeddin Kirmani Tomb, Entrance Façade
 (● ev.BM1, ● ev.SM1, ● ev.SM2)



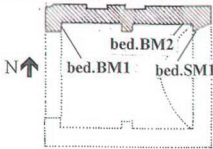
E1.2 Evhadeddin Kirmani Tomb, Plan
 (Redrawn from Dülgerler, 1979)



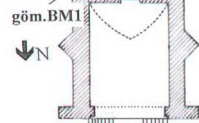
E2.1 Bedreddin Gühertaş Tomb, North Wall,
 Interior (● bed.BM1, ● bed.BM2, ● bed.SM1)



E1.3 Evhadeddin Kirmani Tomb, South Façade
 Interior (● ev.BM2, ● ev.SM3)



E2.2 Bedreddin Gühertaş Tomb
 Plan (Redrawn from Dülgerler,
 1979)



E3.1 Gömeç Hatun Tomb, Plan
 (Redrawn from Dülgerler, 1979)



E3.2 Gömeç Hatun Tomb,
 North Façade



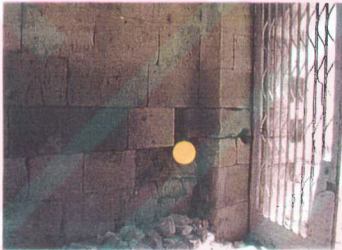
E3.3 Gömeç Hatun Tomb, East
 Façade (● göm. BM1)

APPENDIX F

Zazadin Han



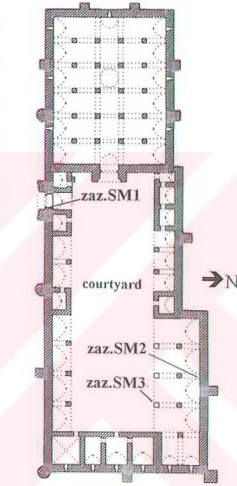
F.1 Zazadin Han, General View



F.3 Entrance Eyvan, Sout-East Corner
(● zaz.SM1)



F.4 Courtyard, North Side Vaults
(● zaz.SM2)



F.2 Zazadin Han, Plan
(Redrawn from Ethem, 1969)



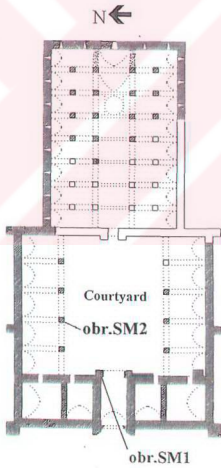
F.5 Courtyard, North Side Vaults
(● zaz.SM3)

APPENDIX G

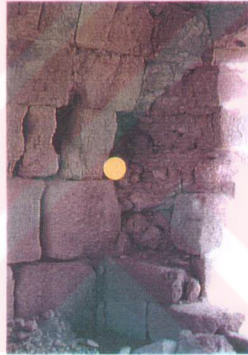
Obruk Han



G1. Obruk Han, General View



G2. Obruk Han, Plan
(Redrawn from Ethem, 1969)



G3. Entrance Eyvan, South-West Corner
(● obr.SM1)



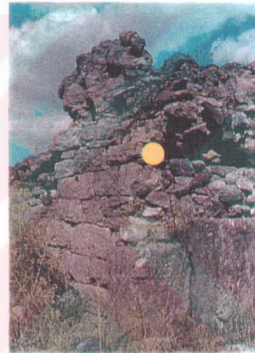
G4. Courtyard, North Side Vaults (● obr.SM2)

APPENDIX H

Kuruçeşme Han



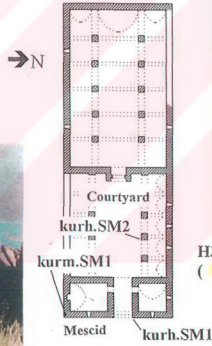
H1. Kuruçeşme Han, Entrance Façade



H3. Entrance Gate, North-East Corner
(● kurh.SM1)



H4. Courtyard, North Side Vaults
(● kurh.SM2)



H2. Kuruçeşme Han, Plan
(Redrawn from Ethem, 1969)



H5. Mescid Space, Interior of the
East Wall and the Vault (● kurm.SM1)

APPENDIX I

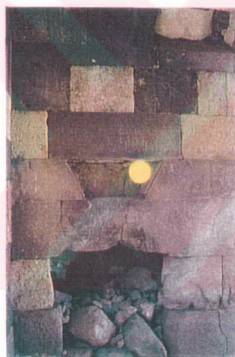
Kızılören Han and the Mescid Building



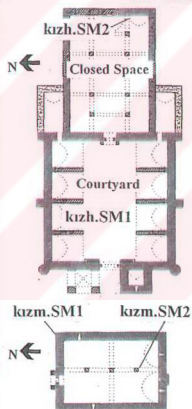
II.1 Kızılören Han, General View



II.2 Mescid Building, General View



II.4 The Han, Entrance Eyvan,
South-West Wall (● kızh.SM1)



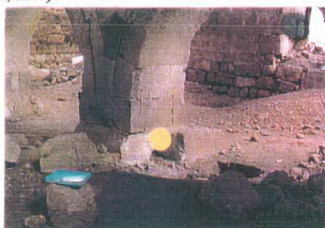
II.3 Kızılören Han and Mescid, Plans
(Redrawn from Ethem, 1969)



II.5 The Han, Closed Space,
Central Vault (● kızh.SM2)



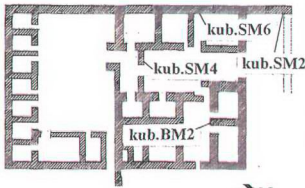
II.6 Mescid Building, North-East Corner,
Exterior (● kızm.SM1)



II.7 Mescid Building, Footing of the third
Pier (● kızm.SM2)

APPENDIX J1

Kubadabad – The Great Palace



J1.1 The Great Palace, Plan
(Modified from Arık, 1968)
Samples have been provided through the
courtesy of Prof. Dr. Rüçhan & Oluş Arık



J1.2 The Great Palace, General View



J1.3 The Great Palace, (● kub.SM2)



J1.4 The Great Palace, (● kub.SM4)



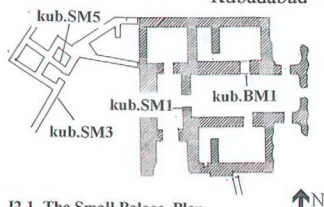
J1.5 The Great Palace, (● kub.SM6)



J1.6 The Great Palace, (● kub.BM2)

APPENDIX J2

Kubadabad – The Small Palace



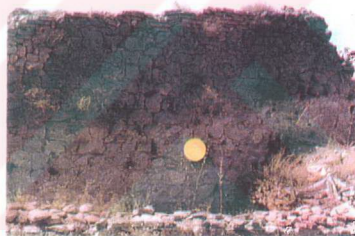
J2.1 The Small Palace, Plan
(Redrawn from Artık, 1992)
Samples have been provided through the
courtesy of Prof. Dr. Rüçhan & Oluş Artık)



J2.2 The Small Palace, General View



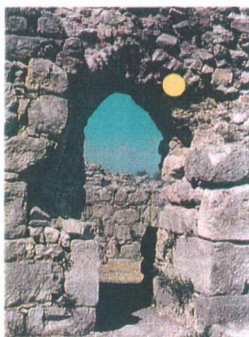
J2.3 The Small Palace, (● kub.SM1)



J2.4 The Small Palace, (● kub.SM3)



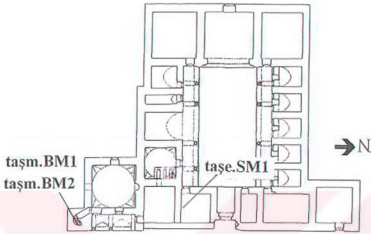
J2.5 The Small Palace, (● kub.SM5)



J2.6 The Small Palace, (● kub.BM1)

APPENDIX K

K1: Taş Medrese and the Mescid K2: Akşehir Ulu Camii
K3: Güdük Minare Mescidi



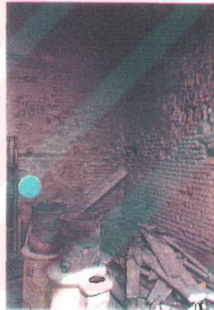
K1.1 Taşmedrese and Mescid, Plan (İpekoğlu, 1993)



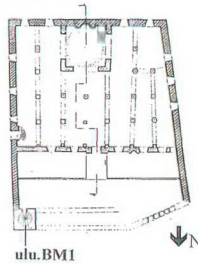
K1.2 Taşmedrese and Mescid, General View
 (● taşm.BM1, ● taşm.BM2)



K2.1 The Minaret of Ulucami
 (● ulu.BM1)



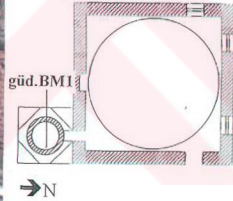
K1.3 Taşmedrese, Eyvan
 (● taşe.SM1)



K2.2 Ulucami, Plan
 (Redrawn from Öney, 1967)



K3.1 Güdük Minareli Mescid, Entrance Façade



K3.2 Güdük Minareli Mescid, Plan
 (Redrawn from Bakurer, 1967)



K3.3 The Minaret of Güdük Minareli Mescid
 (● güd.BM1)

APPENDIX L

**BASIC PHYSICAL PROPERTIES OF STONE AND
BRICK MASONRY MORTARS**

Table L1 Porosity and density of stone masonry mortars

Sample	m_{dry} (g)	m_{sat} (g)	m_{arch} (g)	P (%)	D (g/cm³)
ev.SM1(1)	8,73	11,63	5,35	46,18	1,39
SM1(2)	12,18	16,55	7,46	48,07	1,34
SM1(3)	15,22	19,67	9,10	42,10	1,44
ev.SM1				45,45	1,39
ev.SM2(1)	8,35	10,89	4,97	42,91	1,41
SM2(2)	10,40	13,31	6,15	40,64	1,45
SM2(3)	17,06	21,62	9,93	39,01	1,46
ev.SM2				40,85	1,44
ev.SM3(1)	10,53	13,01	6,33	37,13	1,58
SM3(2)	12,35	15,32	7,36	37,31	1,55
ev.SM3				37,22	1,56
bed.SM1(1)	18,87	23,52	11,58	38,94	1,58
SM1(2)	6,29	7,80	3,87	38,42	1,60
SM1(3)	14,40	18,17	8,85	40,45	1,55
bed.SM1				39,27	1,58
sak.SM1(1)	6,90	8,28	4,00	32,24	1,61
SM1(2)	9,50	11,12	5,24	27,55	1,62
SM1(3)	18,90	22,27	11,08	30,12	1,69
sak.SM1				29,97	1,64
taş.SM1(1)	12,85	15,08	7,90	31,06	1,79
SM1(2)	16,10	18,82	9,93	30,60	1,81
SM1(3)	24,55	29,30	15,16	33,59	1,74
taş.SM1				31,75	1,78
lar.SM1(1)	10,80	13,03	6,66	35,01	1,70
SM1(2)	11,21	13,49	6,76	33,88	1,67
SM1(3)	23,31	28,80	14,39	38,10	1,62
lar.SM1				35,66	1,66

Table L1 continued

kub.SM1(1)	20,11	26,87	12,49	47,01	1,40
SM1(2)	15,84	20,79	9,65	44,43	1,42
SM1(3)	8,36	10,72	5,07	41,77	1,48
kub.SM1				44,40	1,43
kub.SM2(1)	14,69	19,54	9,12	46,55	1,41
SM2(2)	16,76	22,18	10,42	46,09	1,43
SM2(3)	15,18	19,90	9,41	45,00	1,45
kub.SM2				45,88	1,43
kub.SM3(1)	20,10	23,55	12,31	30,69	1,79
SM3(2)	7,95	9,46	4,86	32,83	1,73
SM3(3)	15,85	18,70	9,69	31,63	1,76
kub.SM3				31,72	1,76
kub.SM4(2)	11,94	14,44	7,23	34,67	1,66
SM4(3)	13,01	15,70	7,89	34,44	1,67
kub.SM4				34,56	1,66
kub.SM5(1)	8,12	10,13	5,05	39,57	1,60
SM5(2)	10,54	13,35	6,58	41,51	1,56
SM5(3)	8,03	10,23	4,99	41,98	1,53
kub.SM5				41,02	1,56
kub.SM6(1)	11,26	14,18	6,98	40,56	1,56
SM6(2)	7,81	9,71	4,83	38,93	1,60
SM6(3)	10,46	13,08	6,49	39,76	1,59
kub.SM6				39,75	1,58
kurh.SM1(2)	18,12	20,81	11,24	28,11	1,89
SM1(3)	12,89	15,14	8,02	31,60	1,81
kurh.SM1				29,85	1,85
kurh.SM2(1)	19,65	23,16	12,34	32,44	1,82
SM2(3)	21,68	25,65	13,62	33,00	1,80
kurh.SM2				32,72	1,81
kurm.SM1(1)	21,7	25,32	13,64	30,99	1,86
SM1(2)	20,82	24,52	13,17	32,60	1,83
SM1(3)	14,03	16,71	8,93	34,45	1,80
kurm.SM1				32,68	1,83
kızh.SM1(1)	22,06	25,33	12,11	24,74	1,67
SM1(2)	19,05	21,79	10,46	24,18	1,68
SM1(3)	25,71	30,29	14,31	28,66	1,61
kızh.SM1				25,86	1,65

Table L1 continued

kızh.SM2(1)	13,68	17,99	7,33	40,43	1,28
SM2(2)	21,39	29,56	11,30	44,74	1,17
SM2(3)	12,88	17,56	6,88	43,82	1,21
kızh.SM2				43,00	1,22
kızm.SM1(1)	9,90	12,90	6,05	43,80	1,45
SM1(2)	16,99	21,73	10,26	41,33	1,48
SM1(3)	14,05	18,12	8,49	42,26	1,46
kızm.SM1				42,46	1,46
kızm.SM2(1)	19,74	24,56	11,95	38,22	1,57
SM2(2)	15,10	18,50	9,11	36,21	1,61
SM2(3)	19,96	24,21	11,97	34,72	1,63
kızm.SM2				36,38	1,60
zaz.SM1(2)	14,96	18,58	9,34	39,18	1,62
SM1(3)	12,93	16,62	8,11	43,36	1,52
zaz.SM1				41,27	1,57
zaz.SM2(1)	18,03	23,02	11,18	42,15	1,52
SM2(2)	13,33	16,81	8,19	40,37	1,55
SM2(3)	17,34	21,95	10,77	41,23	1,55
zaz.SM2				41,25	1,54
zaz.SM3(1)	7,81	9,70	4,55	36,70	1,52
SM3(3)	14,51	18,17	8,47	37,73	1,50
zaz.SM3				37,22	1,51
obr.SM1(1)	10,47	13,58	6,20	42,14	1,42
SM1(2)	10,87	14,34	6,49	44,20	1,38
SM1(3)	7,75	10,12	4,63	43,17	1,41
obr.SM1				43,17	1,41
obr.SM2(1)	17,76	22,75	10,33	40,18	1,43
SM2(2)	10,45	13,34	6,07	39,75	1,44
SM2(3)	11,70	15,25	6,81	42,06	1,39
obr.SM2				40,66	1,42

Table L2 Porosity and density of brick masonry mortars

Sample	m_{dry} (g)	m_{sat} (g)	m_{arch} (g)	P (%)	D (g/cm ³)
sah.BM1(1)	13,49	15,81	7,64	28,40	1,65
BM1(2)	12,80	15,00	7,21	28,24	1,64
BM1(3)	21,55	25,54	12,26	30,05	1,62
sah.BM1				28,89	1,64
sam.BM1(1)	10,00	14,18	6,19	52,32	1,25
BM1(2)	16,90	23,39	10,06	48,69	1,27
BM1(3)	11,71	16,66	7,23	52,49	1,24
sam.BM1				51,16	1,25
sam.BM2(1)	17,13	24,42	10,53	52,48	1,23
BM2(3)	16,80	23,82	10,33	52,04	1,25
sam.BM2				52,26	1,24
zen.BM1(1)	13,12	17,15	7,93	43,71	1,42
BM1(2)	10,55	13,98	6,41	45,31	1,39
BM1(3)	14,47	19,11	8,73	44,70	1,39
zen.BM1				44,57	1,40
ev.BM1(1)	9,46	12,71	5,80	47,03	1,37
BM1(2)	9,93	13,56	6,11	48,72	1,33
BM1(3)	13,07	17,65	8,05	47,71	1,36
ev.BM1				47,82	1,35
ev.BM2(1)	14,25	19,62	8,75	49,40	1,31
BM2(2)	9,42	12,76	5,74	47,58	1,34
BM2(3)	18,53	25,18	11,31	47,95	1,34
ev.BM2				48,31	1,33
şek.BM1(1)	11,88	13,27	7,02	22,24	1,90
BM2(2)	19,45	23,01	11,81	31,79	1,74
BM2(3)	13,18	15,37	7,92	29,40	1,77
şek.BM1				27,81	1,80
hoc.BM1(1)	14,01	17,74	8,62	40,90	1,54
BM1(2)	19,48	24,85	11,96	41,66	1,51
BM1(3)	17,25	21,77	10,62	40,54	1,55
hoc.BM1				41,03	1,53
hoc.BM2(1)	15,96	20,04	9,63	39,19	1,53
BM2(3)	17,81	22,02	10,71	37,22	1,57
hoc.BM2				38,21	1,55

Table L2 continued

göm.BM1(2)	15,43	20,14	9,51	44,31	1,45
BM1(3)	11,37	14,55	6,95	41,84	1,50
göm.BM1				43,08	1,47
bed.BM1(1)	19,15	23,01	11,62	33,89	1,68
BM1(2)	14,04	16,78	8,56	33,33	1,71
BM1(3)	26,35	31,68	15,92	33,82	1,67
bed.BM1				33,68	1,69
bed.BM2(1)	10,71	12,86	6,63	34,51	1,72
BM2(2)	13,08	15,87	8,13	36,05	1,69
BM2(3)	13,27	15,93	8,22	34,50	1,72
bed.BM2				35,02	1,71
hat.BM1(1)	10,12	12,75	6,19	40,09	1,54
BM1(2)	9,53	12,07	5,87	40,97	1,54
BM1(3)	22,61	28,51	13,73	39,92	1,53
hat.BM1				40,33	1,54
hat.BM2(1)	11,54	14,34	6,97	37,99	1,57
BM2(2)	9,44	11,78	5,72	38,61	1,56
BM2(3)	15,37	19,06	9,25	37,61	1,57
hat.BM2				38,07	1,56
ef.BM1(1)	7,57	9,63	4,48	40,00	1,47
BM1(2)	19,45	24,54	11,49	39,00	1,49
BM1(3)	19,35	24,11	11,29	37,13	1,51
ef.BM1				38,71	1,49
inc.BM1(1)	5,07	6,67	3,12	45,07	1,43
BM1(2)	6,44	8,30	3,86	41,89	1,45
BM1(3)	6,45	8,23	3,88	40,92	1,48
inc.BM1				42,63	1,45
inc.BM2(1)	7,92	9,86	4,90	39,11	1,60
BM2(2)	12,79	16,02	7,87	39,63	1,57
BM2(3)	20,30	25,39	12,45	39,34	1,57
inc.BM2				39,36	1,58
taşm.BM1(2)	11,39	15,12	6,99	45,88	1,40
BM1(3)	14,20	18,74	8,72	45,31	1,42
taşm.BM1				45,59	1,41
taşm.BM2(1)	15,71	19,99	9,74	41,76	1,53
BM2(2)	17,49	23,34	10,92	47,10	1,41
BM2(3)	13,26	17,17	8,31	44,13	1,50
taşm.BM2				44,33	1,48

Table L2 continued

ulu.BM1(1)	12,50	15,89	7,46	40,21	1,48
BM1(2)	13,19	17,76	8,27	48,16	1,39
BM1(3)	18,60	24,99	11,60	47,72	1,39
ulu.BM1				45,36	1,42
güd.BM1(1)	9,38	12,44	5,83	46,29	1,42
BM1(2)	11,13	14,15	6,68	40,43	1,49
BM1(3)	8,89	11,61	5,46	44,23	1,45
güd.BM1				43,65	1,45
kub.BM1(1)	10,69	14,28	6,61	46,81	1,39
BM1(2)	10,96	14,61	6,81	46,79	1,41
BM1(3)	12,60	16,42	7,83	44,47	1,47
kub.BM1				46,02	1,42
kub.BM2(1)	16,60	19,90	10,17	33,92	1,71
BM2(2)	8,93	10,49	5,45	30,95	1,77
BM2(3)	17,55	20,64	10,59	30,75	1,75
kub.BM2				31,87	1,74

APPENDIX M

PHYSICAL PROPERTIES OF BRICKS USED IN SOME OF THE MONUMENTS

Table M1 Porosity and density of the bricks

Sample	m_{dry} (g)	m_{sat} (g)	m_{arch} (g)	P (%)	D (g/cm ³)
sah.B1(1)	24,34	33,32	14,92	48,80	1,32
B1(2)	22,55	30,68	13,85	48,31	1,34
B1(3)	16,61	22,85	10,29	49,68	1,32
sah.B1				48,93	1,33
sam.B1(1)	20,12	27,81	12,52	50,29	1,32
B1(2)	20,34	28,09	12,75	50,52	1,33
B1(3)	12,37	17,04	7,67	49,84	1,32
sam.B2(1)	22,38	30,99	13,93	50,47	1,31
B2(2)	15,68	21,76	9,75	50,62	1,31
B2(3)	12,30	17,24	7,71	51,84	1,29
sam.B1,B2				50,60	1,31
zen.B1(1)	19,63	29,06	12,61	57,33	1,19
B1(2)	19,01	28,29	12,12	57,39	1,18
B1(3)	15,92	23,72	10,05	57,06	1,16
B1(4)	19,39	28,45	12,23	55,86	1,20
zen.B1				56,91	1,18
ev.B1(1)	23,48	29,55	13,14	36,99	1,43
B1(2)	25,38	31,83	14,57	37,37	1,47
B1(3)	24,37	30,99	13,78	38,47	1,42
B1(4)	25,55	32,23	14,57	37,83	1,45
ev.B1				37,66	1,44
şek.B1(1)	28,27	34,10	16,91	33,92	1,64
B1(2)	22,24	27,52	13,39	37,37	1,57
B1(3)	25,23	30,95	15,10	36,09	1,59
B1(4)	25,72	31,23	15,46	34,94	1,63
şek.B1				35,58	1,61
hoc.B1(1)	51,27	74,30	32,89	55,61	1,24
B1(2)	51,87	74,56	33,26	54,94	1,26
hoc.B1				55,28	1,25

Table M1 continued

göm.B1(1)	22,68	29,83	13,82	44,66	1,42
B1(2)	25,76	33,97	15,44	44,31	1,39
B1(3)	24,21	31,90	14,47	44,12	1,39
B1(4)	24,12	31,74	14,66	44,61	1,41
göm.B1				44,42	1,40
bed.B1(1)	29,52	39,48	18,02	46,41	1,38
B1(2)	32,10	42,79	19,63	46,16	1,39
B1(3)	30,04	40,09	18,27	46,06	1,38
B1(4)	27,43	36,68	16,78	46,48	1,38
bed.B1				46,28	1,38
hat.B1(1)	23,36	30,98	14,43	46,04	1,41
B1(2)	34,85	46,40	21,57	46,52	1,40
B1(3)	11,48	15,25	7,08	46,14	1,41
hat.B2(1)	14,95	20,41	9,31	49,19	1,35
B2(2)	17,19	23,30	10,58	48,03	1,35
B2(3)	16,36	22,28	10,21	49,05	1,36
hat.B1,B2				47,50	1,38
inc.B1(1)	14,14	19,67	8,79	50,83	1,30
B1(2)	19,22	26,75	12,04	51,19	1,31
B1(3)	8,77	12,13	5,43	50,15	1,31
inc.B2(1)	25,75	34,36	15,90	46,64	1,39
B2(2)	25,80	34,93	15,86	47,88	1,35
inc.B1,B2				49,34	1,33
taşm.B1(1)	18,77	23,80	11,21	39,95	1,49
B1(2)	19,04	23,87	11,41	38,76	1,53
taşm.B2(1)	16,78	20,91	9,93	37,61	1,53
B2(2)	21,34	26,48	12,71	37,33	1,55
taşm.B1				38,41	1,52
güd.B1(1)	28,43	36,33	16,88	40,62	1,46
B1(2)	25,99	33,02	15,22	39,49	1,46
güd.B2(1)	29,43	37,22	16,59	37,76	1,43
B2(2)	26,81	33,83	15,36	38,01	1,45
güd.B1				38,97	1,45

APPENDIX N

**ULTRASONIC PULSE VELOCITY MEASUREMENTS
AND MODULUS OF ELASTICITY OF STONE AND
BRICK MASONRY MORTARS**

Table N1 Ultrasonic pulse velocity measurements and modulus of elasticity of stone masonry mortars

Sample	l (mm)	t (s)	V (m/s)	D (kg/m³)	E_{mod} (MPa)
kub.SM1(1)	16	11,18	1431,13	1360	2565,33
SM1(2)	16	12,08	1324,50	1440	2326,57
SM1(3)	22	16	1375,00	1370	2385,47
kub.SM1			1376,88	1390	2425,79
kub.SM2(1)	12	10,04	1195,22	1480	1947,17
SM2(2)	13	11,23	1157,61	1710	2110,43
SM2(3)	14	11,53	1214,22	1520	2063,90
SM2(4)	14	11,2	1250,00	1500	2158,54
kub.SM2			1204,26	1553	2070,01
kub.SM3(1)	12	8,66	1385,68	1640	2900,14
SM3(2)	14	11,5	1217,39	1760	2402,27
SM3(3)	15	12,04	1245,85	1810	2587,36
kub.SM3			1282,97	1737	2629,92
bed.SM1(1)	24	30,2	794,70	1530	889,91
SM1(2)	17	21,25	800,00	1520	895,93
bed.SM1			797,35	1525	892,92
sak.SM1(1)	20	29,35	681,43	1550	662,86
SM1(2)	22	30,4	723,68	1590	766,91
sak.SM1			702,56	1570	714,89
kurh.SM2(1)	21	12,8	1640,63	1650	4090,26
SM2(2)	20	11,7	1709,40	1850	4978,61
SM2(3)	21	10,36	2027,03	1900	7189,87
kurh.SM2			1792,35	1800	5419,58

Table N1 continued

kurm.SM1(1)	25	12,93	1933,49	1880	6472,75
SM1(2)	19	7,92	2398,99	1920	10176,68
kurm.SM1			2166,24	1900	8324,72
kızım.SM1(1)	27	32,5	830,77	1530	972,52
SM1(2)	27	36	750,00	1520	787,43
kızım.SM1			790,38	1525	879,98
zaz.SM1(1)	22	25,65	857,70	1590	1077,25
zaz.SM1			857,70	1590	1077,25
zaz.SM2(1)	23	26,13	880,21	1450	1034,65
SM2(2)	32	36,43	878,40	1550	1101,44
zaz.SM2			879,31	1500	1068,05
obr.SM1(1)	25	36,75	680,27	1420	605,20
SM1(2)	24	28,56	840,34	1470	956,03
obr.SM1			760,30	1445	780,62

Table N2 Ultrasonic pulse velocity measurements and modulus of elasticity of brick masonry mortars

Sample	l (mm)	t (s)	V (m/s)	D (kg)	E _{mod} (MPa)
kub.BM2(1)	17	17,53	969,77	1810	1567,69
BM2(2)	9	6,36	1415,09	1630	3006,12
kub.BM2			1192,43	1720	2286,91
sah.BM1(1)	19	13,45	1412,64	1520	2793,54
BM1(2)	20	13,46	1485,88	1570	3192,40
sah.BM1			1449,26	1545	2992,97
sam.BM1(1)	24	25,37	946,00	1270	1046,73
BM1(2)	22	22,47	979,08	1240	1094,74
BM1(3)	22	23,4	940,17	1330	1082,71
sam.BM1			955,08	1280	1074,73
sam.BM2(1)	19	15,93	1192,72	1270	1663,90
BM2(2)	19	16,06	1183,06	1280	1649,96
BM2(4)	21	19,13	1097,75	1290	1431,68
sam.BM2			1157,84	1280	1581,85

Table N2 continued

zen.BM1(1)	21	19,4	1082,47	1390	1500,02
BM1(2)	19	18,1	1049,72	1400	1420,78
BM1(3)	20	18,16	1101,32	1330	1485,69
BM1(5)	26	27,77	936,26	1350	1089,88
zen.BM1			1042,45	1367	1374,09
ev.BM1(1)	25	32,46	770,18	1350	737,50
BM1(2)	24	28,3	848,06	1370	907,44
ev.BM1			809,12	1360	822,47
hoc.BM1(1)	28	20,32	1377,95	1510	2640,55
BM1(3)	27	22,65	1192,05	1510	1976,13
hoc.BM1			1285,00	1510	2308,34
hoc.BM2(1)	24	19,46	1233,30	1580	2213,31
BM2(2)	24	18,47	1299,40	1580	2456,94
hoc.BM2			1266,35	1580	2335,12
bed.BM1(1)	30	32,13	933,71	1670	1340,87
BM1(2)	27	29,43	917,43	1690	1310,03
BM1(3)	16	18,1	883,98	1630	1173,06
bed.BM1			911,71	1663	1274,65
inc.BM1(1)	21	26,2	801,53	1470	869,76
BM1(3)	23	22,5	1022,22	1480	1424,30
BM1(4)	30	30,86	972,13	1490	1296,84
BM1(5)	20	17,4	1149,43	1450	1764,32
inc.BM1			986,33	1473	1338,80
taşm.BM1(1)	24	35,9	668,52	1450	596,83
BM1(2)	21	27,1	774,91	1470	812,95
BM1(3)	19	25,5	745,10	1380	705,59
taşm.BM1			729,51	1433	705,12
ulu.BM1(2)	18	24,25	742,27	1460	740,84
BM1(4)	20	22,85	875,27	1440	1016,01
ulu.BM1			808,77	1450	878,42
güd.BM1(2)	15	12,9	1162,79	1500	1867,85
BM1(3)	16	13,36	1197,60	1470	1941,75
güd.BM1			1180,20	1485	1904,80
hat.BM2(1)	23	29,3	784,98	1530	868,28
BM2(2)	22	28,5	771,93	1550	850,62
BM2(3)	22	27,4	802,92	1570	932,16
BM2(4)	21	26,4	795,45	1590	926,57
hat.BM2			788,82	1560	894,41

APPENDIX O

UNIAXIAL COMPRESSIVE STRENGTH OF STONE AND BRICK MASONRY MORTARS IN DRY AND WET STATES

Table O1 Uniaxial compressive strength of stone and brick masonry mortars
in dry state

Sample	w (mm)	t (mm)	P (kN)	A (mm ²)	De ²	Is	De	F	Is ₍₅₀₎	UCS (MPa)
<i>Stone masonry mortars</i>										
kub.SM1(1)	33	16	0,7	528	672,27	1,04	25,93	0,74	0,77	10,72
SM1(2)	34	16	1,1	544	692,64	1,59	26,32	0,75	1,19	15,14
kub.SM1									0,98	12,93
kub.SM2(1)	23	12	0,2	276	351,41	0,57	18,75	0,64	0,37	6,37
SM2(2)	22	13	0,3	286	364,15	0,82	19,08	0,65	0,53	8,16
SM2(3)	22	14	0,3	308	392,16	0,76	19,80	0,66	0,50	7,84
SM2(4)	23	14	0,15	322	409,98	0,37	20,25	0,67	0,24	5,07
kub.SM2									0,41	6,86
kub.SM3(1)	25	12	0,8	300	381,97	2,09	19,54	0,66	1,37	17,09
SM3(2)	22	14	0,8	308	392,16	2,04	19,80	0,66	1,34	16,79
SM3(3)	19	15	0,8	285	362,87	2,20	19,05	0,65	1,43	17,68
kub.SM3									1,38	17,18
ev.SM1(1)	35	29	1,5	1015	1292,34	1,16	35,95	0,86	1,00	13,13
SM1(2)	31	25	1,6	775	986,76	1,62	31,41	0,81	1,32	16,48
ev.SM1									1,16	14,80
bed.SM1(1)	29	24	0,25	696	886,17	0,28	29,77	0,79	0,22	4,85
SM1(2)	24	17	0,15	408	519,48	0,29	22,79	0,70	0,20	4,63
SM1(3)	23	17	0,16	391	497,84	0,32	22,31	0,70	0,22	4,85
bed.SM1									0,22	4,78
sak.SM1(1)	37	20	0,1	740	942,20	0,11	30,70	0,80	0,09	3,38
SM1(2)	38	22	0,1	836	1064,43	0,09	32,63	0,83	0,08	3,30
sak.SM1									0,08	3,34

Table O1 continued

kurm.SM1(1)	27	25	2	675	859,44	2,33	29,32	0,79	1,83	21,96
SM1(2)	30	19	1,1	570	725,75	1,52	26,94	0,76	1,15	14,69
SM2(4)	24	23	1,45	552	702,83	2,06	26,51	0,75	1,55	18,98
kurm.SM1									1,49	18,32
kızın.SM1(1)	34	27	0,25	918	1168,83	0,21	34,19	0,84	0,18	4,39
kızın.SM1									0,18	4,39
zaz.SM1(1)	24	22	0,3	528	672,27	0,45	25,93	0,74	0,33	6,01
SM1(2)	24	19	0,2	456	580,60	0,34	24,10	0,72	0,25	5,11
SM1(3)	25	20	0,15	500	636,62	0,24	25,23	0,74	0,17	4,32
zaz.SM1									0,25	5,15
zaz.SM2(1)	35	23	0,25	805	1024,96	0,24	32,01	0,82	0,20	4,60
SM2(2)	35	32	0,1	1120	1426,03	0,07	37,76	0,88	0,06	3,13
SM2(3)	35	24	0,15	840	1069,52	0,14	32,70	0,83	0,12	3,71
zaz.SM2									0,13	3,81
obr.SM1(1)	35	25	0,15	875	1114,08	0,13	33,38	0,83	0,11	3,67
SM1(2)	35	24	0,2	840	1069,52	0,19	32,70	0,83	0,15	4,12
obr.SM1									0,13	3,89
Brick masonry mortars										
kub.BM2(1)	22	17	0,5	374	476,19	1,05	21,82	0,69	0,72	10,17
BM2(2)	23	9	0,2	207	263,56	0,76	16,23	0,60	0,46	7,34
kub.BM2									0,59	8,76
sah.BM1(1)	34	19	0,3	646	822,51	0,36	28,68	0,78	0,28	5,50
BM1(2)	21	20	0,4	420	534,76	0,75	23,12	0,71	0,53	8,10
sah.BM1									0,41	6,80
sam.BM1(1)	32	24	0,35	768	977,85	0,36	31,27	0,81	0,29	5,56
BM1(3)	29	22	0,15	638	812,33	0,18	28,50	0,78	0,14	4,00
sam.BM1									0,22	4,78
sam.BM2(2)	30	19	0,4	570	725,75	0,55	26,94	0,76	0,42	6,92
BM2(4)	21	21	0,2	441	561,50	0,36	23,70	0,71	0,25	5,18
sam.BM2									0,34	6,05
zen.BM1(1)	27	21	0,2	567	721,93	0,28	26,87	0,76	0,21	4,70
BM1(3)	31	20	0,2	620	789,41	0,25	28,10	0,77	0,20	4,55
BM1(4)	32	21	0,1	672	855,62	0,12	29,25	0,79	0,09	3,45
BM1(5)	31	26	0,2	806	1026,23	0,19	32,03	0,82	0,16	4,17
zen.BM1									0,16	4,22
ev.BM1(1)	25	25	0,1	625	795,77	0,13	28,21	0,77	0,10	3,51
BM1(2)	28	24	0,15	672	855,62	0,18	29,25	0,79	0,14	3,94
ev.BM1									0,12	3,72

Table O1 continued

hoc.BM1(1)	29	28	0,65	812	1033,87	0,63	32,15	0,82	0,52	7,96
BM1(2)	27	25	0,55	675	859,44	0,64	29,32	0,79	0,50	7,83
hoc.BM1									0,51	7,90
hoc.BM2(1)	28	27	0,45	756	962,57	0,47	31,03	0,81	0,38	6,49
hoc.BM2									0,38	6,52
bed.BM1(1)	33	30	0,3	990	1260,51	0,24	35,50	0,86	0,20	4,65
BM1(4)	25	19	0,2	475	604,79	0,33	24,59	0,73	0,24	5,03
bed.BM1									0,22	4,84
hat.BM1(2)	32	24	0,25	768	977,85	0,26	31,27	0,81	0,21	4,68
BM1(4)	29	18	0,3	522	664,63	0,45	25,78	0,74	0,34	6,04
hat.BM1									0,27	5,36
hat.BM2(2)	28	22	0,1	616	784,32	0,13	28,01	0,77	0,10	3,52
BM2(3)	28	22	0,1	616	784,32	0,13	28,01	0,77	0,10	3,52
hat.BM2									0,10	3,52
inc.BM1(3)	29	23	0,4	667	849,25	0,47	29,14	0,78	0,37	6,41
BM1(4)	36	30	0,5	1080	1375,10	0,36	37,08	0,87	0,32	5,86
BM1(5)	21	20	0,15	420	534,76	0,28	23,12	0,71	0,20	4,58
inc.BM1									0,30	5,62
taşm.BM1(1)	28	24	0,1	672	855,62	0,12	29,25	0,79	0,09	3,45
BM1(2)	26	21	0,15	546	695,19	0,22	26,37	0,75	0,16	4,20
BM1(3)	29	19	0,1	551	701,55	0,14	26,49	0,75	0,11	3,61
taşm.BM1									0,12	3,75
ulu.BM1(1)	28	22	0,15	616	784,32	0,19	28,01	0,77	0,15	4,04
BM1(3)	28	24	0,2	672	855,62	0,23	29,25	0,79	0,18	4,43
ulu.BM1									0,17	4,24
güd.BM1(1)	41	24	0,4	984	1252,87	0,32	35,40	0,86	0,27	5,38
BM1(2)	31	15	0,3	465	592,06	0,51	24,33	0,72	0,37	6,38
BM1(5)	26	19	0,45	494	628,98	0,72	25,08	0,73	0,52	8,06
güd.BM1									0,39	6,61

Table O2 Uniaxial compressive strength of stone and brick masonry mortars
in wet state

Sample	w (mm)	t (mm)	P (kN)	A (mm ²)	De ²	Is	De	F	Is ₍₅₀₎	UCS (MPa)
<i>Stone masonry mortars</i>										
kub.SM1(1)	33	28	0,7	924	1176,47	0,59	34,30	0,84	0,50	7,82
SM1(4)	33	25	0,7	826	1050,42	0,67	32,41	0,82	0,55	8,31
kub.SM1									0,53	8,07
kub.SM2(3)	31	24	0,5	744	947,29	0,53	30,78	0,80	0,42	6,99
SM2(4)	32	24	0,5	7,68	977,85	0,51	31,27	0,81	0,41	6,88
kub.SM2									0,42	6,94
kub.SM3(1)	29	27	1,15	783	996,95	1,15	31,57	0,81	0,94	12,46
kub.SM3									0,94	12,46
kurm.SM1(1)	29	18	1,3	522	664,63	1,96	25,78	0,74	1,45	17,93
kurm.SM1									1,45	17,91
<i>Brick masonry mortars</i>										
sam.BM1(2)	32	22	0,3	704	896,36	0,33	29,94	0,79	0,27	5,30
BM1(4)	30	17	0,05	510	649,35	0,08	25,48	0,74	0,06	3,08
sam.BM1									0,16	4,19
sam.BM2(1)	30	19	0,25	570	725,75	0,34	26,94	0,76	0,26	5,25
BM2(3)	30	19	0,1	570	725,75	0,14	26,94	0,76	0,10	3,58
sam.BM2									0,18	4,42
zen.BM1(1)	28	19	0,1	532	677,36	0,15	26,03	0,75	0,11	3,65
zen.BM1									0,11	3,64
hoc.BM1(1)	28	27	0,4	756	962,57	0,42	31,03	0,81	0,34	6,04
hoc.BM1									0,34	6,09
hoc.BM2(1)	27	24	0,1	648	825,06	0,12	28,72	0,78	0,09	3,48
BM2(2)	26	24	0,1	624	794,50	0,13	28,19	0,77	0,10	3,51
hoc.BM2									0,10	3,49
bed.BM1(2)	27	27	0,2	729	928,19	0,22	30,47	0,80	0,17	4,31
BM1(3)	27	16	0,05	432	550,04	0,09	23,45	0,71	0,06	3,16
bed.BM1									0,12	3,74
hat.BM1(1)	28	14	0,2	392	499,11	0,40	22,34	0,70	0,28	5,44
hat.BM1									0,28	5,45
hat.BM2(1)	23	23	0,05	529	673,54	0,07	25,95	0,74	0,06	3,06
BM2(4)	24	21	0,05	504	641,71	0,08	25,33	0,74	0,06	3,08
hat.BM2									0,06	3,07

Table O2 Continued

inc.BM1(1)	29	21	0,2	609	775,40	0,26	27,85	0,77	0,20	4,58
BM1(2)	22	19	0,2	418	532,21	0,38	23,07	0,71	0,27	5,30
inc.BM1									0,23	4,94
ulu.BM1(2)	26	18	0,1	468	595,88	0,17	24,41	0,72	0,12	3,77
BM1(4)	30	20	0,1	600	763,94	0,13	27,64	0,77	0,10	3,54
ulu.BM1									0,11	3,65
güd.BM1(3)	35	16	0,1	560	713,01	0,14	26,70	0,75	0,11	3,60
BM1(4)	26	19	0,25	494	628,98	0,40	25,08	0,73	0,29	5,58
güd.BM1									0,20	4,59

APPENDIX P

BINDER /AGGREGATE RATIOS, PARTICLE SIZE DISTRIBUTION IN THE OVERALL COMPOSITION OF MORTAR AND AGGREGATE PARTS OF STONE AND BRICK MASONRY MORTARS

Table P1 B/A ratios, particle size distribution in the mortar and aggregate parts of stone masonry mortars

Sample	B/A ratios		Size distribution in mortar					Size distribution in aggregate part				
	B (%)	A (%)	>1000 (µm)	500 (µm)	250 (µm)	125 (µm)	<125 (µm)	>1000 (µm)	500 (µm)	250 (µm)	125 (µm)	<125 (µm)
kub.SM1	50,72	49,28	13,63	6,65	5,39	3,44	20,17	27,65	13,5	10,94	6,99	40,93
kub.SM2	70,55	29,45	8,24	3,73	3,16	1,94	12,37	27,99	12,68	10,73	6,59	42,01
kub.SM3	64,54	35,46	9,34	7,43	9,01	3,47	6,21	26,34	20,95	25,42	9,79	17,5
kub.SM4	56,42	43,58	8,55	5,95	5,72	2,24	21,11	19,63	13,65	13,12	5,15	48,45
kub.SM5	51,87	48,13	12,23	12,87	14,59	4,20	4,25	25,4	26,74	30,31	8,73	8,82
kub.SM6	53,17	46,83	14,06	11,76	13,06	2,39	5,56	30,02	25,11	27,89	5,10	11,88
ev.SM1	60,21	39,79	7,31	4,09	8,11	9,75	10,53	18,19	10,32	20,45	24,55	26,85
ev.SM2	55,56	44,44	5,17	3,96	11,13	9,74	14,44	11,68	9,13	25,68	22,11	31,90
ev.SM3	52,58	47,42	7,77	4,25	8,50	13,33	13,58	16,48	8,98	17,95	28,16	28,80
bed.SM1	59,35	40,65	9,83	8,64	12,28	5,26	4,63	24,03	21,29	30,30	12,98	11,40
sak.SM1	58,56	41,44	11,79	12,30	10,65	3,81	2,89	28,47	29,67	25,69	9,19	6,98
taş.SM1	52,74	47,26	27,24	7,71	4,02	1,62	6,67	57,63	16,32	8,50	3,42	14,13
lar.SM1	50,13	49,87	11,12	7,86	14,12	10,54	6,23	22,30	15,74	28,33	21,13	12,50
kızh.SM1	43,97	56,03	21,80	11,06	10,31	5,37	7,51	38,90	19,74	18,39	9,57	13,39
kızh.SM2	39,64	60,36	20,13	13,42	13,89	6,58	6,34	33,33	22,24	23,01	10,91	10,51
kızm.SM1	38,46	61,54	24,35	13,04	12,99	5,80	5,36	39,53	21,20	21,13	9,43	8,72
zaz.SM1	66,42	33,58	12,82	5,52	6,59	4,61	4,05	38,11	16,44	19,64	13,76	12,05
zaz.SM2	65,53	34,47	13,59	5,42	6,70	4,53	4,22	39,36	15,75	19,48	13,19	12,22
zaz.SM3	68,80	31,20	10,76	5,74	6,53	4,30	3,88	34,48	18,39	20,91	13,77	12,45
obr.SM1	88,61	11,39	1,18	1,42	2,04	1,76	4,99	10,45	12,50	17,87	15,41	43,77
obr.SM2	80,75	19,25	5,93	1,72	1,66	1,66	8,28	27,98	8,59	8,68	9,05	45,70
taz.SM1	52,80	47,20	3,77	7,55	18,23	12,48	5,39	7,99	16,00	38,62	26,43	11,42
taz.SM2	54,23	45,77	3,76	9,15	19,39	9,38	4,14	8,21	20,00	42,37	20,49	9,04
taz.SM3	53,16	46,84	7,26	9,43	18,08	8,82	3,57	15,49	20,14	38,61	18,84	7,62
taz.SM4	53,98	46,02	5,19	9,96	18,50	8,47	4,27	11,28	21,65	40,20	18,42	9,28

Each row represents the average values of three pieces of the same sample

Table P2 B/A ratios, particle size distribution in the mortar and aggregate parts of brick masonry mortars

Sample	B (%)	A (%)	Size distribution in mortar					Size distribution in aggregate part				
			>1000 (µm)	500 (µm)	250 (µm)	125 (µm)	<125 (µm)	>1000 (µm)	500 (µm)	250 (µm)	125 (µm)	<125 (µm)
kub.BM1	71,07	28,93	8,47	6,84	6,50	2,34	4,78	29,29	23,65	22,48	8,08	16,51
kub.BM2	71,22	28,78	7,46	9,49	8,87	2,12	8,32	20,58	26,17	24,46	5,84	22,95
sah.BM1	60,81	39,19	1,90	6,82	14,19	7,82	8,46	4,90	17,60	36,62	20,15	21,85
sam.BM1	75,38	24,62	2,76	2,70	6,14	5,08	7,94	11,52	11,23	25,50	21,15	32,73
sam.BM2	69,80	30,20	3,78	3,44	9,00	7,74	6,24	12,44	11,21	29,29	25,50	22,41
zen.BM1	58,77	41,23	1,24	1,87	3,82	8,93	25,37	3,02	4,45	8,99	21,60	62,87
ev.BM1	62,44	37,56	5,77	4,20	6,11	9,11	12,38	15,51	11,32	16,47	24,58	33,35
ev.BM2	62,34	37,66	5,01	4,27	6,23	9,31	12,83	13,90	11,17	16,54	24,75	34,44
şek.BM1	50,41	49,59	9,41	12,72	15,59	6,97	4,90	19,00	25,57	31,48	14,09	9,90
hoc.BM1	55,46	44,54	7,81	9,60	12,99	7,78	6,37	17,53	21,55	29,15	17,47	14,29
hoc.BM2	65,32	34,68	5,46	6,80	10,49	7,77	4,16	15,66	19,59	30,24	22,44	12,07
göm.BM1	55,66	44,34	5,68	5,69	12,37	9,55	11,05	12,78	12,77	27,87	21,60	24,98
bed.BM1	54,51	45,49	10,13	9,74	13,35	6,15	6,12	22,25	21,42	29,34	13,53	13,45
bed.BM2	52,22	47,78	9,04	10,36	15,59	7,18	5,60	18,90	21,69	32,62	15,04	11,75
hat.BM1	48,09	51,91	1,88	5,55	16,42	15,12	12,94	3,62	10,70	31,63	29,13	24,93
hat.BM2	46,69	53,31	2,72	5,11	15,05	15,52	14,90	5,10	9,58	28,23	29,12	27,96
ef.BM1	65,26	34,74	2,59	6,26	9,02	14,56	2,32	7,15	15,56	26,85	43,24	7,21
inc.BM1	61,64	38,36	10,01	9,63	9,32	4,28	5,12	26,08	25,11	24,30	11,16	13,35
inc.BM2	56,29	43,71	5,82	7,71	14,25	9,41	6,52	13,51	17,74	32,48	21,38	14,89
taşm.BM1	67,92	32,08	12,78	5,13	4,21	2,05	7,92	39,77	15,94	13,11	6,42	24,76
taşm.BM2	71,37	28,63	12,79	4,52	3,61	2,05	5,66	44,05	15,90	12,97	7,45	19,64
ulu.BM1	61,13	38,87	16,23	5,94	5,28	3,34	8,10	41,70	15,24	13,60	8,62	20,84
güd.BM1	69,95	30,05	14,90	4,17	3,09	1,82	6,07	48,08	14,27	10,63	6,24	20,78
taz.BM1	61,30	38,70	3,83	9,33	16,13	6,93	2,78	9,90	24,11	41,69	17,90	7,19
taz.BM2	63,52	36,48	3,15	6,15	12,75	9,70	4,79	8,63	16,87	34,94	26,59	13,12
taz.BM3	70,02	29,98	2,49	4,78	10,14	7,80	4,77	8,30	15,96	33,82	26,03	15,90
taz.BM4	66,29	33,71	3,31	6,89	13,24	6,28	4,26	9,83	20,45	39,28	18,64	12,62

Each row represents the average values of three pieces of the same sample

APPENDIX R

METAL OKSIDE CONTENTS BY AAS AND COMPLEXOMETRIC TITRATION ANALYSES IN ACID SOLUBLE PARTS AND CEMENTATION INDEX OF STONE AND BRICK MASONRY MORTARS

Table R1 The percentages of CaO, MgO, SiO₂, Al₂O₃ and Fe₂O₃ contents and cementation index (CI) of stone masonry mortars

Sample	%CaO	%MgO	%SiO ₂	%Al ₂ O ₃	%Fe ₂ O ₃	CI
kub.SM1	23,26	2,18	2,24	1,56	1,95	0,35
kub.SM2	37,50	1,45	0,65	0,49	1,08	0,08
kub.SM3	33,73	0,79	0,82	0,97	1,24	0,12
kub.SM4	29,06	0,73	1,74	1,59	1,99	0,27
kub.SM5	27,31	0,00	1,05	1,19	1,62	0,20
kub.SM6	28,33	0,40	1,10	1,00	1,82	0,19
kub.SM	29,87	0,93	1,27	1,13	1,62	0,20
ev.SM1	29,36	1,44	0,63	1,53	0,94	0,13
ev.SM2	29,35	1,01	0,36	1,73	1,15	0,12
ev.SM3	27,49	0,93	0,10	0,21	0,71	0,03
ev.SM	28,73	1,13	0,36	1,15	0,93	0,10
bed.SM1	30,21	2,34	0,62	0,05	0,66	0,07
sak.SM1	28,56	0,74	0,11	0,48	0,19	0,03
taş.SM1	27,47	0,07	0,37	0,91	1,45	0,11
lar.SM1	32,12	2,43	0,63	1,01	0,84	0,10
kurh.SM1	41,76	12,30	0,11	0,16	0,00	0,01
kurm.SM1	35,08	17,43	0,11	0,48	0,00	0,01
kurh.SM	38,42	14,87	0,11	0,32	0,00	0,01
kızh.SM1	22,55	0,20	1,05	2,07	0,84	0,25
kızm.SM1	19,13	0,34	0,48	1,02	0,63	0,15
kızm.SM	20,84	0,27	0,77	1,55	0,74	0,20
zaz.SM1	35,71	0,07	0,32	0,38	0,35	0,04
zaz.SM2	37,44	0,27	0,32	0,16	0,25	0,03
zaz.SM3	35,12	0,27	0,43	0,27	0,25	0,05
zaz.SM	36,09	0,20	0,35	0,27	0,28	0,04
obr.SM1	45,38	0,34	0,16	0,91	0,41	0,06
obr.SM2	34,06	0,41	0,44	1,00	0,35	0,05
obr.SM	39,72	0,38	0,30	0,96	0,38	0,05

Table R1 continued

taz.SM1	26,78	0,46	0,41	0,57	0,30	0,07
taz.SM2	26,52	0,27	0,63	0,48	0,19	0,09
taz.SM3	27,98	0,13	0,52	0,37	0,19	0,07
taz.SM4	29,11	0,13	0,10	0,37	0,10	0,03
taz.SM	27,60	0,25	0,42	0,45	0,20	0,07

Table R2 The percentages of CaO, MgO, SiO₂, Al₂O₃ and Fe₂O₃ contents and cementation index (CI) of brick masonry mortars

Sample	%CaO	%MgO	%SiO ₂	%Al ₂ O ₃	%Fe ₂ O ₃	CI
kub.BM1	36,93	1,43	0,64	1,02	1,07	0,09
kub.BM2	42,61	0,94	0,75	0,49	1,19	0,08
kub.BM	39,77	1,19	0,69	0,76	1,13	0,09
sah.BM1	30,41	0,81	0,13	0,57	0,35	0,04
sam.BM1	42,05	1,00	0,63	0,90	0,52	0,07
sam.BM2	37,47	0,73	0,72	0,98	0,55	0,09
sam.M	39,76	0,87	0,67	0,94	0,54	0,08
zen.BM1	31,39	0,53	0,11	0,38	0,74	0,04
ev.BM1	30,81	0,59	0,10	0,58	0,83	0,05
ev.BM2	28,54	1,65	0,37	0,91	0,74	0,06
ev.BM	29,68	1,12	0,24	0,74	0,79	0,06
şek.BM1	25,06	0,07	0,11	0,37	0,19	0,03
hoc.BM1	27,49	0,00	0,21	0,78	0,30	0,06
hoc.BM2	31,16	0,51	0,49	0,35	0,23	0,06
hoc.BM	29,33	0,26	0,35	0,56	0,26	0,06
göm.BM1	29,89	0,20	0,31	0,47	0,24	0,05
bed.BM1	27,98	1,76	0,10	0,58	0,73	0,05
bed.BM2	29,08	1,39	0,31	0,37	0,51	0,05
bed.BM	28,53	1,58	0,21	0,47	0,62	0,05
hat.BM1	28,24	0,20	0,21	-0,05	0,19	0,02
hat.BM2	23,99	1,53	0,21	0,05	0,30	0,03
hat.BM	26,12	0,87	0,21	0,00	0,25	0,03
ef.BM1	33,08	1,28	0,11	0,74	0,57	0,04
inc.BM1	31,31	0,20	0,52	0,16	0,27	0,06
inc.BM2	29,30	0,07	0,11	0,38	0,35	0,03
inc.BM	30,31	0,14	0,31	0,27	0,31	0,04
taşm.BM1	33,82	0,00	0,53	1,01	1,38	0,10
taşm.BM2	29,50	0,00	0,58	0,80	1,60	0,12
taşm.BM	31,66	0,00	0,55	0,90	1,49	0,11
ulu.BM1	35,43	0,27	0,43	0,91	1,51	0,09
güd.BM1	41,74	0,00	1,05	0,69	1,27	0,11

Table R2 continued

taz.BM1	33,13	0,07	0,31	0,73	0,19	0,05
taz.BM2	34,30	0,07	0,53	0,49	0,09	0,06
taz.BM3	34,38	0,47	0,63	0,48	0,19	0,07
taz.BM4	33,39	0,47	0,64	0,38	0,09	0,07
taz.BM	33,80	0,27	0,53	0,52	0,14	0,06



